Rijkswaterstaat
Ministerie van Infrastructuur en Milieu

RWS INFORMATION

WBI2017 Code Calibration

Reliability-based code calibration and semi-probabilistic assessment rules for the WBI2017

Date 24 June 2017
Status

Colofon

Publisher	Rijkswaterstaat
Information	Robert Slomp
Telephone	0320298532
Fax	
Author	Ruben Jongejan
Lay-out	
Date	24 June 2017
Status	
Versienummer	

Acknowlegdments

This report summarizes the results of studies carried out by various researchers (in alphabetical order): Ferdinand Diermanse (Deltares, dune erosion), Pieter van Geer (Deltares, dune erosion), Wouter ter Horst (HKV, internal erosion), Ruben Jongejan (RMC, calibration procedure, various reviews, block and grass revetments), Maximilian Huber (Deltares, slope stability), Wim Kanning (Deltares, slope stability, asphalt revetments), Dorothea Kaste (Deltares, revetments), Mark Klein Breteler (Deltares, revetments), Wouter Jan Klerk (Deltares, revetments, various reviews), Mark van der Krogt (Deltares, slope stability), Ana Martins Teixeira (Deltares, slope stability, internal erosion), Timo Schweckendiek (Deltares, slope stability, calibration procedure) and Karolina Wojciechowska (HKV, internal erosion). The assistance of prof. Ton Vrouwenvelder (TNO) and Ed Calle (Deltares), who laid the intellectual groundwork for the calibration studies, is gratefully acknowledged. All studies were carried out under the auspices of Robert Slomp (Rijkswaterstaat) and Marcel Bottema (Rijkswaterstaat).

The author would like to thank Ferdinand Diermanse (Deltares), Marcel Bottema (Rijkswaterstaat), Marieke de Visser (Rijkswaterstaat) and Anske van der Laan (Rijkswaterstaat) for their valuable comments on previous versions of this document.

Contents

Summary 9

Samenvatting 10

1 Introduction 11
1.1 Flood risk management in the Netherlands 11
1.2 Towards probabilistic flood protection standards 12
1.2.1 From exceedance probabilities to probabilities of flooding 12
1.2.2 Institutional context 12
1.2.3 The WBI2017 13
1.3 Semi-probabilistic assessment rules 14
1.3.1 Code calibration 14
1.3.2 Semi-probabilistic assessment rules in the WBI2017 15
1.4 Report outline 15
1.5 Target audience 15

2 Semi-probabilistic assessment rules 16
2.1 Basic concepts in reliability engineering 16
2.2 The relations between probabilistic and semi-probabilistic assessments 19

3 Code calibration procedure 25

4 Step 1: Establish reliability requirements 27
4.1 Probabilities of flooding, segments, sections and cross-sections 27
4.2 Reliability requirements per failure mechanism 28
4.3 Cross-sectional reliability requirements per failure mechanism 31
4.3.1 The length effect 31
4.3.2 From cross-sectional reliabilities to system reliability 31
4.3.3 Length effect factors 32

5 Step 2: Establishing the safety format 35
5.1 Analyzing design point values 35
5.2 Defining representative values 36
5.3 Defining representative values for spatial averages 37
5.4 Selecting partial safety factors 38
5.5 β_T-dependent and β_T-invariant partial safety factors 39

6 Step 3: Calibrating partial safety factors 40
6.1 Establishing β_T-invariant safety factors 40
6.2 Establishing a β_T-dependent safety factor 41
6.2.1 Obtaining a relationship between safety factors and target reliabilities 41
6.2.2 The calibration criterion 43
6.2.3 The functional form of a β_T-dependent safety factor 45
6.2.4 The β_T-dependent safety factor and schematization uncertainty 47
6.2.5 The β_T-dependent safety factor and parallel system behavior 48

7 Internal erosion: uplift, heave and piping 50
7.1 Failure mechanism 50
7.1.1 Qualitative description 50
7.1.2 Failure mechanism model 51

7.2 Reliability requirement 53
7.3 Safety format 53
7.3.1 Partial factors and representative values 53
7.3.2 Schematization uncertainty 54
7.4 Calibrated safety factors 54
7.5 Comparison with former assessment rule 58
7.6 Discussion 58

8 Slope instability 60
8.1 Failure mechanism 60
8.1.1 Qualitative description 60
8.1.2 Failure mechanism model 60
8.2 Reliability requirement 62
8.3 Safety format 62
8.3.1 Representative values 62
8.3.2 Partial safety factors 63
8.4 Calibrated safety factors 64
8.5 Comparison with former assessment rule 66
8.6 Discussion 67

9 Dune erosion 68
9.1 Failure mechanism 68
9.1.1 Qualitative description 68
9.1.2 Failure mechanism model 68
9.2 Reliability requirement 69
9.3 Safety format 70
9.4 Calibrated design water level 71
9.5 Comparison with former assessment rule 72
9.6 Discussion 72

10 Block revetment failure caused by wave impacts 73
10.1 Failure mechanism 73
10.1.1 Qualitative description 73
10.1.2 Failure mechanism model 74
10.2 Reliability requirement 75
10.3 Safety format 78
10.3.1 Representative values 78
10.3.2 Partial safety factors 79
10.3.3 Residual strength 79
10.4 Calibrated safety factors 80
10.4.1 Computational results 80
10.4.2 Interpretation and proposal 81
10.5 Comparison with former assessment rule 82
10.6 Discussion 82

11 Asphalt revetment failure caused by wave impacts 83
11.1 Failure mechanism 83
11.1.1 Qualitative description 83
11.1.2 Failure mechanism model 85
11.2 Reliability requirement 85
11.3 Safety format 86
11.3.1 Representative values 86
11.3.2 Partial safety factors 87
11.4 Calibrated safety factors 87

11.5 Comparison with former assessment rule 88
11.6 Discussion 88

12 Grass revetment failure caused by wave impacts 89
12.1 Failure mechanism 89
12.1.1 Qualitative description 89
12.1.2 Failure mechanism model 91
12.2 Reliability requirement 91
12.3 Safety format 92
12.4 Calibrated safety factors 93
12.5 Comparison with former assessment rule 93
12.6 Discussion 95

13 Grass revetment failure caused by wave run-up 96
13.1 Failure mechanism 96
13.1.1 Qualitative description 96
13.1.2 Failure mechanism model 98
13.2 Reliability requirement 98
13.3 Safety format 98
13.4 Calibrated safety factors 99
13.5 Comparison with former assessment rule 100
13.6 Discussion 100

14 Concluding remarks 101

References 103

Appendix A System reliability analysis and the length effect 110
A.1 A method for quantifying system reliability 110
A.2 The length-effect within statistically homogenous sections 112
A.3 From system-level reliability requirements to cross-sectional requirements 114

Appendix B The calibration criterion 116

Summary

The Netherlands is protected against major floods by a system of primary flood defenses. The primary flood defenses have to comply with the flood protection standards from the Water Act. These were updated in January 2017. They are now defined in terms of maximum allowable probabilities of flooding. In the past, the standards were defined in terms of exceedance probabilities of loads that primary flood defenses should be able to safely withstand.

Periodic safety assessments are carried out to establish whether the Dutch primary flood defenses comply with the flood protection standards from the Water Act. Because of the change in the type of standard, a new set of tools and guidelines had to be developed for assessing the safety of primary flood defenses: the WBI2017.

The WBI2017 consists of simple screening methods as well as probabilistic and semi-probabilistic methods for detailed assessments. Semi-probabilistic methods rest on a partial safety factor approach. This approach allows practitioners to evaluate the reliability of flood defenses without having to resort to probability calculus.

To ensure consistency between probabilistic and semi-probabilistic assessments, the WBI2017's semi-probabilistic assessment rules have been code calibrated. This means that appropriate design values (partial safety factors and representative values) have been defined for use in semi-probabilistic assessments.

For reasons of consistency, efficiency and transparency, a standardized code calibration procedure was developed. This report provides an overview of this procedure and discusses its application to the following failure mechanisms:

1. internal erosion (uplift, heave and piping),
2. slope instability (macro instability),
3. dune erosion,
4. block revetment failure caused by wave impacts,
5. asphalt revetment failure caused by wave impacts,
6. grass revetment failure caused by wave impacts,
7. grass revetment failure caused by wave run-up.

Samenvatting

Nederland wordt beschermd tegen overstromingen vanuit buitenwater door een stelsel van primaire waterkeringen. De normen waar deze keringen aan moeten voldoen zijn vastgelegd in de Waterwet. Deze zijn in januari 2017 geactualiseerd. De normen zijn nu gedefinieerd in termen van maximaal toelaatbare overstromingskansen. De normen waren voorheen gedefinieerd als overschrijdingskansen van waterstanden die veilig gekeerd moesten kunnen worden.

De primaire waterkeringen worden periodiek beoordeeld op basis van de normen uit de Waterwet. Vanwege de verandering in het normtype moest daar een instrumentarium voor worden ontwikkeld: het Wettelijk Beoordelings-instrumentarium 2017 of WBI2017.

Het WBI2017 omvat zowel eenvoudige beoordelingsmethoden als probabilistische en semi-probabilistische methoden voor gedetailleerde beoordelingen. Bij een semi-probabilistische beoordeling wordt gerekend met rekenwaarden (representatieve waarden en partiële veiligheidsfactoren). Met een semi-probabilistisch voorschrift kan worden beoordeeld of een waterkering voldoet aan een faalkanseis zonder dat een faalkans berekend hoeft te worden.

Om de consistentie tussen probabilistische en semi-probabilistische beoordelingen te waarborgen zijn de semi-probabilistische voorschriften uit het WBI2017 gekalibreerd. Dit betekent dat geschikte rekenwaarden zijn afgeleid voor toepassing in semi-probabilistische beoordelingen.

Vanwege de consistentie, efficiëntie en transparantie is een gestandaardiseerde kalibratieprocedure ontwikkeld. In dit rapport wordt deze procedure besproken, evenals de toepassing ervan bij de volgende faalmechanismen:

1. opbarsten, heave en piping,
2. macroinstabiliteit,
3. duinafslag,
4. falen steenbekleding onder golfaanval,
5. falen asfaltbekleding onder golfaanval,
6. falen grasbekleding onder golfaanval,
7. falen grasbekleding door golfoploop.

1 Introduction

1.1 Flood risk management in the Netherlands

A major flood in the densely populated, low-lying Netherlands would have catastrophic consequences. Roughly two thirds of the country is at risk of severe flooding (Figure 1). The flood prone parts of the country are divided into major levee systems. Their outer defenses are formed by primary flood defenses. These are natural or man-made barriers such as dunes, levees, sea dikes, dams, and locks that protect the country from large-scale floods. Their total length is approximately 3600 kilometres. The adjective "primary" is used to distinguish these outer defenses from the numerous regional flood defenses and embankments in the polders behind them.

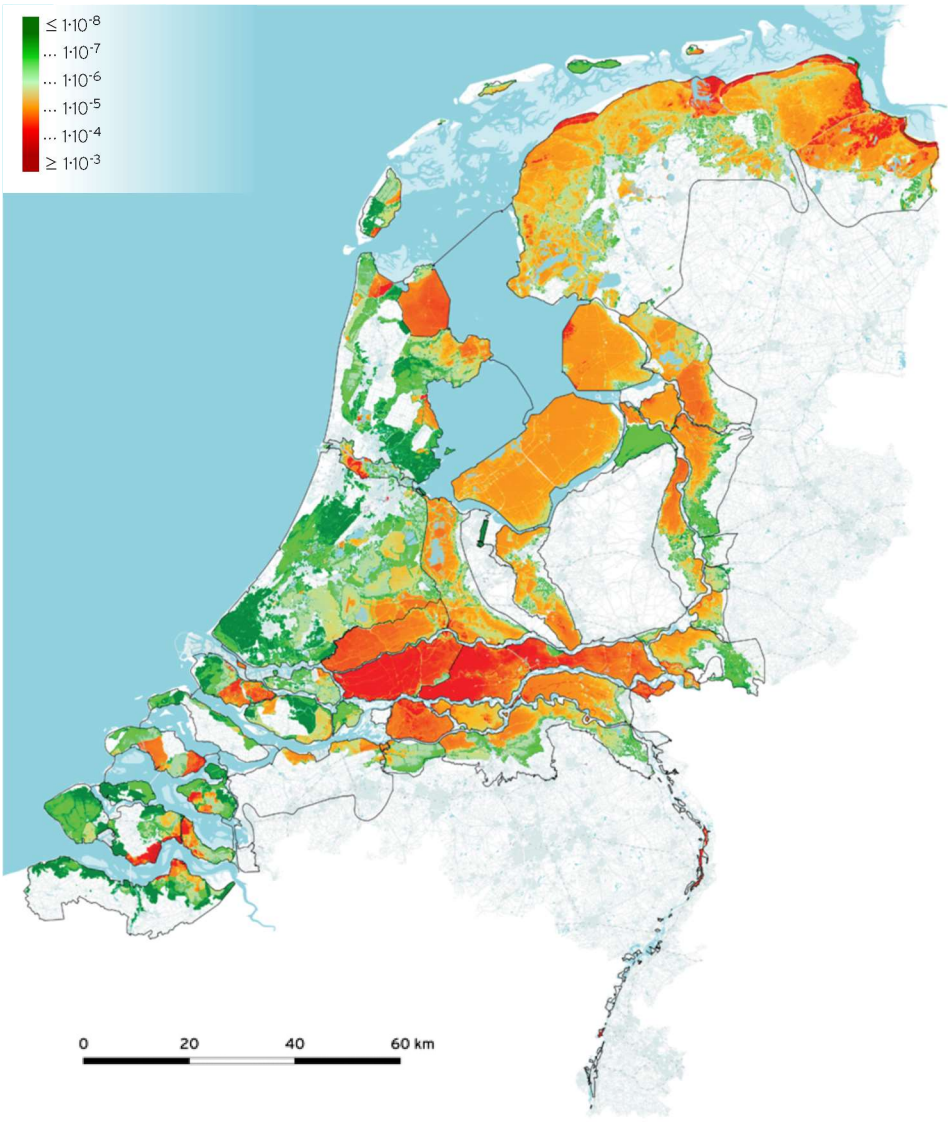

Figure 1. Individual risk in the Netherlands in 2015 according to a national flood risk analysis, called VNK2 (Rijkswaterstaat VNK Project Office 2014: 31).

1.2 Towards probabilistic flood protection standards

1.2.1 From exceedance probabilities to probabilities of flooding

The flood protection standards, which provide the basis for safety assessments and design, were updated in 2017, following an assessment of economic risk, individual risk an societal risk (Jonkman, Jongejan and Maaskant, 2011; Kind, 2014; Van der Most *et al.*, 2014). Since January 1st 2017, the Dutch flood protection standards are defined in terms of maximum allowable probabilities of flooding. They used to be defined in terms of the exceedance probabilities of the hydraulic loads that the primary flood defenses should be able to safely withstand. This change has two important advantages.

First, the new standards bring an end to the ambiguity related to the requirement that flood defenses should be able to "safely withstand" particular loads. This increases the transparency of safety assessments and provides a uniform basis for the development of technical guidelines for different failure mechanisms.

Second, the new standards are more closely related to the risk of flooding deemed acceptable than the old standards (Figure 2). This, in turn, contributes to a more effective and efficient protection of the Netherlands against flooding.

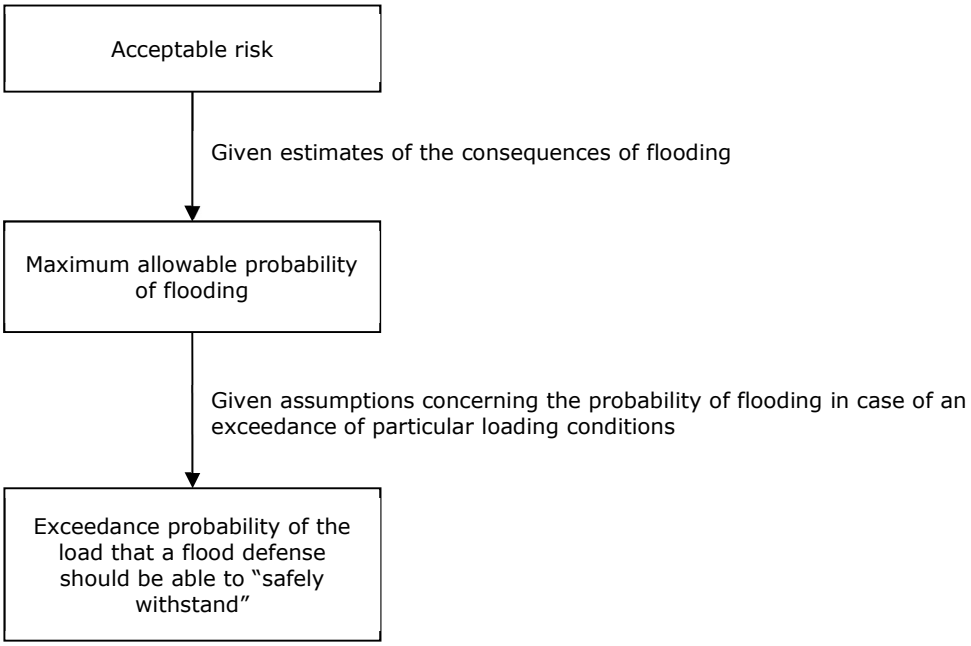

Figure 2. From acceptable risk to probabilities of flooding and probabilities of exceedance (after Jongejan and Calle, 2013).

1.2.2 Institutional context

Most primary flood defenses are managed by water boards. These are the oldest democratic institutions in the Netherlands. Rijkswaterstaat, the executive branch of the Ministry of Infrastructure and the Environment, manages the other primary flood defenses, such as the Eastern Scheldt and Maeslant storm surge barriers. Rijkswaterstaat is also charged with managing the main rivers and maintaining the coastline through periodic renourishments.

The Water Act (in Dutch: "Waterwet") defines the roles, responsibilities and procedures related to, amongst other, periodic safety assessments, coastal zone management, river basin management and the funding of restoration projects. The Water Act also specifies which flood defenses are primary flood defenses and lays down the standards that these flood defenses have to comply with.

The primary flood defenses are periodically tested against the flood protection standards from the Water Act using a set of tools and guidelines provided by the Minister (see e.g. Slomp et al. 2016). Such an official set of tools and guidelines is called a WBI.[1] In principle, every flood defense that fails a safety assessment has to be strengthened. Restoration projects by water boards are subsidized by the national government (50%) and the other water boards (40%), leaving an individual contribution of 10%. This arrangement is overseen by the National Flood Protection Programme (Dutch acronym: HWBP).

In contrast to the official tools and guidelines for safety assessments, the Dutch tools and guidelines for the design of primary flood defenses are not legally binding. In practice, however, they are often strictly followed. This is because they are used by the National Flood Protection Programme for evaluating subsidy applications. The tools and guidelines for design purposes and safety assessments are closely related: flood defenses are essentially designed in such a manner that they will pass future safety assessments for a given period of time.

1.2.3 The WBI2017

To be able to assess whether the primary flood defenses comply with the new flood protection standards, a new set of tools and guidelines for safety assessments had to be developed: the WBI2017. The WBI2017 consists of a Ministerial Order (Ministry of Infrastructure and the Environment, 2016d) with three appendices:

1. Appendix 1: procedural and reporting rules (Ministry of Infrastructure and the Environment, 2016a),
2. Appendix 2: rules for deriving hydraulic loads (Ministry of Infrastructure and the Environment, 2016b),
3. Appendix 3 rules for assessing the strength and reliability of primary flood defenses (Ministry of Infrastructure and the Environment, 2016c).

Appendix 3 of the WBI2017 is similar to the former Safety Assessment Guideline for Primary Flood Defenses (in Dutch: Voorschrift Toetsen op Veiligheid Primaire Waterkeringen, VTV).

Various technical guidelines and software programs have been developed for supporting safety assessments. A notable example is Hydra-Ring, a probabilistic model that can be used for calculating design water levels, quantifying failure probabilities and combining the failure probabilities for different failure mechanisms and/or components. For further details, the reader is referred to the Hydra-Ring technical reference manual (Van Balen *et al.*, 2016).

This report summarizes the basis of the semi-probabilistic assessment rules of Appendix 3 of the WBI2017. These are rules that rest on a partial factor approach. They allow engineers to assess the failure probabilities of flood defenses without having to resort to probability calculus.

[1] The acronym "WBI" stands for "Wettelijk Beoordelingsinstrumentarium". Previously, WBIs were called WTIs. The acronym "WTI" stands for "Wettelijk Toetsinstrumentarium".

Besides semi-probabilistic rules, Appendix 3 of the WBI2017 also covers simple screening rules to quickly evaluate the relevance of particular failure mechanisms. Appendix 3 also refers to models for probabilistic assessments. An overview of the different types of assessments supported by the WBI2017 is given in Figure 3. For further details on the structure of the WBI2017, the reader is referred to the WBI2017 basis document (De Waal, 2016; in Dutch).

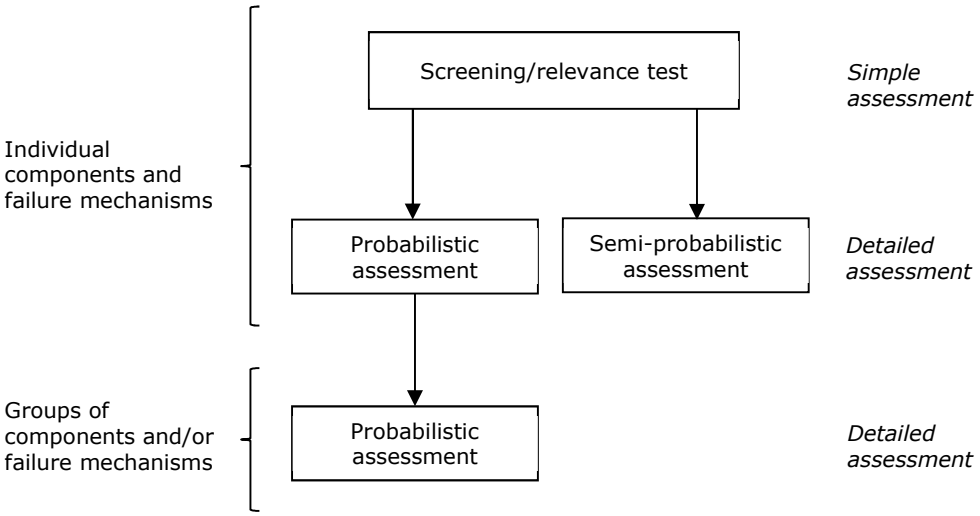

Figure 3. Types of assessments. The names of the different types of assessments are given in italics.

1.3 Semi-probabilistic assessment rules

1.3.1 Code calibration

While Dutch hydraulic engineers were among the first to use probabilistic methods in the design of flood defenses, most notably the Eastern Scheldt barrier (1976-1986) and the Maeslant barrier (1991-1997) (Vrijling, 2001), most engineers are still unfamiliar with probabilistic techniques. This is why semi-probabilistic rules have been developed that can be used alongside, or instead of, such techniques.

Probabilistic and semi-probabilistic approaches are closely related. A semi-probabilistic approach, or partial factor approach, is essentially an indirect, approximate approach to assessing probabilities of failure. To ensure consistency between probabilistic and semi-probabilistic assessments, the safety factors in the existing codes had to be (re)calibrated. This is because the former rules were often based on experience and engineering judgment rather than probabilistic analyses. An explicit link between safety factors and some reliability requirement was often missing.

A standardized code calibration procedure was developed for reasons of efficiency, transparency and consistency across failure mechanisms. This procedure draws upon decades of research and development in this field. The concept of probability based partial factor methods dates back to the 1960s and 1970s (Lind, 1971; CIRIA, 1977; Bazzurro and Cornell, 2004), with early applications to bridge codes in the United States and Canada (Nowak and Lind, 1979) and codes for steel structures (Ravindra and Galambos, 1978). Nowadays, probability based partial factor methods are widely used, with numerous applications in structural and

geotechnical design (e.g. Allen, Nowak and Bathurst, 2005; National Research Council, 2007; Arnold *et al.*, 2013). The Eurocodes are a notable example. These standardized European rules rest on a partial factor approach with an explicit reference to target reliabilities (JCSS, 2001; EN1990, 2002; Faber and Sørensen, 2002).

A novel element in the WBI2017 code calibration procedure and the WBI2017 as a whole concerns the linking of component-level target reliabilities for individual failure mechanisms to system-level requirements. The WBI2017 is among the first set of tools and guidelines for assessments of flood defenses to do so in a systematic manner. Since major levee systems are essentially series systems with little to no redundancy, the distinction between system and component reliabilities is of critical importance for flood defenses.

1.3.2 Semi-probabilistic assessment rules in the WBI2017

Code calibration studies have been carried out for the following failure mechanisms within the context of the development of the WBI2017:

1. internal erosion (uplift, heave and piping),
2. slope instability (macro instability),
3. dune erosion,
4. block revetment failure caused by wave impacts,
5. asphalt revetment failure caused by wave impacts,
6. grass revetment failure caused by wave impacts,
7. grass revetment failure caused by wave run-up.

Assessments for other failure mechanisms will be carried using probabilistic methods or old (uncalibrated) deterministic rules. In future, these deterministic rules will be replaced by probabilistic models or semi-probabilistic assessment rules.

1.4 Report outline

The structure of this report is as follows. Chapter 2 discusses the theoretical foundations of the semi-probabilistic approach, including its link with a fully probabilistic approach. An overview of the WBI2017 code calibration procedure is given in chapter 3. The different steps within this procedure are discussed in greater detail in chapters 4 to 6. Chapters 7 to 13 then present the code calibrated semi-probabilistic assessment rules for the failure mechanisms listed in section 1.3.2. Concluding remarks are given in chapter 14.

1.5 Target audience

This report has been written for practitioners that are familiar with statistics and levee safety assessments. Chapter 2 gives an introduction to (semi-)probabilistic design. For further background on e.g. probability theory and probabilistic design, readers are referred to books on probabilistic reliability analysis (e.g. Bedford & Cooke 2001) or reports such as CUR-publication 190 (CUR, 2002) and the WBI2017 report on the handling of uncertainty in safety assessments (Diermanse, 2017).

2 Semi-probabilistic assessment rules

2.1 Basic concepts in reliability engineering

A flood defense fails when load exceeds resistance.[2] In practice, both load and resistance are uncertain. This uncertainty may arise from natural variability (aleatory uncertainty) or lack of knowledge (epistemic uncertainty) (e.g. Winkler, 1996; Bedford and Cooke, 2001; Der Kiureghian and Ditlevsen, 2009; Diermanse, 2017). The uncertainty related to extreme loads is often largely due to natural variability. The uncertainty related to the resistance of a flood defense against, for instance, piping, arises from to the spatial variability of soil properties, combined with a limited number of measurements and measurement uncertainties. Also, models may produce outputs that differ from reality, giving rise to model uncertainty. In probabilistic and semi-probabilistic assessments of flood defenses in the Netherlands, all uncertainties are treated similarly. No distinctions are made between aleatory and epistemic uncertainties (ENW, 2017).

The probability of failure of a flood defense equals the probability that the uncertain load exceeds the uncertain resistance:

$$P(F) = P(S>R) \quad (1)$$

Where
P(·) Probability
F Failure
R Resistance
S Load

A limit state function, or failure function, is an indicator function that returns a negative value in case of failure:

$$P(F) = P(S>R) = P(Z<0) \quad (2)$$

Where
Z Limit state function (e.g. Z=R-S or Z=1–S/R)

There are various techniques for calculating failure probabilities, such as numerical integration and Monte Carlo simulation. The First Order Reliability Method (FORM) is an efficient, approximate method for calculating failure probabilities (Rackwitz, 2001). This method is discussed in greater detail below because several important concepts in reliability engineering are related to FORM, such as design points, influence coefficients and reliability indices. For further details, the reader is referred to CUR-publication 190 (CUR, 2002).

In a FORM-analysis, the limit state function is normalized and linearized at the design point. The design point is the combination of parameter values on the failure surface (Z=0) with the highest probability density. This is shown schematically in Figure 4. The plus and minus signs are such that the influence coefficient is negative for a load variable and positive for a resistance variable, in line with convention.

[2] The terms load and demand are treated as synonyms throughout this report. The same applies to the terms resistance and capacity.

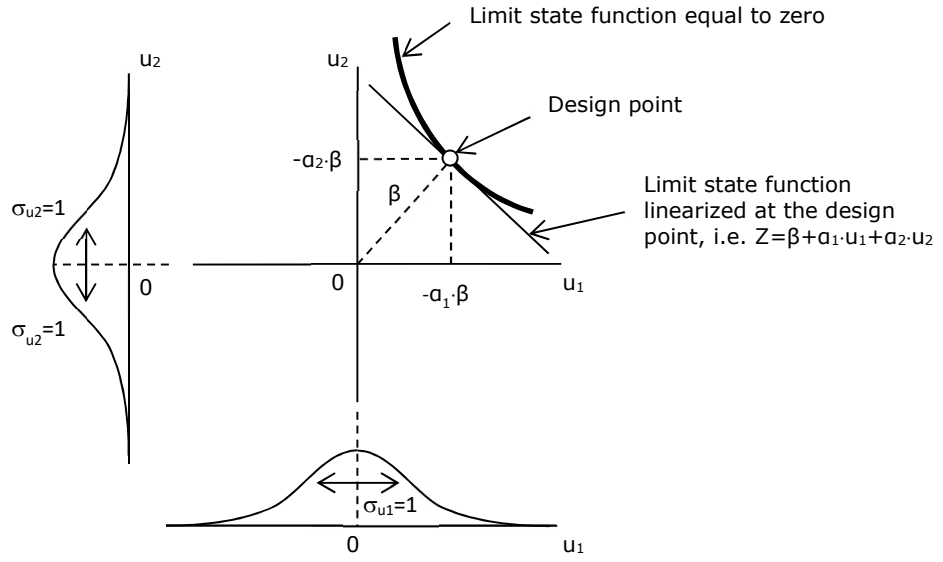

Figure 4. Two standard normally distributed variables, a non-linear limit state function and a linearized limit state function at the design point.

The linearized and normalized limit state function has the following functional form:

$$Z = \beta + \Sigma(\alpha_i \cdot u_i) \qquad \text{with} \qquad \Sigma\alpha_i^2=1 \tag{3}$$

Where

β Reliability index (Hasofer and Lind, 1974)

α_i Influence coefficient for stochastic variable X_i

u_i Independent, standard normally distributed variable (mean equal to 0 and standard deviation equal to 1)

The variance of the linearized and normalized limit state function is equal to the sum of the variances of the independent variables u_i weighted with their squared influence coefficients:

$$\sigma_Z^2 = \Sigma(\alpha_i \cdot \sigma_i)^2 = \Sigma(\alpha_i^2 \cdot 1) = \Sigma(\alpha_i^2) \tag{4}$$

Where

σ_Z Standard deviation of Z (note: σ_Z^2 is the variance of Z)

σ_i Standard deviation of standard normally distributed variable u_i (note: $\sigma_i=1$)

Since the sum of the squared influence coefficients is equal to one, the limit state function given by equation (3) is also normally distributed with a standard deviation equal to one. Since the means of the independent stochastic variables u_i are all equal to zero, the expected value of the limit state function given by equation (3) is equal to β.

The probability density function of the linearized and normalized limit state function is shown schematically in Figure 5. The probability that this limit state function is smaller is zero, indicating failure, is given by the hatched area.

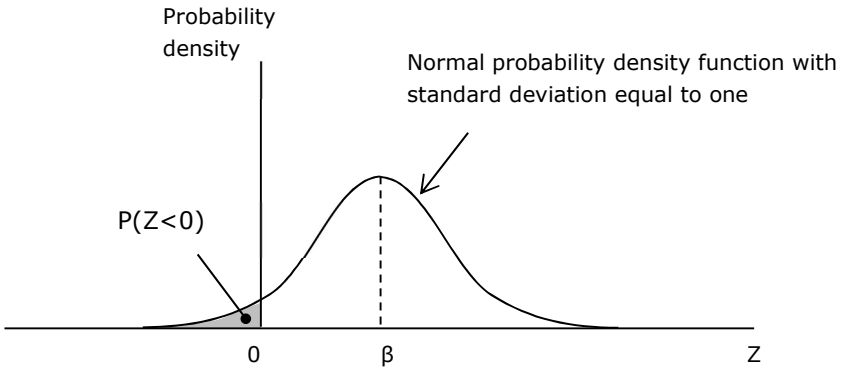

Figure 5. A normally distributed limit state function with a standard deviation equal to one and an expected value equal to β.

The absolute value of the influence coefficient of a stochastic variable is a measure of the relative importance of the uncertainty related to that stochastic variable. The squared value of an influence coefficient corresponds to the fraction of the variance of the linearized and normalized limit state function that can be attributed to a stochastic variable.

The relationship between the probability of failure and the reliability index is as follows, see also Figure 5:

$$P(F) = P(Z<0) \tag{5}$$

$$P(F) = P(\beta+u<0) \tag{6}$$

$$P(F) = P(u<-\beta) \tag{7}$$

This probability equals:

$$P(F) = \Phi(-\beta) \tag{8}$$

Where
$\Phi(\cdot)$ Standard normal distribution function (cdf)
β Reliability index
u Standard normally distributed variable

Because of the symmetry of u, equation (7) is equivalent to:

$$P(F) = P(u>\beta) \tag{9}$$

So that equation (8) is equivalent to:

$$P(F) = 1-\Phi(\beta) \tag{10}$$

Both expressions (8) and (10) are commonly used. The relationship between the reliability index and the probability of failure is shown in Figure 6.

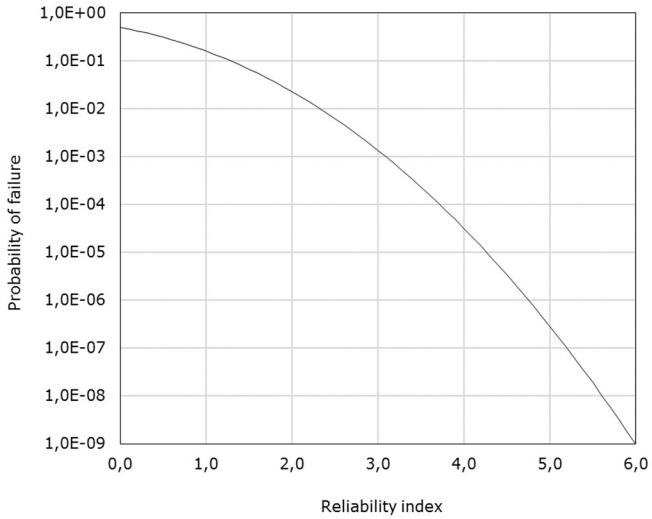

Figure 6. Probability of failure versus reliability index.

Generally, a FORM-analysis yields a close approximation of the probability of failure. FORM is exact when the limit state function is linear and all stochastic variables are independent and normally distributed.

2.2 The relations between probabilistic and semi-probabilistic assessments

Probabilistic and semi-probabilistic safety assessments are closely related. Both rely on the same reliability requirements, the same limit state functions and the same probability distributions of the stochastic variables. The only difference lies in the fact that a semi-probabilistic approach rests on a number of simplifications and approximations, giving it the appearance of a deterministic procedure.

In probabilistic safety assessments, engineers consider the probability that the ultimate limit state is exceeded, i.e. that load (S) exceeds resistance (R). The failure probability, P(S>R), should not exceed some maximum allowable or target failure probability (P_T).

In semi-probabilistic assessments, analysts consider the difference between the design values of load (S_d) and strength (R_d): S_d should not exceed R_d. Design values are representative values such as 5^{th} or 95^{th} quantile values or 1/1,000 yr^{-1} water levels, factored with partial safety factors, see equations (11) and (12). Note that the definitions from the Eurocodes are adopted here, similar terms may have different meanings in other codes. Design values are calculated as follows:

$$S_d = S_{rep} \cdot \gamma_S \quad (11)$$

$$R_d = R_{rep} / \gamma_R \quad (12)$$

Where
S_d Design value of the uncertain load
S_{rep} Representative value of the uncertain load
γ_S Partial safety factor for the uncertain load
R_d Design value of the uncertain resistance
R_{rep} Representative value of the uncertain resistance
γ_R Partial safety factor the uncertain resistance

Design values, and hence (partial) safety factors, should be defined in such a manner that $S_d \leq R_d$ when the structure complies with the reliability requirement, i.e. $P(S>R) \leq P_T$. The relationship between probabilistic and semi-probability safety assessments is shown schematically in Figure 7.

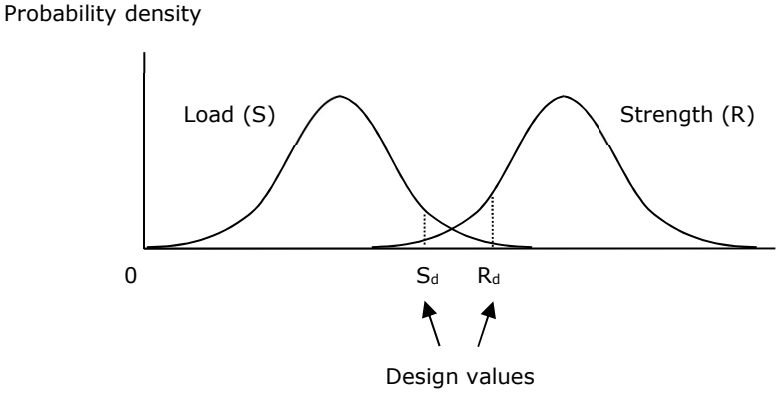

Fully probabilistic assessment: evaluate whether $P(R<S) \leq P_T$
Semi-probabilistic assessment: evaluate whether $S_d \leq R_d$

Figure 7. The probability density functions of load (S) and strength (R), and the design values of load (S_d) and strength (R_d).

A close relationship between probabilistic and semi-probabilistic assessments can be obtained by equating the design values of the different stochastic variables to their design point values, for structures that just comply with the reliability requirement.

Design points values can be obtained from FORM-analyses, see section 2.1. The value of a stochastic variable at the design point depends on:

1. its distribution,
2. its FORM-influence coefficient and
3. the reliability index.

For a structure that just complies with the reliability requirement, so that $\beta = \beta_T$, the design point value of a stochastic variable is given by the following expression:

$$X_d = F_X^{-1}(\Phi(-\alpha_X \cdot \beta_T)) \quad (13)$$

or, equivalently:

$$X_d = F_X^{-1}(1-\Phi(\alpha_X \cdot \beta_T)) \quad (14)$$

Where

$F_X^{-1}(\cdot)$ Inverse of the cumulative distribution function of stochastic variable X
X_d Design value of stochastic variable X
$\Phi(\cdot)$ Standard normal distribution function
β_T Target reliability index
α_X Influence coefficient for stochastic variable X ($\alpha_X \geq 0$ for resistance parameters and $\alpha_X \leq 0$ for load parameters)

The above is illustrated in Figure 8.

FORM-analysis

Example for a non-linear limit state function with two stochastic variables, X_1 and X_2. These variables have been transformed into standard normal variables U_1 and U_2.

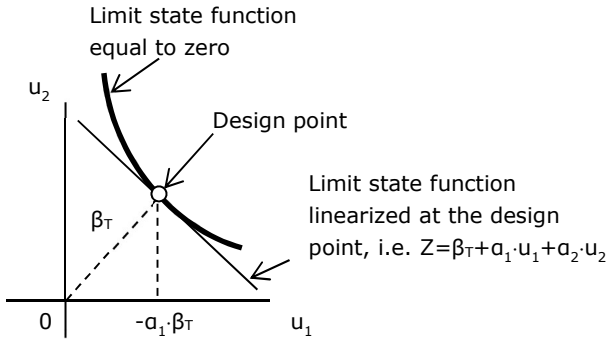

Probability density function of u_1

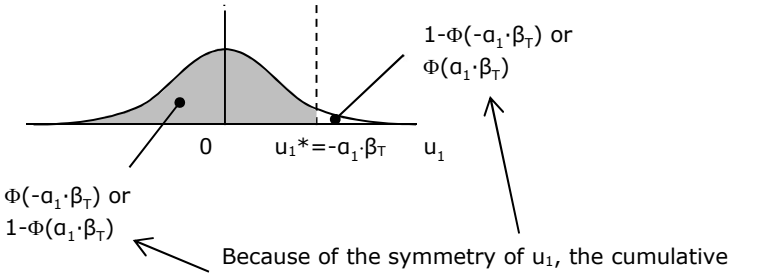

Because of the symmetry of u_1, the cumulative probability of u_1* is equal to the exceedance probability of $-u_1$*, i.e. $\Phi(u_1^*)$ is equal to $1-\Phi(-u_1^*)$ and $\Phi(-\alpha_1 \cdot \beta_T)$ is equal to $1-\Phi(\alpha_1 \cdot \beta_T)$.

Probability density function of X_1

The cumulative probability of $X_{1,d}$ equals the cumulative probability of u_1*.

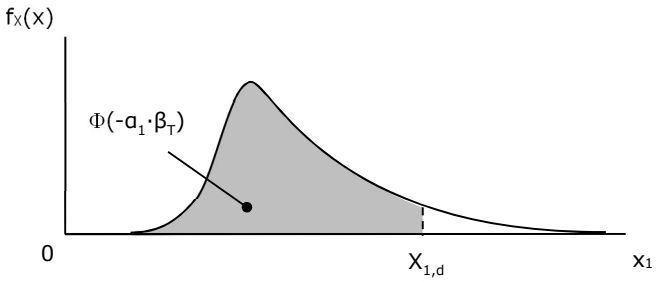

Cumulative distribution function of X_1

The cumulative probability of $X_{1,d}$ equals the cumulative probability of u_1*

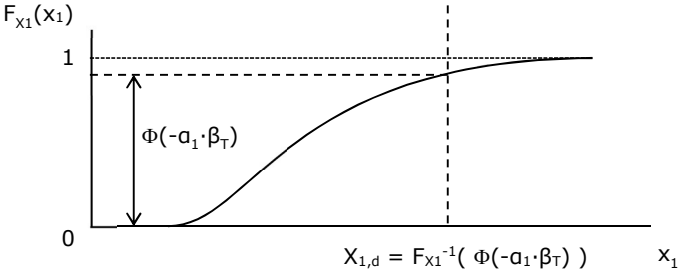

Figure 8. From FORM influence coefficient and target reliability index to design point value. The plus and minus signs are such that the influence coefficient is negative for a load variable and positive for a resistance variable, in line with convention.

For a normally distributed stochastic variable, equation (13) yields:

$$X_d = \mu_X - \alpha_X \cdot \beta_T \cdot \sigma_X \qquad (15)$$

Where
μ_X Mean value of the normally distributed variable X
σ_X Standard deviation of the normally distributed variable X

For a lognormally distributed stochastic variable, equation (13) yields:

$$X_d = \exp\{ -\alpha_X \cdot \beta_T \cdot (\ln(1+v_X^2))^{1/2} \} \qquad (16)$$

Where
v_X Coefficient of variation of the lognormally distributed variable X

Representative values of resistance parameters are often 5% quantile values. Figure 9 shows which combinations of squared influence coefficients (α_x^2) and target reliability indices (β_T) then lead to a partial factor greater than 1 ($R_d<R_{rep}$) or smaller than 1 ($R_d>R_{rep}$). The dividing line between the two is independent of the distribution of R. For a load variable with a representative value equal to its 95% quantile value, the dividing line is identical to the line in Figure 9.

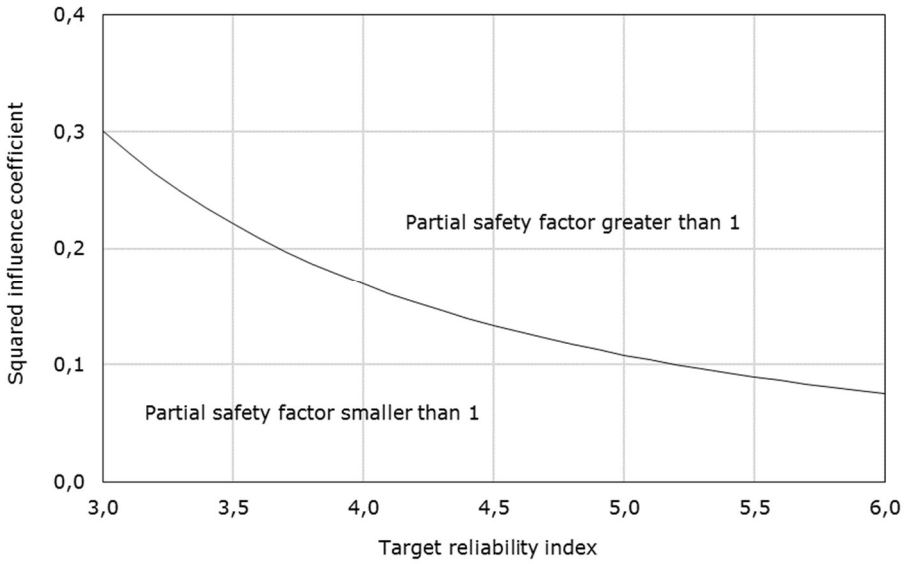

Figure 9. The dividing line between partial safety factors that are greater than or smaller than 1.0 for a representative value of a resistance parameter equal to its 5% quantile value or a representative value of a load parameter equal to its 95% quantile value.

A numerical example illustrating the link between reliability indices, influence coefficients, design values, representative values and partial factors is given below.

Numerical example
Consider the resistance of a gravity dam against sliding. The horizontal force (S) on the dam and the resistance of the dam against sliding (R) are uncertain. Note that this hypothetical case study has been greatly simplified for illustrative purposes.

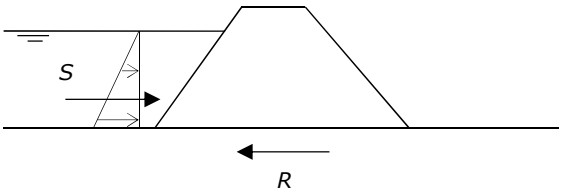

The resistance of the dam against sliding (R) is normally distributed with μ_R=1000 kN/m and σ_R=100kN/m. The annual maxima of the load (S) are normally distributed with μ_S=500 kN/m and σ_S=100 kN/m (note: if the horizontal force acting on the gravity dam is normally distributed, the water level obviously is not). The limit state function is:

$$Z = R - S$$

Since R and S are both normally distributed, this limit state function is also normally distributed, with $\mu_Z = \mu_R - \mu_S$ = 1000-500 = 500 kN/m and $\sigma_Z = (\sigma_R^2+\sigma_S^2)^{1/2} = (100^2+100^2)^{1/2}$ = 141 kN/m. The failure probability, i.e. the probability that the limit state function Z is smaller than zero, equals $\Phi(-\mu_Z/\sigma_Z) = \Phi(-3.53) = 2.03.10^{-4}$ per year.

The result of a FORM-analysis would be:

- *Reliability index: β = 3.53*
- *Influence coefficients: $\alpha_R^2 = \alpha_S^2 = 0.5$, or $\alpha_R = 0.707$ and $\alpha_S = -0.707$*
- *Design point values:*
    - *$P(S<S_d) = \Phi(-\alpha_S \cdot \beta) = \Phi(-(-0.707)\cdot 3.53) = \Phi(2.5) = 0.9938$ per year, so that S_d=750kN/m. Note that the exceedance probability $P(S>S_d)$ equals 1-0.9938 = 0.0062 per year.*
    - *$P(R<R_d)=\Phi(-\alpha_R \cdot \beta)=\Phi(-0.707\cdot 3.53)=\Phi(-2.5)=0.0062$, so that R_d=750kN/m.*

  Note that R_d and S_d have to be the same, since Z=0 at the design point.

The design values S_d and R_d could be defined by an exceedance probability of 0.0062 per year and a cumulative probability of 0.0062. The design values could also be split into representative values and partial factors.

If S_{rep} were a load with an exceedance probability of 1% per year and R_{rep} a resistance with a cumulative probability of 5%, the partial load and resistance factors would be as follows:

$\gamma_S = S_d / S_{rep} = 750 / 733 = 1.02$
$\gamma_R = R_{Rep} / R_d = 836 / 750 = 1.11$

Partial factors could be derived along similar lines for more complex limit state functions, with more numerous and not normally distributed stochastic variables.

For simplicity, it has so far been assumed that load and resistance are not themselves functions of different stochastic variables. In case they are, equations (11) and (12) may be rewritten to:

$$S_d = f(S_{1,d} , S_{2,d} , \dots , S_{n,d}) \quad (17)$$

$$R_d = f(R_{1,d} , R_{2,d} , \dots , R_{n,d}) \quad (18)$$

or:

$$S_d = f(S_{1,rep} \cdot \gamma_{S1} , S_{2,rep} \cdot \gamma_{S2}, \dots , S_{n,rep} \cdot \gamma_{Sn}) \quad (19)$$

$$R_d = f(R_{1,rep} / \gamma_{R1} , R_{2,rep} / \gamma_{R2}, \dots , R_{n,rep} / \gamma_{Rn}) \quad (20)$$

According to equations (19) and (20), the number of partial factors equals the number of stochastic variables. It is often practical to limit the number of partial factors. This can be done by combining different partial factors into a single safety factor or by introducing an overall safety factor, e.g.:

$$S_d = \gamma_S \cdot f(S_{1,rep}, S_{2,rep} , \dots , S_{n,rep}) \quad (21)$$

$$R_d = f(R_{1,rep}, R_{2,rep}, \dots , R_{n,rep}) / \gamma_R \quad (22)$$

A complicating factor when defining appropriate design values is that the influence coefficient of a stochastic variable typically varies from case to case. This is because the relative importance of the uncertainty related to a stochastic variable may depend on local circumstances. This also means that design values, and hence partial safety factors, should ideally be different for each case. This gives rise to a tradeoff between simplicity and accuracy: partial safety factors that are broadly applicable may sometimes be too conservative. Differentiating between groups of cases may improve the accuracy of semi-probabilistic assessments, but it may also complicate assessments and lead to confusion and error. The broad applicability of partial factors can be verified by comparing the results of probabilistic and semi-probabilistic assessments for a wide range of conditions.

3 Code calibration procedure

The objective of a code calibration study is to define design values (representative values and partial safety factors) in such a manner that semi-probabilistic and probabilistic verifications give broadly similar results. This is why the WBI2017 code calibration procedure revolves around comparisons between probabilistic assessments and assessments with partial safety factors.

A summary of the WBI2017 calibration procedure is given below. The first three steps in the calibration procedure will be discussed in greater detail in the following chapters.

1 Establish the reliability requirement. For each failure mechanism, a reliability requirement has to be derived from the standard of protection. From this requirement, a cross-sectional reliability requirement has to be derived, taking into account the length-effect.[3]

2 Establish the safety or code format. This step comprises the following:
- 2.1 Establish a test set that covers a wide range of cases. The test set members are real-life or hypothetical cross-sections of flood defenses. Their reliabilities should be broadly consistent with the cross-sectional reliability requirements from step 1.
- 2.2 Calculate influence coefficients for each test set member.
- 2.3 Based on the outcomes of the calculated influence coefficients and practical considerations, define representative values and decide on the safety factors that are to be included in the semi-probabilistic assessment rule.

3 Establish the numerical values of the safety factors. This step comprises the following:
- 3.1 Establish the values of all but one safety factor, on the basis of the calculated influence coefficients and a specific target reliability index. These safety factors will be called β_T-invariant safety factors because they do not depend on the reliability requirement from step 1 (the symbol β_T stands for a target reliability index).
- 3.2 For a range of values of the remaining (β_T-dependent) safety factor or design value: change the strength of each test set member (e.g. by changing its dimensions) such that $R_d=S_d$. When this condition is fulfilled, each (modified) test set member would just pass a semi-probabilistic assessment. Alternatively, calculate the values of the β_T-dependent safety factors or design values for which $R_d=S_d$.
- 3.3 Calculate the probability of failure of each (modified) test set member. The objective of this step is to establish a relationship between the value of the β_T-dependent safety factor and the probability of failure for each test set member.
- 3.4 Select sufficiently safe β_T-dependent safety factors.

4 Compare the calibrated semi-probabilistic assessment rule to previous assessments rules. Differences should be understood.

[3] Note that in many WBI2017-calibration reports, the length effect is considered in step 3.4, when safety factors are defined for a range of cross-sectional reliability requirements.

An overview of the calibration procedure is given in Figure 10.

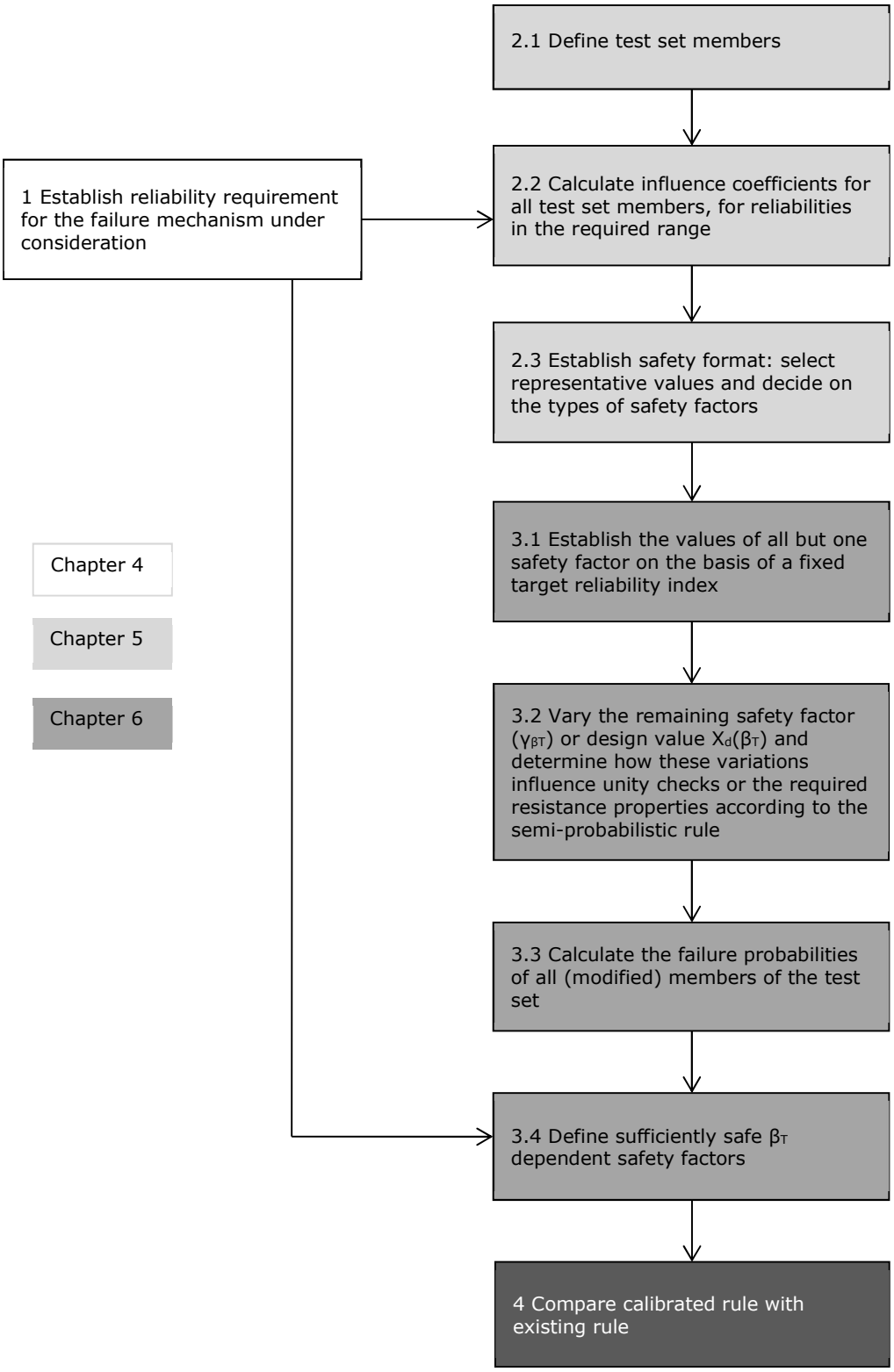

Figure 10. Schematic overview of the calibration procedure.

4 Step 1: Establish reliability requirements

This chapter discusses the derivation of the reliability requirements that are needed for calibration purposes. It starts with maximum allowable probabilities of flooding for segments, then moves to reliability requirements for individual failure mechanisms and ends with cross-sectional reliability requirements for individual failure mechanisms.

4.1 Failure mechanisms, segments, sections and cross-sections

The Dutch flood protection standards are defined in terms of maximum allowable probabilities of flooding[4]. These standards apply to segments (in Dutch: "trajecten"), as defined by the Water Act. Segments range from about 5 to 40 kilometers in length. The maximum allowable probabilities of flooding range from 1/100 per year to 1/100,000 per year.

The failure of a segment (failure = flooding) can be caused by numerous failure mechanisms, see Figure 11. The probability that a failure mechanism manifests itself somewhere within a segment is typically greater than the probability that it manifests itself at a particular location.

Sections are defined here as continuous lengths in which load and resistance properties are statistically homogeneous. Sections could be dikes, structures or dunes. The term "cross-sectional length" is used here to refer to a length in which the spatial variability of demand and capacity along the dike can be ignored when evaluating a limit state function.[5] Segments may consist of numerous sections, and sections of numerous cross-sectional lengths, see also Figure 12.

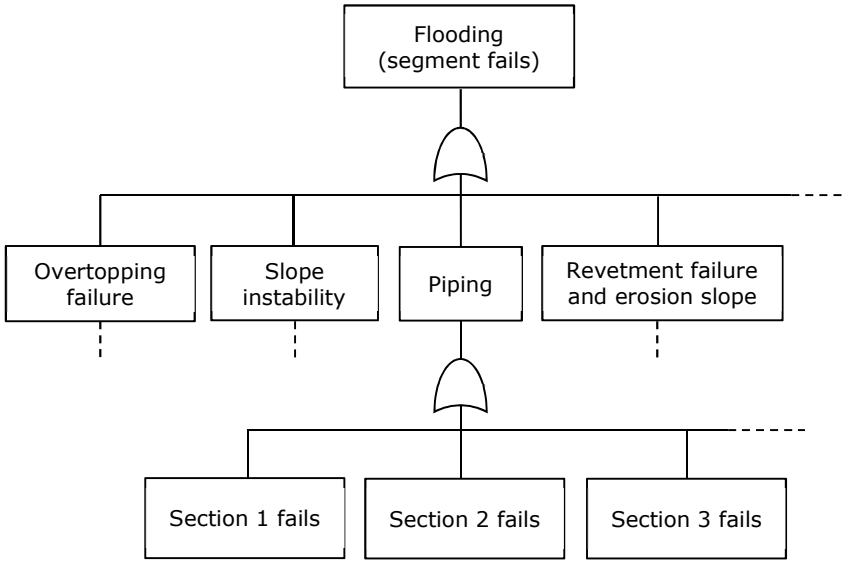

Figure 11. Fault tree for a segment.

[4] The Water Act also gives signal values. For calibration purposes, this distinction is irrelevant.
[5] Demand and capacity may concern point values or spatial averages.

When engineers evaluate the reliability of e.g. a dike section using a semi-probabilistic method, they typically carry out a two-dimensional analysis for a cross-section that is deemed representative for all other cross-sections within that dike section. This explains why partial safety factors ultimately rest on cross-sectional, not sectional, target reliabilities.

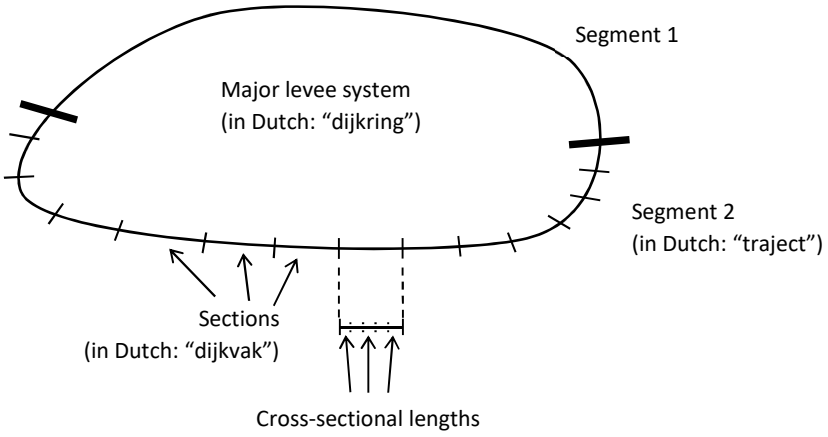

Figure 12. Major levee system, segments, sections and cross-sections.

Note that different terms and definitions can be found in literature for similar concepts. For instance, according to a USACE guideline (USACE, 2013: I-5): "A levee reach is defined for the purpose of risk analysis as a continuous length of levee exhibiting homogeneity of construction, geotechnical conditions, hydrologic and hydraulic loading conditions, consequences of failure, and possibly other features relevant to performance and risk". The main differences with a "section", as defined above, concerns the fact that only features related to performance are considered here and that a "section" could also be a dune or a structure.

4.2 Reliability requirements per failure mechanism

For calibrating a semi-probabilistic assessment rule for a particular failure mechanism, a reliability requirement for that failure mechanism is needed. The combined probabilities of the different failure mechanisms should not exceed the maximum allowable probability of flooding. To ensure that this requirement is met, the reliability requirements for the failure mechanisms should be defined in such a manner that their combined probability of failure cannot exceed the maximum allowable probability of flooding. This will certainly be the case when the sum of the maximum allowable failure probabilities per failure mechanism equals the maximum allowable probability of flooding.[6] This is shown schematically in Figure 13.

[6] In WBI2017-software, these percentages add up to 105%. This is because the reliability requirements for failures of block, grass and asphalt revetments are presented separately in the WBI2017 and have been summed up. The combined failure probability of different types of revetments is assumed to be smaller than the sum of the failure probabilities per revetment type, however.

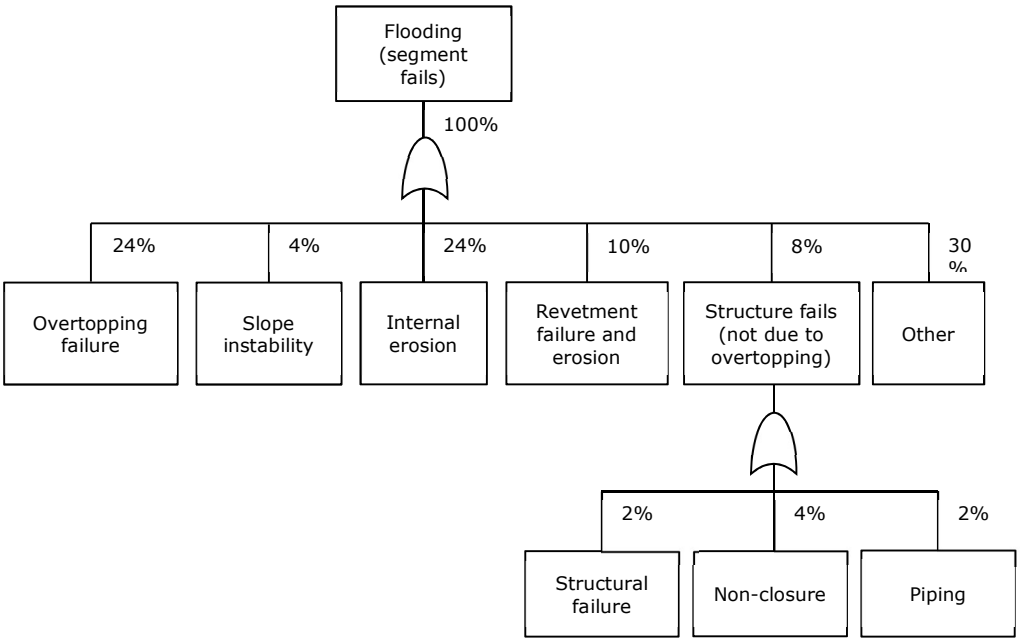

Figure 13. Fault tree with different failure mechanisms. The percentages add up to 100%.

Table 1 shows the default failure probability budgets for segments that consist of dunes and segments that mostly consist of levees. The percentages in Table 1 are based on the expected relative importance of the different failure mechanisms. These expectations are based on VNK2-data as well as a number of expert sessions with representatives of research institutes (TNO, Deltares, Delft University of Technology), engineering consultancies, water boards and Rijkswaterstaat.

Table 1. Maximum allowable failure probabilities per failure mechanism, defined as a percentage of the maximum allowable probability of flooding.

Type of flood defense	**Failure mechanism**	**Type of segment**	
		Sandy coast	**Other (levees)**
Levee and structure	Overtopping	0%	24%
Levee	Piping	0%	24%
	Macro instability of the inner slope	0%	4%
	Revetment failure and erosion	0%	10%
Structure	Non-closure	0%	4%
	Piping	0%	2%
	Structural failure	0%	2%
Dune	Dune erosion	70%	0% / 10%*
Other		30%	30 / 20%*
Total		**100%**	**100%**

* A few segments consist of a combination of levees and dunes. For those segments, the 30% for "other" may be reduced to 20%, to obtain 10% for dune erosion. This pragmatic choice avoids the need for a third failure probability budget.

The default failure probability budgets shown in Table 1 merely serve as a reference or starting point: they may be adapted to local circumstances. When the contributions of the different failure mechanisms to the probability of flooding differ strongly from the percentages shown in Table 1, holding on to these percentages

would lead to unnecessarily conservative requirements for some failure mechanisms (together with needlessly lenient requirements for other). This, in turn, could trigger unnecessary restoration projects. Note that the opposite, i.e. not noticing the need for a restoration project because of a mismatch between the failure probability budget and the actual relative importance of the different failure mechanisms, is impossible. This is because the percentages in Table 1 add up to 100%: relatively lenient requirements for some failure mechanisms will always be associated with relatively stringent requirements for other failure mechanisms.

While the optimal failure probability budget is different for each segment, experience from design projects indicates that the default failure probability budgets are broadly reasonable. This is because changes in maximum allowable failure probabilities by e.g. a factor 2 are typically of little practical importance. Changing a maximum allowable probability of failure of e.g. 10^{-5} per year to 2.10^{-5} per year corresponds to a change in reliability indices of merely a factor 1.04. The associated change in design values will be even smaller. This means that the use of percentages that differ from the ones shown in Table 1 will yield broadly similar results, as long as they stay within the ranges shown in Table 2.

Table 2. The ranges that are obtained by changing the default percentages from Table 1 by about a factor 2.

Type of flood defense	**Failure mechanism**	**Type of segment**	
		Sandy coast	**Other (levees)**
Levee and structure	Overtopping	0%	10%-50%
Levee	Piping	0%	10%-50%
	Macro instability of the inner slope	0%	2%-10%
	Revetment failure and erosion	0%	5%-20%
Structure	Non-closure	0%	2%-10%
	Piping	0%	1%-5%
	Structural failure	0%	1%-5%
Dune	Dune erosion	35%-140%	0% / 5%-20%
Other		15-60%	15%-60% / 10%-40%

It is sometimes proposed to adopt relatively small percentages for failure mechanisms that can occur with relatively little warning, such as slope instability, to further reduce the risk of flooding. Doing so cannot be traced back to flood protection standards however: the Water Act only says that the combined probability of failure should be smaller than the maximum allowable probability of flooding. It says little about individual failure mechanisms.[7]

[7] The Water Act only gives separate reliability requirements for the closure operation of several storm surge barriers.

4.3 Cross-sectional reliability requirements per failure mechanism

4.3.1 *The length effect*

When the resistance against a particular failure mechanism is uncertain and spatially variable, it is uncertain (1) which spot is the weakest and (2) how weak this weakest spot is. This explains why people that inspect levees during high waters do not stand still: the probability that they observe a sign of weakness increases with every step they take. When the probability of a relatively weak spot increases with length, so does the probability of a breach. This phenomenon is known as the length effect (Figure 14). Note that the spatial variability of loading conditions can also lead to a length effect: the probability of observing a particular load *somewhere* can be higher than the probability of observing it *at any specific location*.

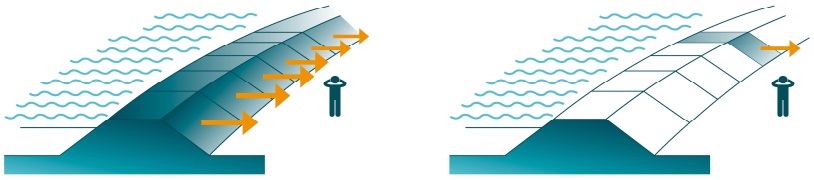

Figure 14. The length effect: the greater the number of cross-sections that could fail independently, the greater the probability of flooding.

Because of the length effect, a system level failure probability is not necessarily the same as the highest cross-sectional failure probability. Consequently, system-level and cross-sectional reliability requirements are not necessarily the same.

4.3.2 *From cross-sectional reliabilities to system reliability*

For a discussion about the way in which cross-sectional reliability requirements can be derived from system level requirements, it is instructive to start in the opposite direction, with a discussion of the way in which cross-sectional reliabilities relate to the reliability of a system as a whole. Only a single failure mechanism is considered here for reasons of simplicity.

Each segment can be thought of as a series system, consisting of numerous cross-sectional lengths (grouped into sections), see also Figure 12. The failure probability of such a series system equals:

$$P(F_{system}) = P(Z_1<0 \cup Z_2<0 \cup \ldots Z_n<0) \quad (23)$$

where
Z_i Limit state function for cross-sectional length i (i = 1..n)

The failure probability of a series system lies between the following bounds:

- Lower bound (perfectly correlated limit state functions):

$$P(F_{system}) = \max(P(Z_i)<0) \quad (24)$$

- Upper bound (independent limit state functions):

$$P(F_{system}) = 1 - \Pi_{i=1\ldots n}(1 - P(Z_i<0)) \quad (25)$$

For sufficiently small failure probabilities, the upper bound can be approximated by:

$$P(F_{system}) \approx \Sigma(P(Z_i<0)) \quad (26)$$

When the limit state functions of the different cross-sectional lengths are strongly correlated, the system failure probability tends to the lower bound. This is the case for e.g. overtopping failure. When the limit state functions are weakly correlated, the system failure probability tends to the upper bound. This is the case for e.g. geotechnical failure.

The difference between the upper and the lower bounds is strongly influenced by variations in cross-sectional failure probabilities. A single weak spot may strongly influence the reliability of a series system, regardless of spatial correlations.

For further details on the quantification of system failure probabilities, see Appendix A.

4.3.3 Length effect factors

As discussed in section 4.3.2, a system failure probability will be higher than the highest cross-sectional failure probability in case of imperfect spatial correlations. In such cases, the cross-sectional reliability requirement will have to be stricter than the system-level reliability requirement:

$$P_{T,cross} = P_T / N \qquad (\text{with } P_T = \omega \cdot P_{max}) \quad (27)$$

where

- $P_{T,cross}$ Cross-sectional target failure probability for the failure mechanism under consideration
- P_T Target failure probability for an entire segment for the failure mechanism under consideration
- N Length effect factor for the failure mechanism under consideration ($N \geq 1$)
- ω Fraction of the maximum allowable probability of flooding that has been reserved for the failure mechanism under consideration ($0<f\leq1$), see also Table 1
- P_{max} Maximum allowable probability of flooding or standard of protection

In theory, estimates of the length effect factor could be obtained from probabilistic analyses for entire segments (see Appendix A). A possible procedure, aimed at finding a cross-sectional requirement that minimizes the number of sections that have to be strengthened, is shown in Figure 15. In practice, the data for such probabilistic analyses is often missing, meaning that decisions have to be made on the basis of the available material and engineering judgment.

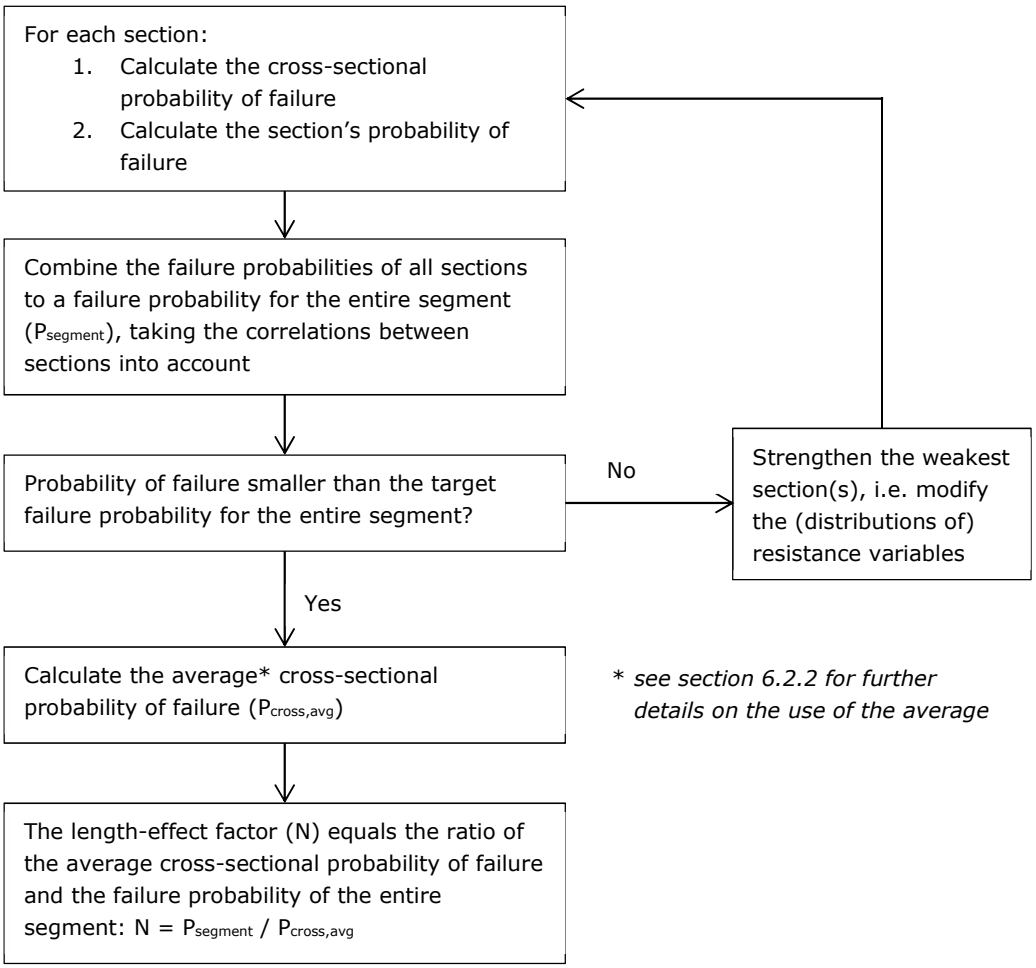

Figure 15. The derivation of a length-effect factor from probabilistic analyses for entire segments (also see Appendix A).

When the length effect depends strongly on the length of a segment rather than e.g. variations in the orientations of the different sections, the length effect factor (N) can be written as a function of:

1. the length of a segment (L),
2. the length of independent, equivalent stretches (b),
3. the fraction of the total length of the segment that should be taken into account in the calculation of the length-effect factor (a).

The following approximation could be used:

$$N = \max\{ a \cdot L / b , 1 \} \quad (28)$$

The parameters a and b describe a segment that consists of different sections in a simplified, equivalent manner, as shown in Figure 16. The failure probability of a segment is usually determined by a relatively short distance over which the probabilities of failure are relatively high, which is expressed by the a-value. Note that failure probabilities are usually plotted on a log-scale because they easily vary over several orders of magnitude.

Within the "critical length" (i.e. "a · L"), the effect of spatial correlation decay can be modelled by means of "independent equivalent lengths". This is reflected by the b-value.

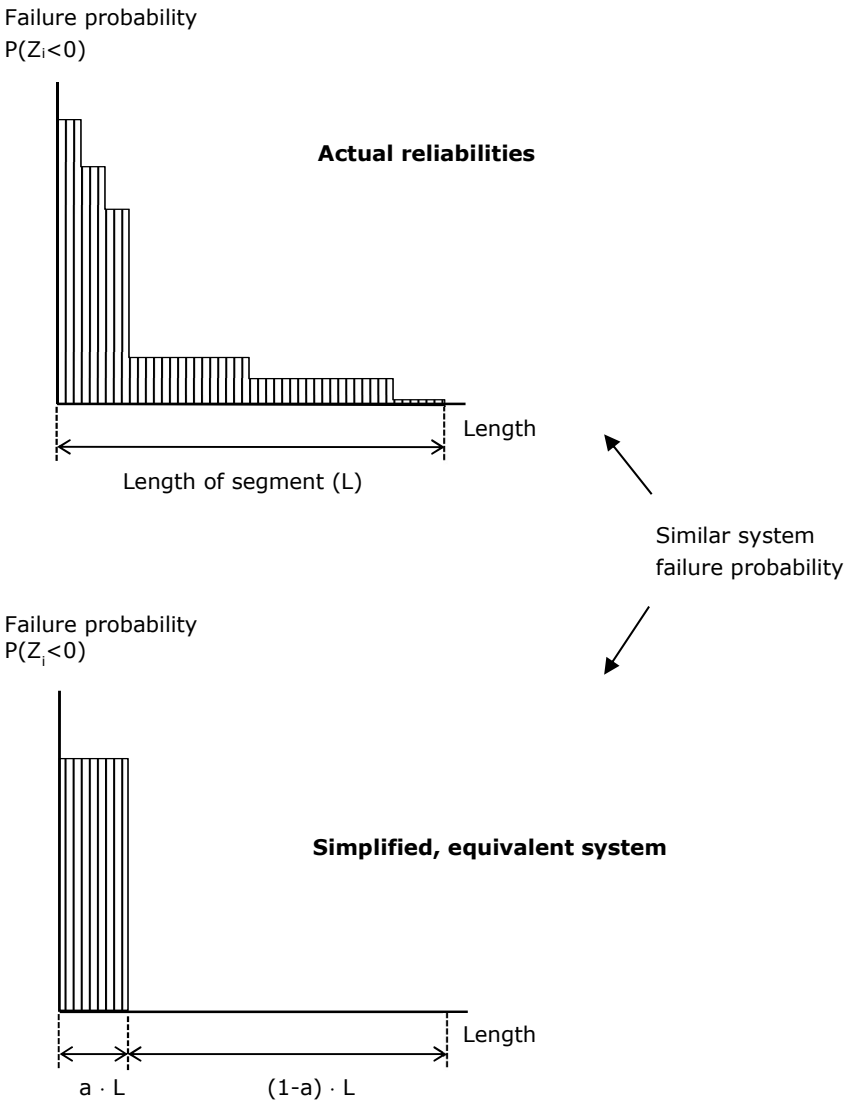

Figure 16. A simplified, equivalent way of describing a segment's reliability (the widths of the bars are independent equivalent lengths, or b-values).

As an approximation, equation (28) is commonly written as:

$$N = 1 + a \cdot L / b \tag{29}$$

Equation (29) has previously been used to define cross sectional reliability requirements for slope stability assessments (ENW, 2007a). It has been reused in the WBI2017 for slope stability and internal erosion.

5 Step 2: Establishing the safety format

A safety format or code format is the outline of a semi-probabilistic rule. It concerns the following:

1. the definitions of the representative values (e.g. a material property with a cumulative probability of 5% or 50%, or a water level with an exceedance probability of 1/1,000 per year),
2. the types of partial safety factors that are to be included in the semi-probabilistic assessment rule (e.g. model and material factors).

Once the safety format has been established, the values of the partial safety factors can be determined.

5.1 Analyzing design point values

As discussed in section 2.2, design values should ideally be based on design point values. An analysis of design point values can inform decisions pertaining to the definition of suitable representative values and the types of partial factors that should be introduced. If the design point value of a stochastic variable differs strongly from its average value, the use of a relatively unfavourable design value in semi-probabilistic assessments would be optimal. This can be achieved via a relatively unfavourable representative value, or via a relatively high partial safety factor.

The cumulative probability of a stochastic variable's design point value depends on the relative importance of the uncertainty related to this variable (its influence coefficient), and the target reliability index, see also equation (13) in section 2.2. This is shown schematically in Figure 17.

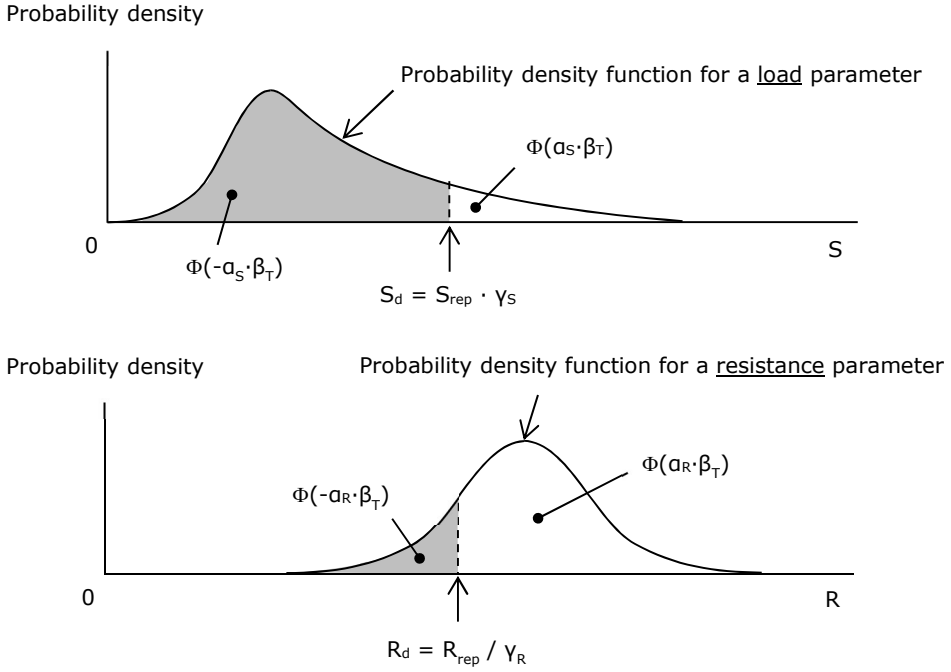

Figure 17. The relationship between an influence coefficients ($\alpha_{X)}$, target reliability index (β_T) and design values (X_d). A design value can be split into a partial factor (γ_X) and a representative value (X_{rep}).

Insight into influence coefficients and reliability indices can be obtained from FORM analyses for a broad range of cases, i.e. schematizations of real-life or hypothetical flood defenses that are considered representative for the area of application of the semi-probabilistic assessment rule. All possible conditions that could strongly influence the outcomes of probabilistic evaluations should be covered by the test set (e.g. different water systems or stratigraphies). Since relevant conditions vary per failure mechanism, a different test set has to be established for each failure mechanism.

5.2 Defining representative values

The representative value of a stochastic variable can be defined by a quantile value. For resistance variables this is often a 5%-quantile value or an average value. The choice of quantile typically rests on the following considerations:

1. Consistency with current practice: avoiding unnecessary changes helps to avoid confusion and error.
2. Representative values should be defined as uniformly as possible. The consistent use of 5% quantiles is preferable over the use of e.g. a 10% quantile for variable X_1, a 25% quantile for X_2, a 55% quantile for variable X_3 and so on.
3. Average values are relatively easy to calculate but their use is only advised when the relative importance of the uncertainty related to stochastic variables is small. Put differently, this is only advisable when the design point values obtained from probabilistic evaluations are close to average values.

For most failure mechanisms, it was decided to define the representative value of the hydraulic load by an exceedance probability that is equal to the maximum allowable probability of flooding. The only exceptions are dune erosion and the erosion of grass revetments on the outer slope. For these failure mechanisms, the design value of the hydraulic load is β_T-dependent and specified by a β_T-dependent exceedance probability.

The reasons for equating the exceedance probabilities of the representative loading conditions for most failure mechanisms to maximum allowable probabilities of flooding are purely pragmatic. In theory, these representative values could be defined by different quantiles. While this would be most accurate, it could easily lead to confusion and error. Defining these representative values by a single fixed quantile for all flood defenses and failure mechanisms would also have significant drawbacks. First, it would lead to highly variable safety factors since the standards range from 1/100 to 1/100,000 per year. Second, it would lead to more conservative semi-probabilistic assessment rules since the regional variations in e.g. water level distributions and physical maxima cannot accurately be dealt with by factoring representative hydraulic loads that are far from their design point values.

It is stressed that the meaning of the representative value of the water level differs from the meaning of the former normative water level (in Dutch: "maatgevend hoogwater"). The representative value of the water level is not "the" water level that a flood defense should be able to safely withstand. Note that the representative values of the hydraulic loads could also be defined by different quantiles/probabilities of exceedance. That would merely lead to different partial safety factors.

The design values of model uncertainty parameters are usually not split into representative values and partial factors. This is because their design values are typically constants. The design value of a model uncertainty parameter is commonly referred to as a model factor (a safety factor). This terminology formally implies a representative value equal to 1.

5.3 Defining representative values for spatial averages

It is important to note that some stochastic variables concern spatial averages. For instance, the block width is defined as the average width of blocks in an area of 1 m^2. Similarly, the undrained strength (s_u) that is to be used in limit equilibrium stability analyses is the local average of the spatially variable undrained strength. In both cases, the definition of the representative value relates to a quantile from the distribution of a spatial average, not the distribution of point values. The difference between a distribution of point values and the distribution of some spatial average of point values is illustrated by Figure 18.

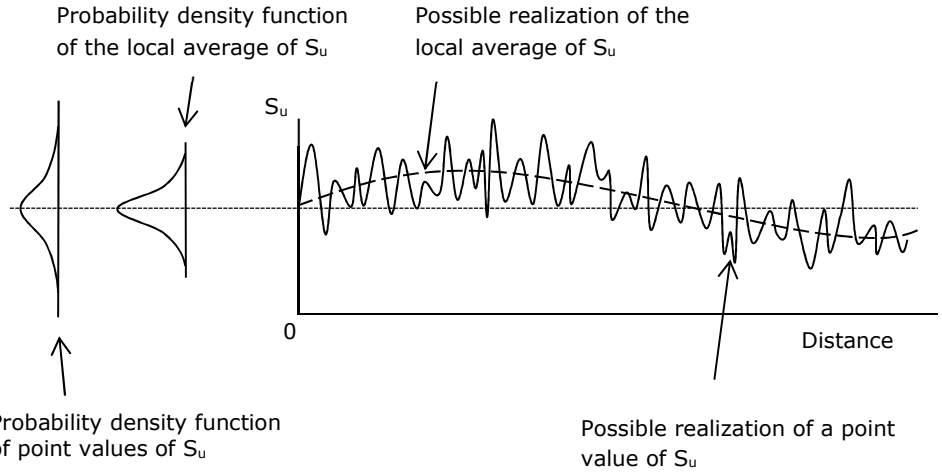

Figure 18. Illustration of the difference between the distribution of point values and the distribution of the local average of point values.

As an example, consider the distribution of the local average of the undrained shear strength. The standard deviation of this distribution follows from (after TAW 2001)[8]:

$$\sigma_{Su,avg} = s_{Su} \cdot \{ (1-\delta) + \delta \cdot \Omega^2 + 1 / n \}^{1/2} \qquad (30)$$

where

$\sigma_{Su,avg}$	Standard deviation of the local average of the undrained shear strength
s_{Su}	Standard deviation of measured undrained shear strength
δ	Fraction of the total variance that can be attributed to fluctuations of point values of the undrained shear strength relative to the local mean
Ω	Variance reduction factor; $0 \leq \Omega \leq 1$
n	Number of measurements

[8] The technical report deals with the local averages of the effective friction angle and the effective cohesion. The same procedures are used for undrained strength parameters in the WBI2017 (Ministry of Infrastructure and the Environment, 2016g).

The Dutch Technical Report on Geotechical Structures (TAW, 2001) assumes that all vertical fluctuations average out over a slip surface, i.e. $\Omega^2 = 0$. This is in line with a widely used assumption in geotechnical engineering that the (vertical) average of the shear strength of a deposit is a good indicator of the shear strength at that particular location.

When measurements originate from an area in which regional variations are unimportant (a local data set), δ is roughly equal to 1. The widely used value for regional data sets (δ = 0,75) stems from a Dutch design guideline for river dikes (TAW, 1989). This value was subsequently used in Appendix 2 of the Dutch Technical Report for Geotechical Structures (TAW, 2001). Attemps were later made by Calle and Van der Meer (1997) and Calle (2007; 2008) to validate this educated guess.

The standard deviation of the *local average* of the undrained shear strength is smaller than the standard deviation of the *point values* of the undrained shear strength, see Figure 18. Spatial averaging thus influences the representaive value that ought to be used in slope stability analyses.

5.4 Selecting partial safety factors

Partial safety factors are ideally introduced for all stochastic variables, especially for the ones with design point values that differ significantly and unfavourably from their representative values. Doing so ensures the closest possible link between probabilistic and semi-probabilistic assessments.

Similar to the choice of representative values, the choice of safety factors mostly rests on a trade-off between practicality and accuracy. While the introduction of a large number of partial factors, each being marginally different from 1, could be most accurate, it would also be impractical and error-prone.

The number of partial safety factors can sometimes be reduced without any loss of accuracy. Consider for instance the following limit state function:

$$Z = S_1 \cdot S_2 - R_1 \cdot R_2 \tag{31}$$

A semi-probabilistic assessment could be carried out by feeding the limit state function with design values:

$$Z = S_{1,d} \cdot S_{2,d} - R_{1,d} \cdot R_{2,d} \tag{32}$$

or:

$$Z = (\gamma_{S1} \cdot S_{1,rep}) \cdot (\gamma_{S2} \cdot S_{2,rep}) - (R_{1,rep} / \gamma_{R,1}) \cdot (R_{2,rep} / \gamma_{R,2}) \tag{33}$$

Rearranging terms gives:

$$Z = (\gamma_{S1} \cdot \gamma_{S2}) \cdot (S_{1,rep} \cdot S_{2,rep}) - (R_{1,rep} \cdot R_{2,rep}) / (\gamma_{R,1} \cdot \gamma_{R,2}) \tag{34}$$

which can be simplified to:

$$Z = \gamma_S \cdot (S_{1,rep} \cdot S_{2,rep}) - (R_{1,rep} \cdot R_{2,rep}) / \gamma_R \tag{35}$$

or even to:

$$Z = 1 - \gamma \cdot (S_{1,rep} \cdot S_{2,rep}) / (R_{1,rep} \cdot R_{2,rep}) \quad (36)$$

The above explains why overall safety factors could be introduced for piping, uplift, heave and revetment failures without any or significant loss of accuracy.

5.5 β_T-dependent and β_T-invariant partial safety factors

Design values, and hence partial factors, depend on the target reliability index (β_T). It would be impractical, however, if all partial factors were to vary from segment to segment. This is why it was decided to derive the values of all but one partial factor for a fixed reliability index (β_{basis}) and to either include a safety factor that also corrects for the difference between β_{basis} and β_T ($\gamma_{\beta T}$) or to define the design value of the hydraulic load as a function of β_T. The latter was done for dune erosion and grass revetment failure. For these failure mechanisms, the uncertainty related to the hydraulic load dominates the other uncertainties, making it possible to obtain a close relationship between probabilistic and semi-probabilistic assessments by defining the hydraulic load as a function of β_T.

The factor $\gamma_{\beta T}$ is conceptually similar to an importance factor that depends on a reliability class (see e.g. the Eurocodes) or a consequence factor that accounts for the consequences of failure (e.g. Fenton and Naghibi, 2014). Note that consequences are inversely related to acceptable probabilities of failure.

6 Step 3: Calibrating partial safety factors

This chapter discusses the calibration of partial safety factors for semi-probabilistic assessments. The objective of a calibration study is to select safety factors that are sufficiently safe but not too conservative.

6.1 Establishing β_T-invariant safety factors

In principle, all partial factors could be defined as a function of the target reliability. It is more practical, however, to fix the values of all but one safety factor or design value. Otherwise, engineers would have to recalculate all safety factors whenever the target reliability changes.

Each β_T-invariant safety factor is based on the following inputs:

1. the distribution of the stochastic variable to which the safety factor applies,
2. the representative value of the stochastic variable to which the safety factor applies (see chapter 5),
3. an influence coefficient that is considered representative for the stochastic variable to which the safety factor applies.
4. a fixed or basic reliability index (β_{basis}). Because safety factors smaller than 1 are counter-intuitive, such values are best avoided. By choosing a relatively low fixed reliability index, the chances of having to work with a β_T-dependent safety factor smaller than 1 can be kept small.

With the abovementioned inputs, the values of β_T-invariant safety factors for load and resistance variables can be derived from:

$$\gamma_S = S_d / S_{rep} = F_S^{-1}(1-\Phi(\alpha_S \cdot \beta_{basis})) / S_{rep} \quad (37)$$

$$\gamma_R = R_{rep} / R_d = R_{rep} / F_R^{-1}(1-\Phi(\alpha_R \cdot \beta_{basis})) \quad (38)$$

where

γ_S	Partial safety factor for load variable S
S_d	Design value of load variable S
S_{rep}	Representative value of load variable S
γ_R	Partial safety factor for resistance variable R
R_d	Design value of resistance variable R
R_{rep}	Representative value of resistance variable R
$F_S^{-1}(\cdot)$	Inverse of the cumulative distribution of load variable S
$F_R^{-1}(\cdot)$	Inverse of the cumulative distribution of resistance variable R
$\Phi(\cdot)$	Cumulative standard normal distribution
α_S	Influence coefficient of a load variable S
α_R	Influence coefficient of a resistance variable R
β_{basis}	Chosen reliability index

For example, for a normally distributed resistance variable with a representative value that is the 5% quantile value, the β_T-invariant safety factor follows from:

$$\gamma_R = R_{rep} / R_d = (\mu_R - 1.65 \cdot \sigma_R) / (\mu_R - \alpha_R \cdot \beta_{basis} \cdot \sigma_R) \quad (39)$$

where
μ_R Mean value of R
σ_R Standard deviation of R

This is because $\Phi(1.65) = 0.95$ so that $1-\Phi(1.65) = 0.05$, which corresponds to the 5% quantile value.

6.2 Establishing a β_T-dependent safety factor

6.2.1 Obtaining a relationship between safety factors and target reliabilities

An equation governing the value of the β_T-dependent safety factor can be obtained from a comparison of probabilistic and semi-probabilistic calculations for different values of the β_T-dependent safety factor. This involves the following steps:

1. For a range of values of the β_T-dependent safety factor, change the dimensions (e.g. berm width) of the test set members so that they that would just pass a semi-probabilistic assessment.
2. Subsequently, calculate the reliability indices or probabilities of failure for each modified test set member.

An example is shown in Figure 19. The example concerns the stability of the inner slope of a levee. For a higher β_T-dependent safety factor, the berm has to be bigger for the levee to pass a semi-probabilistic assessment. A levee with a bigger berm has a higher reliability index, which can be shown by carrying out a probabilistic analysis. Hence, there is a positive correlation between the value of the β_T-dependent safety factor and the reliability implied by the semi-probabilistic rule.

In step 1 above we modified the test set by increasing or decreasing the size of the berm in such a way that the resulting levee would just pass a semi-probabilistic assessment.

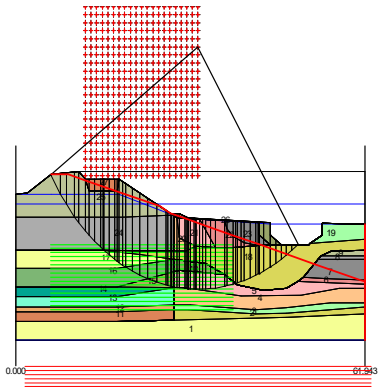

(γ=1.0 , β=3,57)

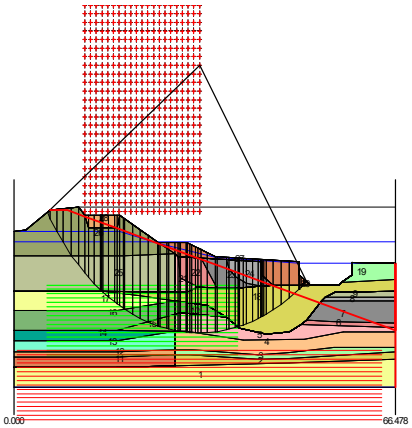

(γ=1.3 , β=5,20)

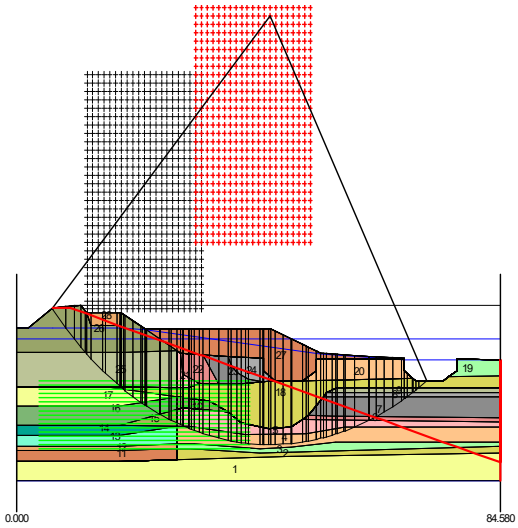

(γ=1.5 , β=7,39)

Figure 19. A higher value of the β_T-dependent safety factor means that a flood defense has to be more reliable to pass a semi-probabilistic assessment.

The relationship between the target reliability index and the value of the β_T-dependent safety factor $\gamma_{\beta T}$ may vary from one test set member to another. This is shown schematically in Figure 20.

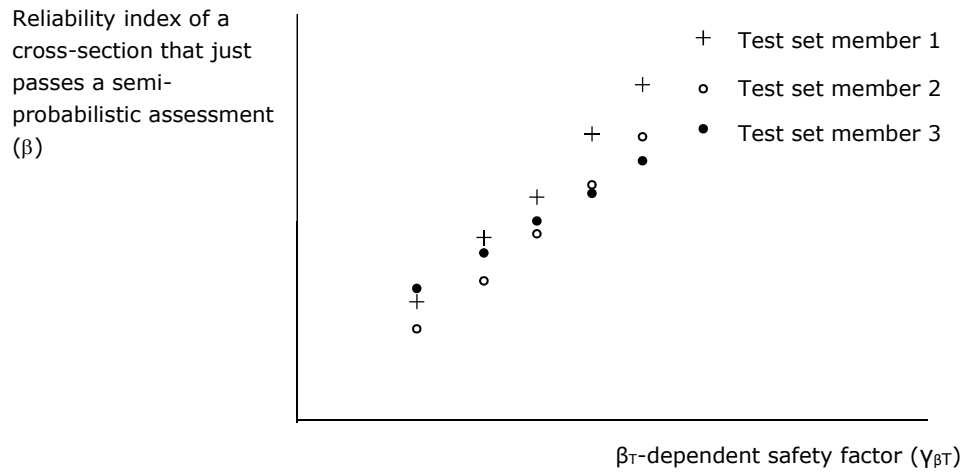

Figure 20. The relationship between the β_T-dependent safety factor and the implied reliability varies from one test set member to another.

6.2.2 *The calibration criterion*

Because the relationship between β_T and the $\gamma_{\beta T}$ varies from one test set member to another, a calibration criterion is required to decide upon a relationship that can be applied universally. Such a relationship should be sufficiently safe but not too conservative. The calibration criterion holds that a semi-probabilistic rule may be considered sufficiently safe when probabilities of failure are *on average* equal to or smaller than the target probability of failure. This criterion is based on economic considerations (see Appendix B of this report). A target failure probability can be specified at the level of entire segments, sections or cross-sectional lengths.

It often proved practical to work at the level of cross-sectional lengths in a code calibration study. Doing so for clusters of test set members with similar characteristics gives insight into the benefits of introducing different β_T-dependent safety factors for different types of cases. An example of such a clustering analysis is given in Figure 21 below.

It is stressed that the requirement that probabilities of failure should *on average* be small enough does not mean that the actual reliability is allowed to be smaller than the target reliability in 50% of cases. This is because the probabilities of failure of different cross-sections are, in practice, far from symmetrically distributed. Unlike cross-sectional failure probabilities, the reliability indices of different cross-sections usually fall within a relatively narrow band. When the spatial distribution of cross-sectional reliability indices is approximately Gaussian with a standard deviation of 0.5, the average cross-sectional probability of failure corresponds roughly to the 20%-quantile of the cross-sectional reliability indices. This can easily be verified numerically.

The above assumption is illustrated in Figure 21: the $\beta_{20\%}$-values are given by the dashed lines, the reliability indices that correspond to the average failure probabilities are given by continuous lines. Both lines are in good agreement in the two upper graphs. There is a clear divergence in the lower graph, albeit in a range

of reliability indices that is largely outside the area of interest[9]. This divergence occurs because the average probability of failure is relatively sensitive to low-reliability outliers (relatively low reliability indices).

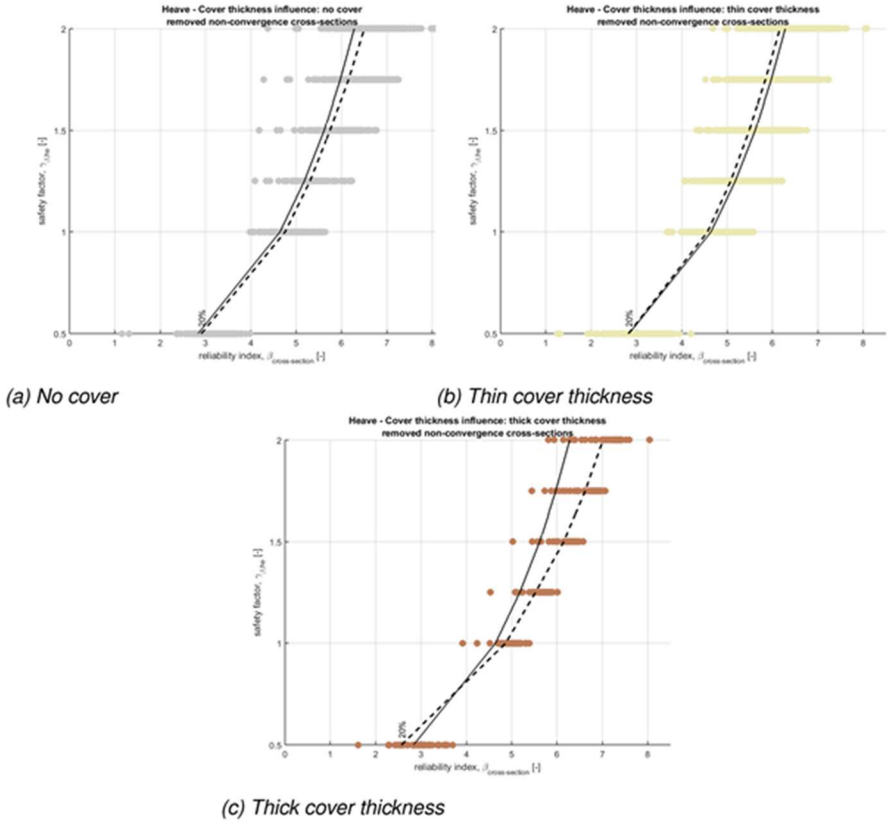

Figure 21. Example of a clustering analysis for heave (Teixeira et al. 2016: p. 101, fig. H.3).

The calibration criterion explicitly allows some cross-sectional failure probabilities to be higher than the cross-sectional target failure probability. This means that conclusions about the adequacy of a semi-probabilistic assessment rule cannot be drawn on the basis of a comparison of the outcomes of a semi-probabilistic and a probabilistic assessment for an *individual* cross-section. Meaningful conclusions can only be drawn when large numbers of cross-sections are considered.

The requirement that probabilities of failure should *on average* be small enough is inconsistent with an assessment procedure in which sections that fail to pass a semi-probabilistic assessment are re-assessed using probabilistic methods. Doing so would disturb the balance between sections with relatively high and low reliabilities. When probabilistic assessments are carried out, this should ideally be done for all sections, not than just for the ones that failed to pass the semi-probabilistic assessment.

[9] Using the default failure probability budget, default length effect factors and maximum allowable probabilities of flooding, the target reliability index for internal erosion is smaller than 5.1 for all but one segment (30-4). For segment 30-4, which protects a nuclear power, it is about 5.3. This segment lies in an open estuary where high water levels have relatively short durations which lowers the probability of this failure mechanism leading to flooding.

6.2.3 *The functional form of a β_T-dependent safety factor*

Each β_T-dependent safety factor is a function of the cross-sectional target reliability. The latter depends on:

1. the standard of protection,
2. the failure probability budget,
3. the length-effect factor.

The standard of protection generally influences the β_T-dependent safety factor in a different manner compared to the failure probability budget and the length effect factor. This is because the exceedance probabilities of the representative and/or design loads have been linked to the standard of protection. A stricter standard of protection therefore leads to both a smaller cross-sectional target failure probability and a less favourable design load, see section 5.2. Changes in the failure probability budget and the length effect factor do not do so.

For the same cross-sectional target reliability, the β_T-dependent safety factor should be smaller when the representative value of the hydraulic load is less favourable. The relationship between β_T and $\gamma_{\beta T}$ is therefore different for different standards of protection. This is shown schematically in Figure 22.

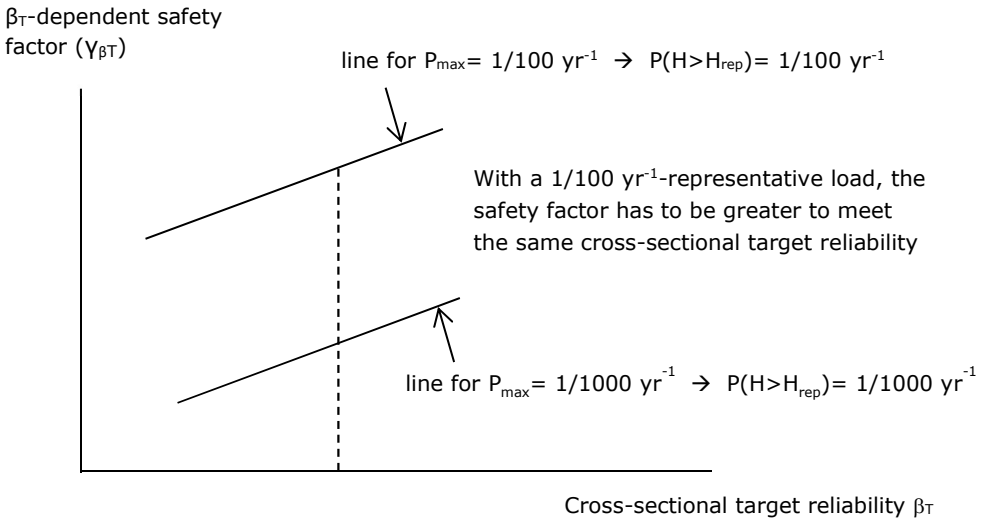

Figure 22. The β_T-dependent safety factor as a function of the cross-sectional target reliability, for two different standards of protection (P_{max}). The representative value of the water level (H_{rep}) is linked to the standard of protection.

A stricter standard of protection leads to a higher target reliability but also to a higher representative load. This may lead to a β_T-dependent safety factor that is broadly similar across a range of standards of protection (for a given length-effect factor). This is shown schematically in Figure 23.

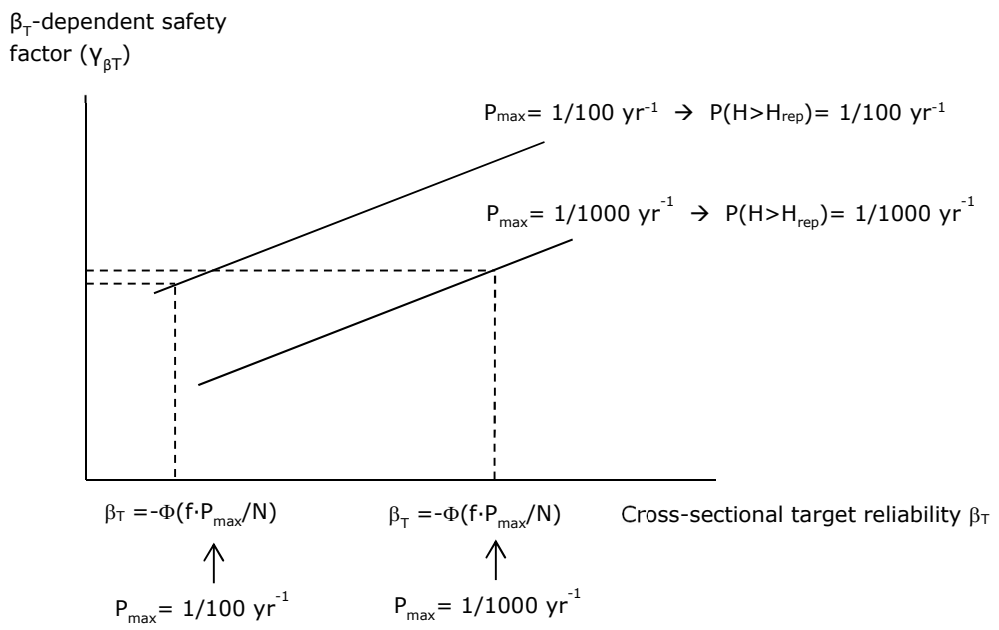

Figure 23. Because the standard of protection (P_{max}) influences both the cross-sectional target reliability and the representative value of the water level (H_{rep}), the β_T-dependent safety could be similar for different standards of protection.

Since the relationship between design (point) values and reliability indices is often approximately linear within the relevant range of cross-sectional target reliabilities, a β_T-dependent safety factor can often be written in the following form:

$$\gamma_{\beta T} = a \cdot \beta_{max} + b \cdot \beta_{T,cross} + c \tag{40}$$

with

$$\beta_{max} = -\Phi^{-1}(P_{max}) \tag{41}$$

and

$$\beta_{T,cross} = -\Phi^{-1}(P_{T,cross}) \quad \text{with} \quad P_{T,cross} = f \cdot P_{max} / N \tag{42}$$

where

$\gamma_{\beta T}$	β_T-dependent safety factor
a,b,c	Constants
P_{max}	Standard of protection or maximum allowable probability of flooding
f	Fraction of the maximum allowable probability of flooding that has been reserved for the failure mechanism under consideration ($0<f\leq1$), see also Table 1
N	Length effect factor ($N\geq1$)

6.2.4 *The β_T-dependent safety factor and schematization uncertainty*

The description of a complex reality in terms of model inputs is called a schematization. Because data is normally incomplete and imprecise, there can be significant uncertainty related to the schematization that best describes reality.

The uncertainty related to the precise properties of a soil layer could be interpreted as a form of schematization uncertainty. The term schematization uncertainty is reserved here, however, for uncertainties that cannot be described by continuous stochastic variables, such as the uncertainty related to stratigraphy. This distinction between continuous and discrete uncertainties greatly simplifies probabilistic and semi-probabilistic assessments.

As an illustration of the way in which schematization can be dealt with in probabilistic assessments, consider a slope stability assessment in case of an uncertain stratigraphy. For each possible stratigraphy, the probability of slope instability will be different. By combining these conditional probabilities of failure with the probabilities of each possible stratigraphy, the (unconditional) probability of failure can be obtained as follows (see ENW 2012):

$$P(F) = \sum(P(F \cap S_i)) \quad \text{with} \quad \sum P(S_i)=1 \tag{43}$$

or:

$$P(F) = \sum(P(F \mid S_i) \cdot P(S_i)) \quad \text{with} \quad \sum P(S_i)=1 \tag{44}$$

where
$P(\cdot)$ Probability
F Failure
S_i Stratigraphy i or more generally: scenario i

Note that the scenarios have to be mutually exclusive and collectively exhaustive.

In a semi-probabilistic assessment, the calibrated relationship between the β_T-dependent safety factor and the cross-sectional reliability requirement may be used inversely to obtain a (safe) estimate of the conditional probability of failure per scenario $P(F \mid S_i)$:

$$P(F \mid S_i)_{estimate} = \Phi(-g^{-1}(\gamma_{\beta T}^*)) \tag{45}$$

where
$g(\cdot)$ function that relates the value of the β_T-dependent safety factor ($\gamma_{\beta T}$) to the cross-sectional target reliability $\beta_{T,cross}$, see also equation (40)
$\gamma_{\beta T}^*$ Value of the β_T-dependent safety factor ($\gamma_{\beta T}$) for which the flood defense would just pass a semi-probabilistic assessment, or $R_d=S_d$.

Having estimated the conditional probability of failure for each scenario, an estimate of the probability of failure can be obtained as follows:

$$P(F)_{estimate} = \sum\{ P(F \mid S_i)_{estimate} \cdot P(S_i) \} \quad \text{with} \quad \sum P(S_i)=1 \tag{46}$$

This probability estimate has to be smaller than the cross-sectional target probability of failure.

As shown above, schematization uncertainties can be dealt with in semi-probabilistic assessments by using the equation governing the β_T-dependent safety factor inversely. No safety factor for schematization uncertainties is required.

The abovementioned semi-probabilistic procedure has been implemented in the WBI2017. This procedure is impractical, however, for the design of flood defenses. This is because the design process is an iterative process. According to the abovementioned procedure, semi-probabilistic evaluations would have to be carried out for all scenarios every time a design is changed during the design process. This is why an alternative semi-probabilistic procedure has been developed for design purposes. It rests on the same logic and equations as the abovementioned procedure but allows for a different work flow.

In the alternative procedure, a schematization factor is applied to the outcome of a semi-probabilistic evaluation for a "base schematization" (ENW, 2012). The numerical value of this schematization factor depends on:

1. the probabilities of the schematizations that are more pessimistic than the base schematization and
2. the differences between the outcomes of semi-probabilistic assessments for these schematizations and the outcome for the base schematization.

This procedure allows engineers to more efficiently work towards a design that complies with the reliability requirement, as they can work with a single schematization during most of the design process.

6.2.5 *The β_T-dependent safety factor and parallel system behavior*

Some failure mechanisms display parallel system behavior. For example, a levee can only fail due to internal erosion when uplift, heave and piping all occur. Failure, in this case, requires the limit state functions for all three sub-failure mechanisms (uplift, heave and piping) to be smaller than zero:

$$P(F) = P(Z_{up}<0 \cap Z_{he}<0 \cap Z_{pip}<0) \quad (47)$$

or:

$$P(F) = P(\max\{Z_{up}, Z_{he}, Z_{pip}\}<0) \quad (48)$$

The upper bound of this failure probability equals the smallest of the probabilities for the three individual sub-mechanisms:

$$P(F) \leq \min\{ P(Z_{up}<0) , P(Z_{he}<0) , P(Z_{pip}<0) \} \quad (49)$$

In case of parallel system behavior and schematization uncertainty, failure probabilities should first be calculated per scenario, taking into account the different sub-mechanisms. The resulting failure probabilities per scenario should only then be weighed by scenario probabilities and combined to a safe estimate of the parallel system's probability of failure. A safe estimate of the probability of failure can be obtained from:

$$P(F) \leq \sum_i(P(S_i) \cdot \min_j\{ P(Z_j<0 \mid S_i) \}) \quad (50)$$

Reversing the order of the calculations, i.e. first combining the scenarios per sub-mechanism and then taking the minimum across the three sub-mechanisms, would be incorrect. This is because a stratigraphy cannot vary across sub-mechanisms.

Numerical example
To illustrate the importance of the order of the calculations when dealing with parallel system behavior and schematization uncertainty, consider uplift, heave and piping for a case with two possible stratigraphies. A safe estimate of the probability of failure can be obtained by:

1. *taking the smallest failure probability per sub-failure mechanism per scenario and multiplying it with the scenario probability and*
2. *summing up the results for the different scenarios.*

$P(S_i)$	$P(Z_{up}<0 \mid S_i)$	$P(Z_{he}<0 \mid S_i)$	$P(Z_{pip}<0 \mid S_i)$	$P(S_i)\cdot min_j\{ P(Z_j<0 \mid S_i) \}$
0.5	*1.00E-03*	*1.00E-02*	*1.00E-04*	*5.00E-05*
0.5	*1.00E-04*	*1.00E-04*	*1.00E-02*	*5.00E-05*
			Sum	***1.00E-04***

First calculating the failure probabilities per sub-mechanism and then taking the minimum would give a different, incorrect result:

$P(S_i)$	$P(Z_{up}<0 \mid S_i)$	$P(Z_{he}<0 \mid S_i)$	$P(Z_{pip}<0 \mid S_i)$
0.5	*1.00E-03*	*1,00E-02*	*1,00E-04*
0.5	*1.00E-04*	*1,00E-04*	*1,00E-02*
$P(Z_j<0)$	***5.50E-04***	***5,05E-03***	***5,05E-03***
$min_j\{ P(Z_j<0) \}$	***5.50E-04***		

In semi-probabilistic assessments, safe estimates of $P(Z_{up}<0|S_i)$, $P(Z_{he}<0|S_i)$ and $P(Z_{pip}<0|S_i)$ for a cross-sectional length can be obtained by using the β_T-$\gamma_{\beta T}$ relationship inversely, as explained in the previous section. These safe estimates can then be combined using the procedure outlined above to obtain a safe estimate of P(F). This safe estimate of the cross-sectional failure probability can then be compared to the cross-sectional target failure probability.

7 Internal erosion: uplift, heave and piping

This chapter gives a summary of the WBI2017 code calibration study for internal erosion (see Teixeira et al. 2016). This failure mechanism is often referred to as piping. To avoid misunderstanding, the term piping is used here for a sub-failure mechanism that involves progressive pipe growth. Piping is a necessary but not a sufficient condition for dike failure. For further details about internal erosion assessments for dikes, the reader is referred to the WBI2017 schematization guideline (Ministry of Infrastructure and the Environment, 2016h).

7.1 Failure mechanism

7.1.1 Qualitative description

A high water level may lead to high pore pressures in an aquifer. When the cover layer lifts up, causing cracks to the surface, concentrated seepage may lead to the transport of suspended sand particles from the aquifer (heave). This can lead to the growth of a pipe from the landside of the levee to the riverside (piping). When the full-grown pipe widens, the dike can become unstable and fail. The sequence of events leading to instability and failure is shown schematically in Figure 24. For further details, the reader is referred to the WBI2017 phenomenological description of this failure mechanism (’t Hart, De Bruijn and De Vries, 2016).

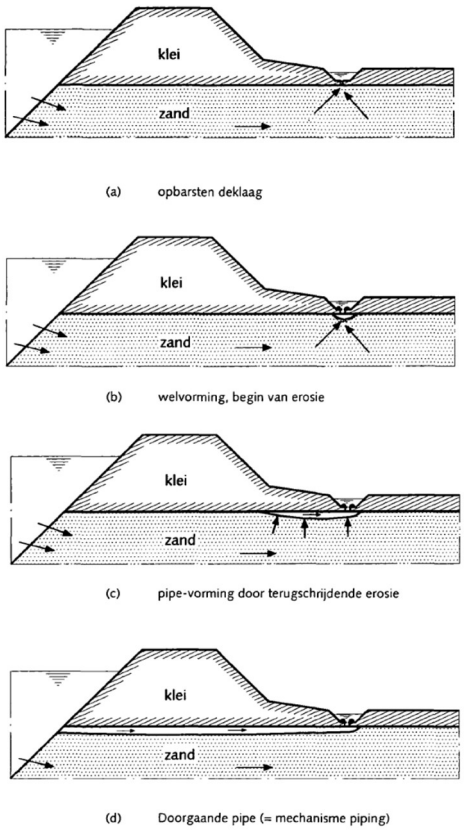

Figure 24. Uplift, heave and piping (TAW 1999: p.16).

7.1.2 Failure mechanism model

The WBI2017 failure mechanism model for internal erosion comprises three sub-mechanisms: uplift, heave and piping. Failure due to internal erosion is assumed to (only) occur when all sub-failure mechanisms manifest themselves, see Figure 25.

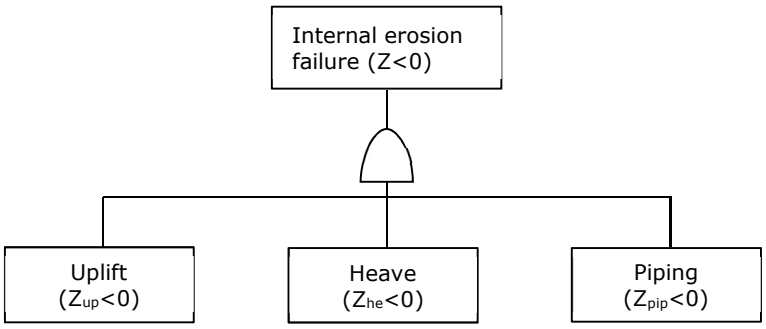

Figure 25. Fault tree for failure due to internal erosion.

Internal erosion

The limit state for internal erosion is given by:

$$Z = \max\{ Z_{up}, Z_{he}, Z_{pip} \} \quad (51)$$

where

Z_{up}	Limit state function for uplift
Z_{he}	Limit state function for heave
Z_{pip}	Limit state function for piping

Uplift

The limit state function for uplift (Z_{up}) is given by:

$$Z_{up} = m_u \cdot \Delta\varphi_{c,u} - (\varphi_{exit} - h_{exit}) \quad (52)$$

with

$$\Delta\varphi_{c,u} = D_{cover} \cdot \gamma_{eff,cover} / \gamma_{water} \quad (53)$$

$$\gamma_{eff,cover} = \gamma_{sat,cover} - \gamma_{water} \quad (54)$$

$$\varphi_{exit} = h_{exit} + (H - h_{exit}) \cdot r_{exit} \quad (55)$$

where

m_u	Model factor for uplift
φ_{exit}	Piezometric head at exit point
h_{exit}	Phreatic level at the exit point
D_{cover}	Effective thickness of the cover layer
γ_{water}	Volumetric weight of water
$\gamma_{sat,cover}$	Saturated volumetric weight of the cover layer
H	water level on the riverside
r_{exit}	Damping factor at the exit point

Heave
The limit state function for heave (Z_{he}) is given by:

$$Z_{he} = i_c - i \quad (56)$$

with

$$i = (\varphi_{exit} - h_{exit}) / D_{cover} \quad (57)$$

$$\varphi_{exit} = h_{exit} + (H - h_{exit}) \cdot r_{exit} \quad (58)$$

where:
i_c Critical heave gradient

Piping
The limit state function for piping (Z_{pip}) is based on the Sellmeijer 2011-model (Sellmeijer *et al.*, 2011):

$$Z_{pip} = m_p \cdot H_c - (H - h_{exit} - r_c \cdot D_{cover}) \quad (59)$$

with

$$H_c = F_{resistance} \cdot F_{scale} \cdot F_{geometry} \cdot L \quad (60)$$

$$F_{resistance} = \eta \cdot \gamma_{sub,particles} / \gamma_{water} \cdot \tan(\theta_{sellmeijer,rev}) \quad (61)$$

$$F_{scale} = d_{70,m} / (\kappa \cdot L)^{1/3} \cdot (d_{70} / d_{70,m})^{0.4} \quad (62)$$

$$\kappa = \nu_{water} / g \cdot k \quad (63)$$

$$F_{geometry} = 0{,}91 \cdot (D/L)^c \quad (64)$$

$$c = 0.04 + 0.28 / \{ (D/L)^{2.8} - 1 \} \quad (65)$$

where

m_p	Model factor for piping
r_c	Reduction factor
η	White's drag coefficient
$\gamma_{sub,particles}$	Submerged volumetric weight of sand particles
$\theta_{sellmeijer,rev}$	Bedding angle of sand grains for the 2011 Sellmeijer rule
$d_{70,m}$	Mean value of the d_{70} in small scale tests
d_{70}	70% quantile of the grain size distribution of the piping-sensitive layer
k	Darcy permeability of the aquifer
ν_{water}	Kinematic viscosity of water
g	Gravitational acceleration
D	Thickness of the aquifer
L	Seepage length

7.2 Reliability requirement

The cross-sectional reliability requirement for internal erosion is given by:

$$P_{T,cross} = \omega \cdot P_{max} / (1 + a \cdot L / b) \quad (66)$$

where

- $P_{T,cross}$ Cross-sectional target failure probability for the failure mechanism under consideration (here: internal erosion)
- ω Fraction of the maximum allowable probability of flooding that has been reserved for the failure mechanism under consideration
- P_{max} Maximum allowable probability of flooding, i.e. the standard of protection
- a The piping-sensitive fraction of the segment
- L Length of the segment
- b The length of independent, equivalent stretches within the piping-sensitive part of the segment

The piping-sensitive fraction of the segment is 0.9 for piping sensitive segments (segments 31-1 to 44-1 and 47-1 to 95-1) and 0.4 for other cases (Förster *et al.*, 2015). It was decided to adopt a generic value b = 350 m following the recommendations of a study by Lopez de la Cruz et al. (2010).[10]

7.3 Safety format

7.3.1 Partial factors and representative values

It was decided to introduce β_T-dependent safety factors for uplift, heave and piping (one β_T-dependent safety factor for each sub-failure mechanism), without separate β_T-invariant partial factors for particular stochastic variables. This has to do with the relations between the different stochastic variables within the limit state functions: the overall β_T-dependent safety factors are (exactly or by approximation) equal to the product of calibrated partial factors for the individual stochastic variables, see also section 5.4. The semi-probabilistic assessment rules for the three sub-failure mechanisms have the following formats. The subscripts "rep" refer to representative values.

Uplift (γ_{up}):

$$D_{cover,rep} \geq \gamma_{up} \cdot \gamma_{water} \cdot (H_{rep} - h_{exit,rep}) \cdot r_{exit,rep} / (\gamma_{sat,cover,rep} - \gamma_{water}) \quad (67)$$

Heave (γ_{he}):

$$D_{cover,rep} \geq \gamma_{he} \cdot (H_{rep} - h_{exit,rep}) \cdot r_{exit,rep} / i_{c,rep} \quad (68)$$

Piping (γ_{pip}):

$$\gamma_{pip} \cdot H_{c,rep} \geq H_{rep} - h_{exit,rep} - r_{c,rep} \cdot D_{cover,rep} \quad (69)$$

An overview of stochastic variables and their representative values is given in Table 3. All variables from section 7.1.2 that are not mentioned in this table are treated as deterministic in the WBI2017.

[10] The schematization guideline says b=300m rather than 350m (Ministry of Infrastructure and the Environment, 2016h). This difference has no practical significance.

Table 3. Stochastic variables and representative values for uplift, heave and piping.

Symbol	Unit	Description	Distribution	Representative value
D_{cover}	m	Total thickness of the cover layer	Lognormal	5%-value
H	m	Water level on the water side relative to NAP	From probabilistic load model	Exceedance probability equal to standard of protection
h_{exit}	m	Phreatic level at the exit point relative to NAP	Normal	5%-value
r_{exit}	-	Damping factor at exit point	Lognormal	95%-value
$\gamma_{sat,cover}$	kN/m^3	Saturated volumetric weight of the cover layer	Shifted lognormal, shift=$10kN/m^3$	5%-value
i_c	-	Critical heave gradient	Lognormal	0.3
L	m	Seepage length	Lognormal	5%-value
D	m	Thickness of the aquifer	Lognormal	95%-value
d_{70}	m	70%-quantile of the grain size of the aquifer	Lognormal	5%-value
k	m/s	Permeability of the aquifer	Lognormal	95%-value
m_p	-	Model factor for piping	Lognormal	1.0 (see section 5.2)
m_u	-	Model factor for uplift	Lognormal	1.0 (see section 5.2)

7.3.2 Schematization uncertainty

In case of uncertainty related to stratigraphy, the β_T-dependent safety factors should be used inversely to assess whether the cross-sectional reliability requirement for internal erosion is met. Semi-probabilistic assessments are first carried out per failure mechanism per stratigraphy/scenario, and then combined into an overall-verdict. For further details, see section 6.2.5.

7.4 Calibrated safety factors

Probabilistic calculations were performed using Hydra-Ring for a large number cross-sections, using data from the VNK2-project, see Figure 26. Initial calculations led to concerns about unrealistically large required seepage lengths. While the Sellmeijer model was developed and tested for homogeneous conditions, real-life cases are strongly heterogeneous. To obtain more realistic outputs, it was decided to introduce default values for the coefficients of the permeability (k) and the d_{70}, i.e. cov(k)=0.50 and cov(d_{70})=0.12, largely on the basis of engineering judgement (Rijkswaterstaat, 2016).

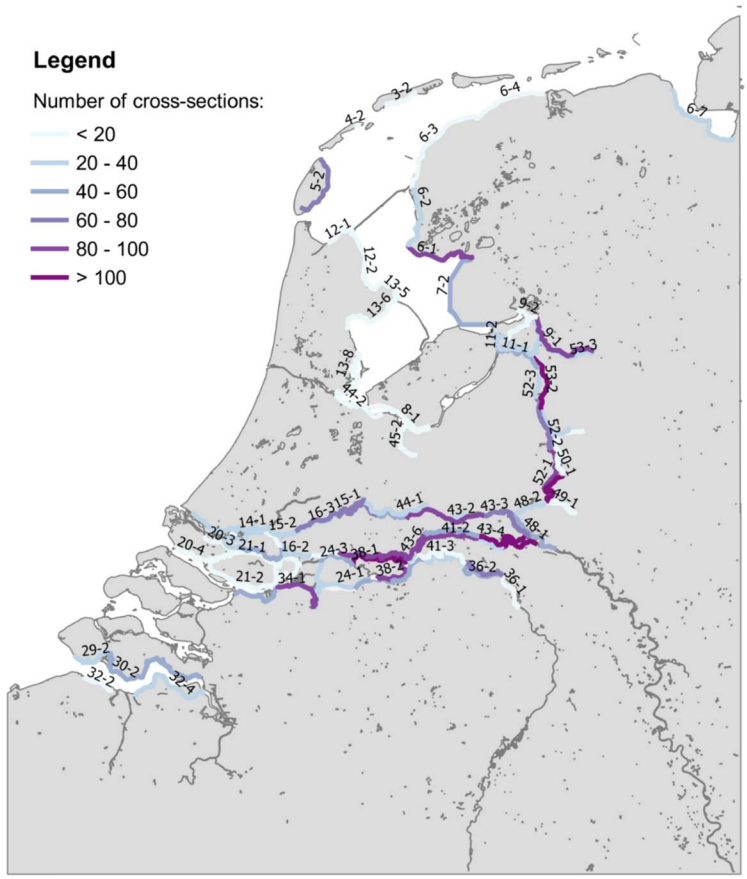

Figure 26. The number of cases per segment.

For each sub-failure mechanism, all test set members (cross-sections) were modified so that they would just pass a semi-probabilistic assessment, assuming a range of values of the β_T-dependent safety factor. This was done by changing the cover layer thickness (for uplift and heave) and the seepage length (for piping). Probabilities of failure were then calculated for each modified cross-section. Results are shown in Figure 27-Figure 29. These figures show the average probability of failure across all cross-sections, for different values of the standard of protection (dots). The results showed no obvious regional or other type of clustering. The fitted β_T-$\gamma_{\beta T}$-relationships are shown by continuous lines.

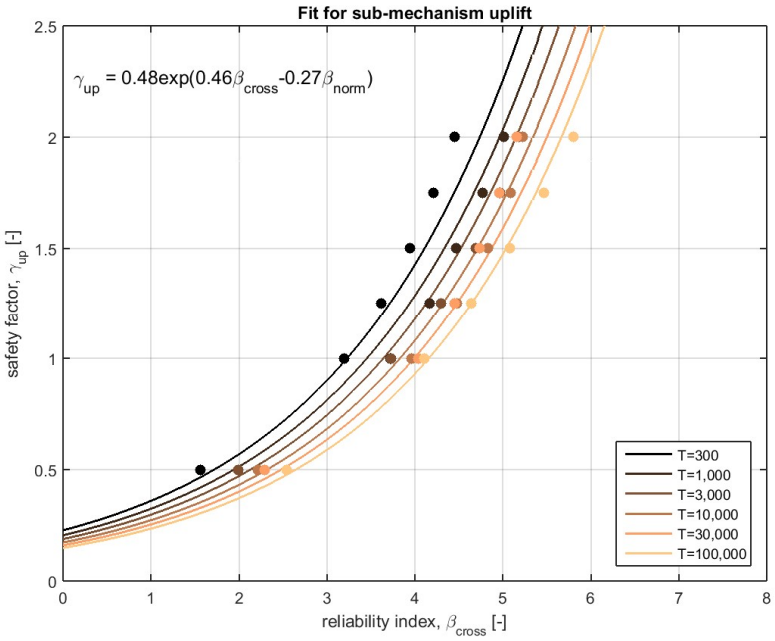

Figure 27. Average failure probabilities for uplift and fitted relationships.

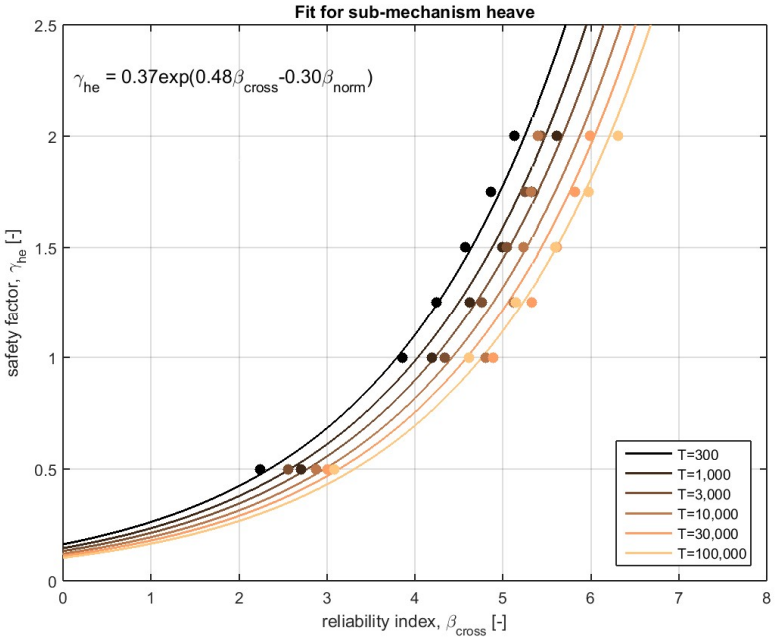

Figure 28. Average failure probabilities for heave and fitted relationships.

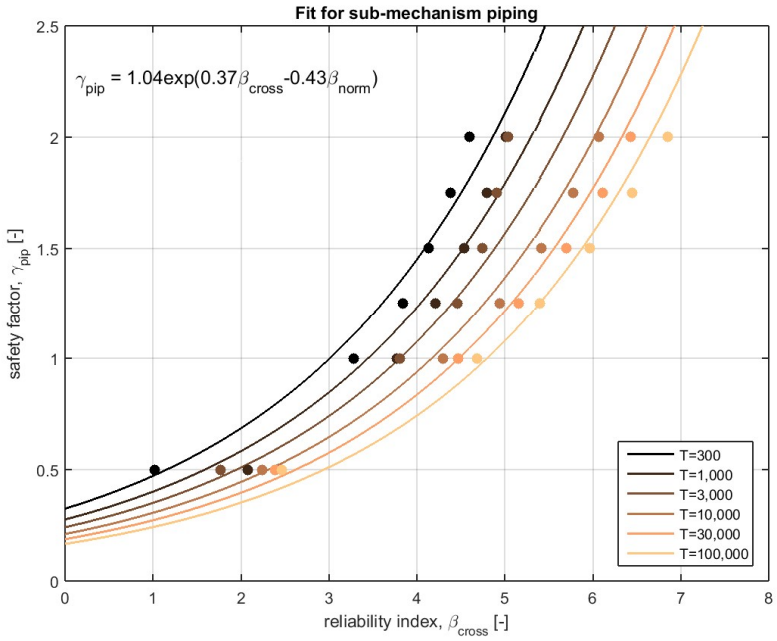

Figure 29. Average failure probabilities for piping and fitted relationships.

The fitted relationships are exponential because a linear relationship for reliability indices greater than 3 would lead to unacceptable errors for relatively low reliability indices, see also Figure 27-Figure 29. Reliability indices of e.g. 2-3 for low factors of safety could still be relevant in piping assessments since relatively unfavourable stratigraphies may have relatively small probabilities. A linear relationship between the β_T-dependent safety and β_T, fitted to the results for β_T>3, would lead to a significant overestimation of cross-sectional reliabilities for low factors of safety.

As shown in Figure 27-Figure 29, the β_T-dependent safety factor should be smaller for a given β_T-value when the standard of protection is higher. This is because the representative value of the outside water level is linked to the standard of protection (see also section 6.2.3). A higher standard of protection leads to a higher design water level. When the design water level is higher but the cross-sectional target reliability stays the same, a smaller safety factor suffices.

The inverse relationships between the safety factors and β_T are given by the following equations:

For uplift:

$$\beta_{up} = 1/0.46 \cdot (\ln(\gamma_{up}/0.48) + 0.27 \cdot \beta_{max}) \quad (70)$$

For heave:

$$\beta_{he} = 1/0.48 \cdot (\ln(\gamma_{he}/0.37) + 0.3 \cdot \beta_{max}) \quad (71)$$

For piping:

$$\beta_{pip} = 1/0.37 \cdot (\ln(\gamma_{pip}/1.04) + 0.43 \cdot \beta_{max}) \quad (72)$$

with

$$\beta_{max} = -\Phi^{-1}(P_{max}) \quad (73)$$

The inverse relationships above can be used in the semi-probabilistic assessment procedure discussed in section 7.3.2.

7.5 Comparison with former assessment rule

Piping
A code calibration study in 2010 with the updated Sellmeijer equation and the old standards led to safety factors ranging from 1.2 for $\beta_T \leq 4$ to 1.6 for $\beta_T = 5.5$, regardless of the standard of protection (Lopez de La Cruz *et al.*, 2010). For maximum allowable probabilities of flooding of 1/10,000 yr^{-1} (common along the main rivers), the newly calibrated safety factor is less stringent than the 2010-safety factor. Differences are in the order of 10%. For higher standards, the differences are greater than 10%. For relatively low standards of protection (e.g. 1/300 yr^{-1}), the new safety factors are more conservative.

Uplift
The β_T-dependent safety factor for uplift applies to the representative value of the effective volumetric weight. It gives broadly similar results compared to the former safety factor on the saturated volumetric weight of cover layers. Note that the value of a safety factor on an effective volumetric weight cannot be compared directly to the value of a safety factor on a saturated volumetric weight.

Heave
Previously, the heave mechanism was only considered within the context of advanced assessments.

7.6 Discussion

Time is not a variable in the limit state functions that underlie WBI2017 safety assessments for internal erosion, see section 7.1.2. In regions where high water levels are likely to last only several hours, the assumption of stationary conditions would be overly conservative. Guidance on the use of the Sellmeijer model under non-stationary conditions is provided by the Schematization guideline for internal erosion (Ministry of Infrastructure and the Environment, 2016h) and the Dutch technical report on pore pressures (TAW, 2004). Also, a simple screening rule is used in the WBI2017 that rests on the time to failure (Ministry of Infrastructure and the Environment, 2016c; Rijkswaterstaat, 2016).

The resistance against internal erosion is highly sensitive to "minor geological details" (Terzaghi, 1929). The Sellmeijer-model is a process-based model that has been developed and tested for uniform, homogeneous and horizontal soil layers. Real-life conditions often differ considerably from these idealized conditions. This may lead to ambiguity concerning the precise definition of model inputs in real-life cases. For instance, the d_{70} is the 70% quantile of a grain size distribution. In a uniform, homogeneous sand layer, the d_{70} of every individual sample is the same. In reality, individual samples show considerable point to point variation. This makes the probability distribution of the d_{70} (and hence its representative value) depend on the volume of sand for which the 70% quantile is calculated.

A similar difficulty concerns the definition of the permeability of the aquifer (k) in real-life, heterogeneous conditions. As a pragmatic solution, average values and coefficients of variation were defined for d_{70} and k for different types of soils, largely on the basis of expert judgment and the realism of model outputs (Rijkswaterstaat, 2016). Such pragmatism is illustrative for the trade-off between model uncertainty and parameter uncertainty when more accurate, process-based models require inputs that are not readily available or that deviate from idealized/experimental conditions.

The various probabilistic sensitivity analyses that were performed within the context of the code calibration study (not presented here) helped inform the choices related to the distributions of d_{70} and k. The distribution parameters of d_{70} and k that were finally used for calibration purposes are the same as the default values in the WBI2017 schematization guideline for internal erosion (Ministry of Infrastructure and the Environment, 2016h).

8 Slope instability

This chapter gives a summary of the WBI2017 code calibration study for slope stability (see Kanning, et al. 2016). For further details about slope stability assessments, the reader is referred to the WBI2017 schematization guideline (Ministry of Infrastructure and the Environment, 2016g).

8.1 Failure mechanism

8.1.1 Qualitative description

When the inner slope of a levee becomes unstable during a high water event, the resulting deformations can lead to e.g. overtopping and hence flooding. In the Netherlands, this failure mechanism is also called macro-instability to distinguish it from micro-instability: the instability of relatively thin layers at the surface of an inner slope due to seepage (TAW, 2001). The macro-instability failure mechanism is shown schematically in Figure 30. For further details, the reader is referred to the WBI2017 phenomenological description of this failure mechanism (’t Hart, De Bruijn and De Vries, 2016).

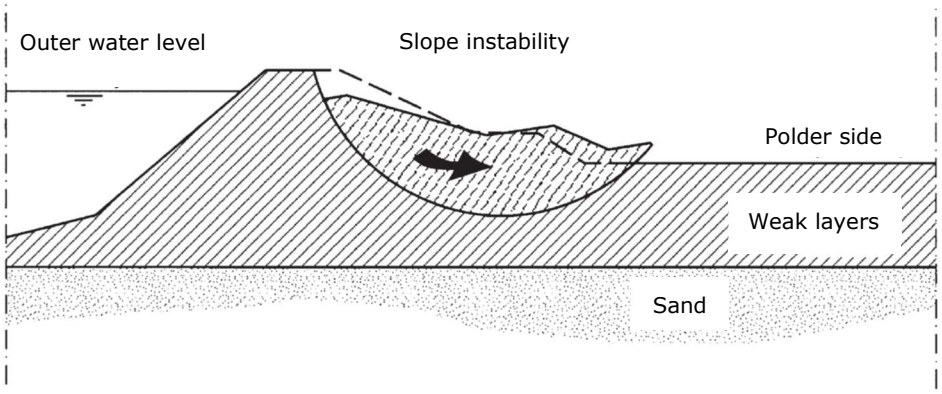

Figure 30. Macro-instability (adapted from TAW 2001: figure 5.3.1, p. 102)

8.1.2 Failure mechanism model

The default WBI2017 model for slope stability assessments is the Uplift-Van model (Ministry of Infrastructure and the Environment, 2016g). This is an extension of Bishop’s model that assumes that the slip plane is composed of a horizontal part bounded by two circular parts (active and passive) to accommodate uplift of the blanket layer, which is common in the Netherlands (Van, 2001), see Figure 31. Other available models in the WBI2017 are Bishop’s model (Bishop, 1955) and the Spencer-Van der Meij model (Spencer, 1967; Van der Meij and Sellmeijer, 2010). The latter model does not impose restrictions on the shape of a slip plane.

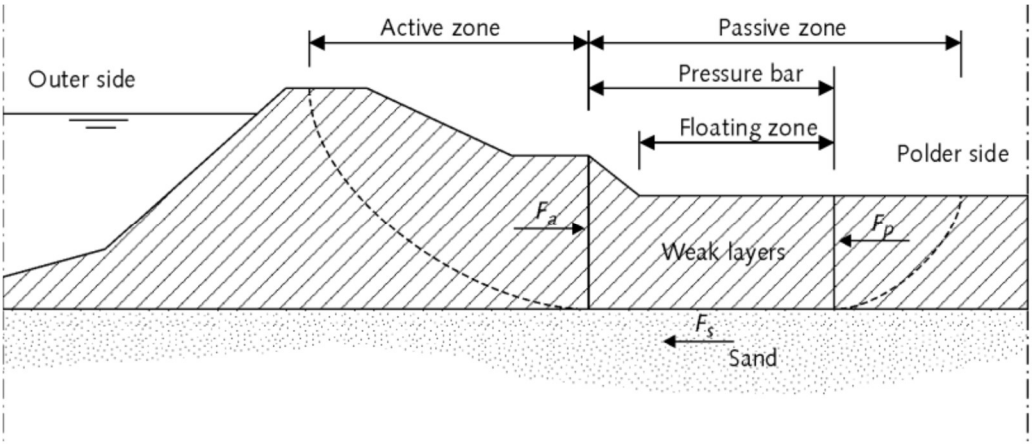

Figure 31. The Uplift-Van model with a slip plane composed of a bar bounded by two circular parts.

In these limit equilibrium models, the stability for every possible slip plane is expressed as the ratio of the resisting moment to the driving moment:

$$SF = M_R / M_D \tag{74}$$

where

SF Ratio of the resisting moment to the driving moment. This ratio is also known as a stability factor or factor of safety. It should be noted that SF is a stochastic variable, not a safety factor in a semi-probabilistic context.

M_R Resistance moment

M_D Driving moment

The lowest stability factor of the numerous possible slip plane determines the stability factor of the cross-section under consideration.

The resistance against sliding (M_R in equation (74)) is determined by the shear strengths of soils. In the WBI2017, the shear strength is modelled on the basis of Critical State Soil Mechanics (CSSM) (Schofield and Wroth, 1968), using the Stress History And Normalized Soil Engineering Properties (SHANSEP) approach (Ladd and Foot, 1974). Slope stability assessments in the Netherlands were previously based on the Mohr-Coulomb model.

All of the abovementioned sliding and constitutive models are available in D-GeoStability (Deltares, 2016).

The distributions of M_R and M_D are functions of various stochastic and deterministic variables. Since soil properties are spatially variable, so are M_D and M_R. Random fields models are available for dealing with spatial variability in limit equilibrium analyses (VanMarcke, 1977; Calle, 1985; Vanmarcke, 2011) and in more advanced numerical analyses (Griffiths and Fenton, 2004; Boulanger and Montgomery, 2016). As an approximation, the material properties can be averaged over the expected dimensions of a slip plane in a limit equilibrium stability analysis. Slope stability analyses can then be performed on the basis of random averages. This is the approach used in the WBI2017.

The limit state function can be written as follows:

$$Z = SF / m_S - 1 \quad (75)$$

where
m_S Model uncertainty

To obtain a probability of failure, conditional probabilities of failure are first calculated for a series of water levels (usually 5). The probability distribution of the critical water level, or fragility curve, is then be obtained via interpolation. Combining this fragility curve with the probability distribution of the annual water level extremes gives the probability of failure.

All slope stability calculations in the code calibration study were performed with the Uplift-Van model in the beta version of D-GeoStability of May 9th, 2016. The Deltares Water Net Creator was used to draw phreatic lines and calculate water pressures as a function of the outer water level.

8.2 Reliability requirement

The cross-sectional reliability requirement for slope instability is given by:

$$P_{T,cross} = \omega \cdot P_{max} / (1 + a \cdot L / b) \quad (76)$$

where
$P_{T,cross}$ Cross-sectional target failure probability for the failure mechanism under consideration (here: slope instability)
ω Fraction of the maximum allowable probability of flooding that has been reserved for the failure mechanism under consideration
P_{max} Maximum allowable probability of flooding or standard of protection
a The fraction of the segment deemed sensitive to slope instability
L Length of the segment
b The length of independent, equivalent stretches within the relevant part of the segment

Deriving values for a and b on the basis of system reliability analyses is complicated by the fact that probabilistic slope stability analyses are time consuming and costly, making it difficult to carry out such analyses for entire segments. This is why it was decided to adopt a = 1/30 ≈ 0.033 and b = 50 m, following part 2 of the guideline for the design or river levees (LOR2, TAW 1989) and current practice (which is already semi-probabilistic).

8.3 Safety format

8.3.1 Representative values

An overview of representative values is given in Table 4. The use of 5%-quantiles for material properties is in line with standard geotechnical engineering practice in the Netherlands. Note that all quantiles in Table 4 relate to the distributions of local averages.

Table 4. Representative values in slope stability assessments.

Symbol	Unit	Description	Distribution	Representative value
γ_{unsat}	kN/m^3	Mean unit weight of soil above phreatic level	Deterministic	-
γ_{sat}	kN/m^3	Mean weight of soil below phreatic level	Deterministic	-
S	-	Undrained shear strength ratio	Lognormal	5%-value
m	-	Strength increase exponent	Lognormal	5%-value
σ'_{vy}	kN/m^2	Vertical yield stress	Lognormal	5%-value
L_i	m	Leakage length	Lognormal	50%-value
IL	m	Intrusion length	Lognormal	50%-value
PL	m	Phreatic line relative to NAP	Deterministic	Default value (see Kanning & Van der Krogt 2016)
H	m	Water level on the water side relative to NAP	From probabilistic load model	Exceedance probability equal to standard of protection (see section 5.2)
c’	kN/m^2	Effective cohesion	Lognormal	5%-value
tan(φ’)	-	Tangent of effective friction angle	Lognormal	5%-value
m_S	-	Model uncertainty factor (different for Bishop, Uplift-Van and Spencer-Van der Meij)	Lognormal	1.0 (see section 5.2)

8.3.2 Partial safety factors

For reasons of consistency with former rules for slope stability assessments, the following safety factors were considered:

1. model factors (for a given value of β_T called β_{basis})
2. material factors (for a given value of β_T called β_{basis})
3. a β_T-dependent safety factor

According to the semi-probabilistic assessment rule, the following condition has to be met:

$$SF_d / (\gamma_d \cdot \gamma_{\beta T}) > 1 \qquad (77)$$

where

SF_d Design values of the stability factor, calculated with the use of the representative values from Table 4 and material factors (-)

γ_d Model factor (-)

$\gamma_{\beta T}$ β_T-dependent safety factor (-)

8.4 Calibrated safety factors

To derive β_T-invariant safety factors, influence coefficients were calculated for 48 cases from 27 different locations. These cases reflect the variations that can be found in the Netherlands with respect to geometry, geology, water level distribution, dike material, uplift/no uplift etc. An overview of the calculated squared influence coefficients is given in Figure 32.

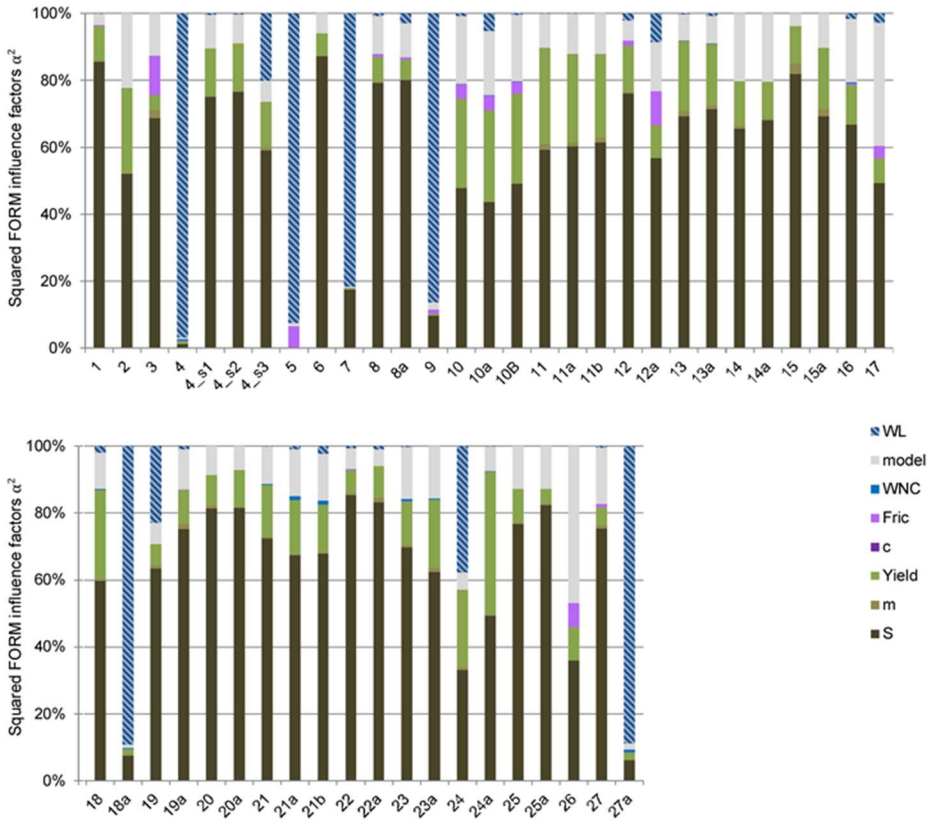

Figure 32. Overview of squared influence coefficients.

When uplift or blanket layer rupture do not play a role, as is the case for most test set members, the calculated influence coefficients of the water level are close to zero. This implies that the design point values of the water level have relatively high annual exceedance probabilities of exceedance. This, in turn, implies that the stability of dikes is relatively insensitive to the water level. This may be explained by the CSSM-framework, together with considerable uncertainty related to material properties, as well as the schematization of the phreatic line. The low (computed) sensitivity to the outer water level is conservative in the present context since it increases the apparent relative importance of the uncertainty related to the other stochastic variables.

Model factors

The model factors rest on a squared influence coefficient of the model uncertainty parameter of 0.15, β_{basis} = 4.3 and a representative value equal to 1 (so that the design value of the model uncertainty parameter equals the partial factor). The resulting model factors are shown in Table 5.

Table 5. Model factors for semi-probabilistic slope stability analyses. For background information on the distribution parameters, the reader is referred to Van Duinen (2014).

Sliding model	Distribution type	Mean value	Standard deviation	Model factor (γ_d)
Bishop*	lognormal	1.025	0.050	1.11
Uplift-Van	lognormal	1.005	0.033	1.06
Spencer-Van der Meij	lognormal	1.008	0.035	1.07

* The model factor for the Bishop model is not covered by the code calibration report (Kanning, *et al.*, 2017).

Material factors

A material factor greater than one is only obtained for $\beta_{basis} = 4.3$ when the influence coefficient of a material property (α_m) is greater than 1,645 / 4.3 = 0.38, or $\alpha_m^2 = 0.38^2 = 0.15$. Since safety factors smaller than 1 are counter-intuitive and therefore error-prone, such factors are best avoided. On the basis of the squared influence coefficients shown in Figure 32, a material factor greater than 1 would only have to be considered for the undrained shear strength ratio (S). This material factor would be equal to 1.3 for $\beta_{basis} = 4.3$, a FORM influence coefficient of 0.8 (or $\alpha_m^2 = 0.64$) and a coefficient of variation of 0.15.

The use of a material factor for the undrained shear strength ratio of 1.3 does not lead to significantly greater accuracy than the use of a material factor equal to 1.0 and a higher β_T-dependent safety factor. For practical reasons, it was therefore decided to use material factors equal to 1.0 for all material properties.

β_T-dependent safety factor

To derive a β_T-dependent safety factor, reliability indices and stability factors were calculated for all 48 cases, see Figure 33. The calculated stability factors rest on the model and material factors mentioned above and the representative values from Table 4. Varying the exceedance probabilities of the representative values of the outer water level was shown to have virtually no impact on the calculated stability factors. This is why Figure 33 does not distinguish between cases with different standards of protection. This is also why the β_T-dependent safety factor ($\gamma_{\beta T}$) was not defined as a function of the standard of protection (to which these exceedance probabilities are linked).

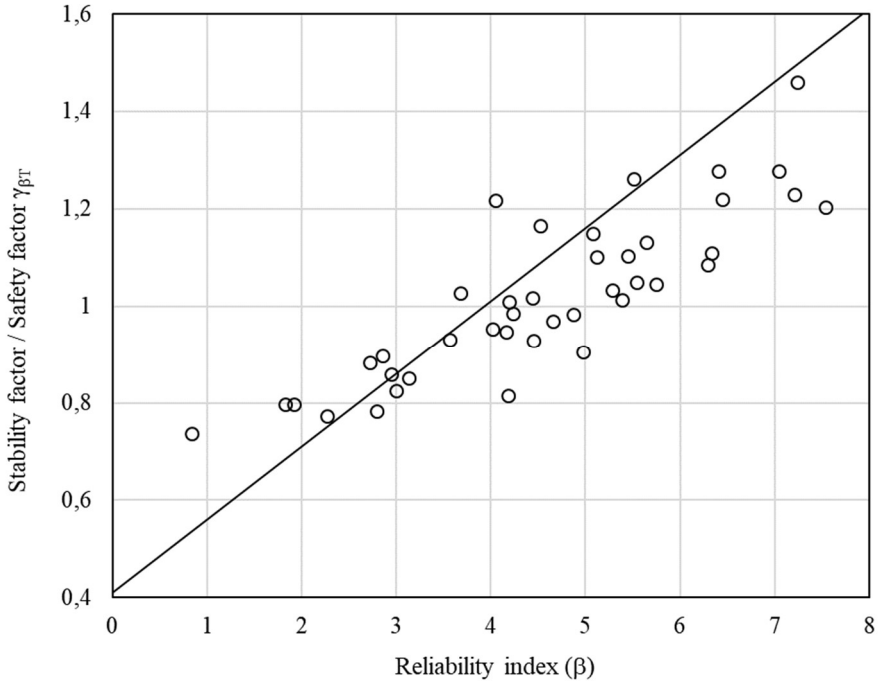

Figure 33. The relationship between the calculated reliability indices (horizontal axis) and the corresponding stability factors (vertical axis).

The β_T-dependent safety factor ($\gamma_{\beta T}$) is based on linear least squares regression for cases with $3.5<\beta<6.5$. The offset of the resulting linear relationship has been increased so that the β_T-value associated with each value of $\gamma_{\beta T}$ corresponds to a 20%-quantile (see also section 6.2.2). The resulting β_T-dependent safety factor, shown in Figure 33 by a continuous line, is given by:

$$\gamma_{\beta T} = 0.15 \cdot \beta_{T,cross} + 0.41 \qquad (78)$$

where

$\gamma_{\beta T}$ β_T-dependent safety factor
$\beta_{T,cross}$ Cross-sectional target reliability index

The β_T-dependent safety factor is not a function of the standard of protection, for the reasons mentioned above.

8.5 Comparison with former assessment rule

The CSSM-modelling framework has not previously been used in the Netherlands. The safety factors for CSSM-stability assessments cannot meaningfully be compared to the former safety factors for stability assessments on the basis of the Mohr-Coulomb model. While the CSSM-modelling framework is new to the Netherlands, the use of the new code calibrated assessment rule for the design of flood defenses has not led to unexpected results.

8.6 Discussion

For most test cases, the calculated reliability indices and stability factors are insensitive to the (uncertainty related to the) outer water level. This suggests that it might be possible to update reliability estimates on the basis of performance observations. New tools and guidelines for reliability updating are currently under development (Schweckendiek and Kanning, 2016).

Potential interactions between overtopping and slope stability were left aside in the calibration study. Overtopping may lead to infiltration, causing the phreatic line to rise. Also, in case of overtopping, superficial slip circles that by themselves do not directly endanger the stability of the levee may damage the inner slope, leading to failure caused by progressive erosion. A procedure for dealing with the interactions between slope instability and overtopping has been developed separately (Jongejan and De Visser, 2017).

It is expected that the code calibrated safety factors can also be safely applied for assessing the stability of a levee's outer slope in case of a rapid drawdown. Verifying this expectation is something for a future update of the WBI2017.

9 Dune erosion

This chapter gives a summary of the WBI2017 code calibration study for dune erosion (see Diermanse & Van Geer 2016). For further details about dune erosion assessments, the reader is referred to the WBI2017 schematization guideline (Ministry of Infrastructure and the Environment, 2016e).

9.1 Failure mechanism

9.1.1 Qualitative description

The Dutch coastal flood defenses are mostly dunes. When a storm surge, combined with the astronomical tide, leads to a water level exceeds the level of a dune foot, waves will reach and erode the dune. Sand is then transported seaward and the dune front recedes. The breaching of a dune during a storm event will lead to flooding.

An eroded dune profile will gradually recover In the period following a storm event due to onshore sediment transport and aerial transport towards the dune. In case of e.g. longshore transport gradients, periodic beach nourishments are required to maintain a sufficiently safe dune profile.

For further details about dune erosion and coastal zone management in the Netherlands, the reader is referred to the ENW technical report on dune erosion (ENW, 2007b) and the WBI2017 phenomenological report (’t Hart, De Bruijn and De Vries, 2016).

9.1.2 Failure mechanism model

The dune erosion used in the WBI2017 is the 2-dimensional Duros+ model, a volumetric sediment balance model (Roscoe and Diermanse, 2011). For a given initial dune profile, the Duros+ model calculates an erosion volume, an *initial* erosion profile and an *initial* position of the setback line (in Dutch: “afslagpunt”) on the basis of the following inputs:

1. the highest water level during the storm event under consideration,
2. the maximum significant wave height on deep water during the storm event,
3. the peak period,
4. the grain size (the median value of the grain size distribution).

In the probabilistic model, two additional stochastic variables are considered (Alkyon, Delft Hydraulics | WL and Delft University of Technology, 2007):

1. the uncertainty related to storm duration,
2. model uncertainty.

Both uncertainties are expressed in terms of linear additions to the erosion volume calculated by Duros+. These additions are used to calculate the *final* position of the setback line. The dune fails when this setback line lies landward or the critical setback line (in Dutch: “maatgevend afslagpunt”). The procedure is shown schematically in Figure 34, The figure shows the initial erosion volume (A) and the additional erosion volume (ΔA), as well as the position of the setback line before and after accounting for the uncertainties related to the storm duration and the dune erosion model.

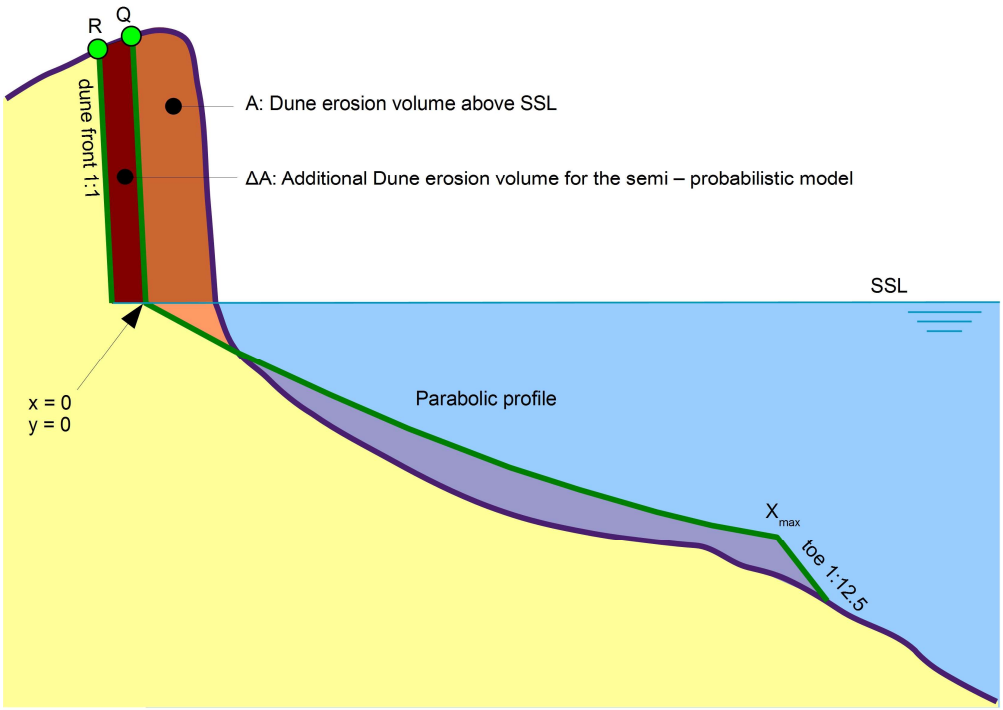

Figure 34. Initial setback line location (Q) and final setback line location (R) after correcting for the uncertainties related to the storm duration and the dune erosion model.

9.2 Reliability requirement

The cross-sectional reliability requirement for dune erosion is given by:

$$P_{T,cross} = P_T / N = \omega \cdot P_{max} / N \quad (79)$$

where

- $P_{T,cross}$ Cross-sectional target failure probability for the failure mechanism under consideration (here: dune erosion)
- P_T Target failure probability for an entire segment for the failure mechanism under consideration (here: dune erosion)
- N Length effect factor
- ω Fraction of the maximum allowable probability of flooding that has been reserved for the failure mechanism under consideration
- P_{max} Maximum allowable probability of flooding, i.e. the standard of protection

An overview of the values of the different parameters that determine the cross-sectional reliability requirement is given in Table 6.

Table 6. Parameter values pertaining to the cross-sectional reliability requirement for dune erosion.

Parameter		Motivation
N	2	Probabilistic calculations for dune segments showed N-values of 1 to 1.5 (HKV, 2015), in line with experiences from the VNK2 project. This implies that N=2 is a safe choice. The N-value is not defined as a function of the length of a segment since there is no room for meaningful optimization: N cannot be smaller than 1.
ω	0.7 (0.1)	The default value for most cases is 0.7, see Table 1. The default value of 0.1 only applies to exceptional cases.

9.3 Safety format

An overview of the representative values of the different stochastic variables is given in Table 7, together with the distributions of the stochastic variables. Largely because of the strong similarities with the semi-probabilistic rule from the WTI2011, it was decided to leave the definitions of the representative values of all stochastic variables except the water level unchanged. This prevents unnecessary changes to working practices and parameter values stored in databases. It also leads to design values that are close to design point values, which is reflected by the exceptional agreement between the outcomes of a number of probabilistic and semi-probabilistic calculations, see section 9.4.

Table 7. Stochastic variables and representative values for dune erosion assessments.

Symbol	Unit	Description	Distribution	Representative value
H	m	Water level relative to NAP	From probabilistic load model	β_T-dependent design value (see below)
H_s	m	Significant wave height	From probabilistic load model	Expected value, given the water level
T_p	s	Peak wave period	From probabilistic load model	Expected value, given the water level
D_{50} (or D_{reken})*	m	50% quantile of local grain size distribution	D_{50} is assumed to be normally distributed, with μ and σ being site-specific	Location specific values stored in databases. These are slightly smaller than average values
C_d	m^3/m	Additional erosion volume due to the uncertainty related to storm duration	Normal distribution, μ=0 m^3/m, σ=0.1V, with V being the initial erosion volume	(see ΔA)
C_m	m^3/m	Additional erosion volume due to the uncertainty related to storm duration	Normal distribution, μ=0 m^3/m, σ=0.15A, with A being the initial erosion volume	(see ΔA)
ΔA (=C_d+C_m)	m^3/m	Additional erosion volume	Normal distribution, μ=0 m^3/m, σ=0.25A, with A being the initial erosion volume	1.25

* The representative value of D_{50} is denoted as D_{reken} in the WBI2017 Schematization Guideline (Ministry of Infrastructure and the Environment, 2016e) and the ENW Technical report (ENW, 2007b), not as $D_{50,rep}$.

9.4 Calibrated design water level

A close relationship between probabilistic and semi-probabilistic assessments can be obtained with a design water level with an exceedance probability equal to about two times the cross-sectional target failure probability for an entire segment for dune erosion (see Figure 35), i.e.:

$$P(H>H_d) = 2.15 \cdot \omega \cdot P_{max} / N \quad (80)$$

Since N=2, the expression used above in the WBI2017 is almost identical to:

$$P(H>H_d) \approx \omega \cdot P_{max} \quad (81)$$

where

H_d Design water level

ω Fraction of the maximum allowable probability of flooding that has been reserved for dune erosion

P_{max} Maximum allowable probability of flooding, i.e. the standard of protection

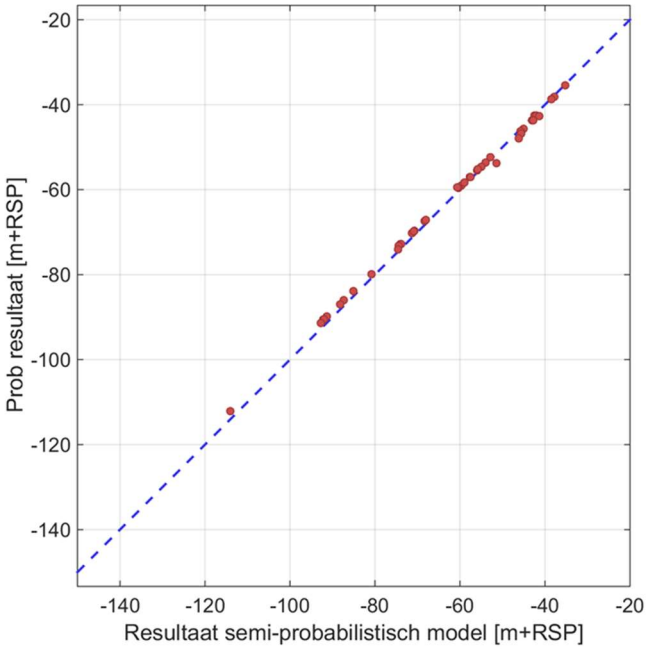

Figure 35. Comparison between the required positions of the critical setback line according to semi-probabilistic (horizontal axis) and probabilistic (vertical axis) assessments. Results shown for 45 dune profiles from different coastal segments.

The close correspondence between the results of probabilistic and semi-probabilistic assessments can be explained by the consistent, considerable relative importance of the uncertainty related to the water level, see Figure 36. This means that the exceedance probabilities of the design point values of the water level are close to the calculated probabilities of failure.

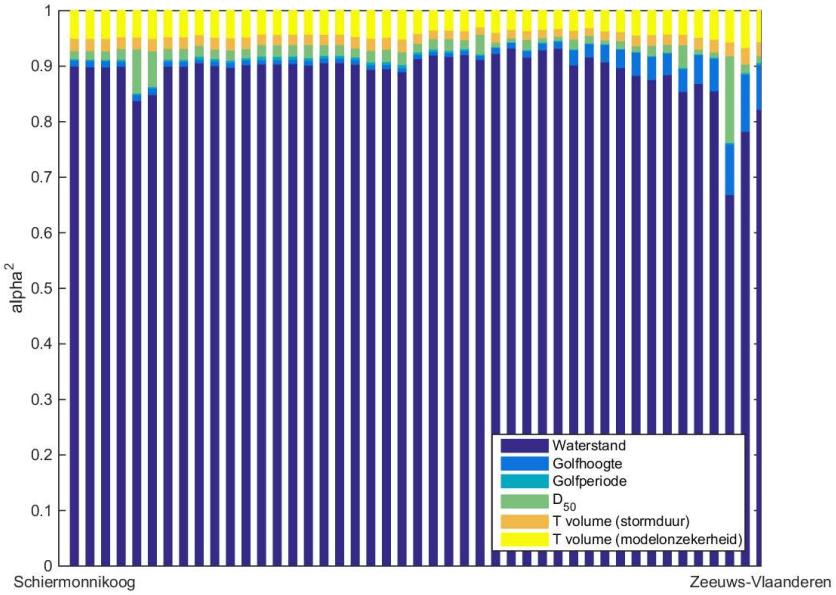

Figure 36. Squared influence coefficients of the different stochastic variables (water level in dark blue). Results shown for 45 dune profiles from different coastal segments, from Schiermonnickoog (north-east) to Zeeuws-Vlaanderen (south-west).

9.5 Comparison with former assessment rule

The calibrated WBI2017-assessment rule for dune erosion is practically identical to the former WTI2011-rule. In the WTI2011, the cross-sectional target failure probability for dune erosion was set at 10% of the value of the old standard of protection (an exceedance probability). The design water level was subsequently defined as a water level with an exceedance probability equal to 2.15 times this cross-sectional target failure probability for dune erosion. This design water level was called "rekenpeil" in Dutch. The exact same design water level can be obtained by adding 2/3 decimate heights[11] to the water level with an exceedance probability equal to the old standard of protection (this procedure is better known by practitioners).

9.6 Discussion

For locations where e.g. longshore transport gradients during storms prohibit the use of Duros+, more advanced, process-based dune erosion models such as XBeach will have to be used. Design values for XBeach have not yet been calibrated.

[11] The decimate height is the difference between two water levels with exceedance probabilities that differ by a factor 10.

10 Block revetment failure caused by wave impacts

This chapter gives a summary of the WBI2017 code calibration study for the failure of block revetments caused by wave impacts (see Jongejan & Klein Breteler 2015). For further details about assessments of block revetments, the reader is referred to the WBI2017 schematization guideline (Ministry of Infrastructure and the Environment, 2016i).

10.1 Failure mechanism

10.1.1 Qualitative description

Breaking waves may generate uplift pressures. These pressures are transmitted through the filter layer of the revetment to the region next to the impact zone (see Figure 37). When the uplift pressures are sufficiently high, blocks can be pushed out.

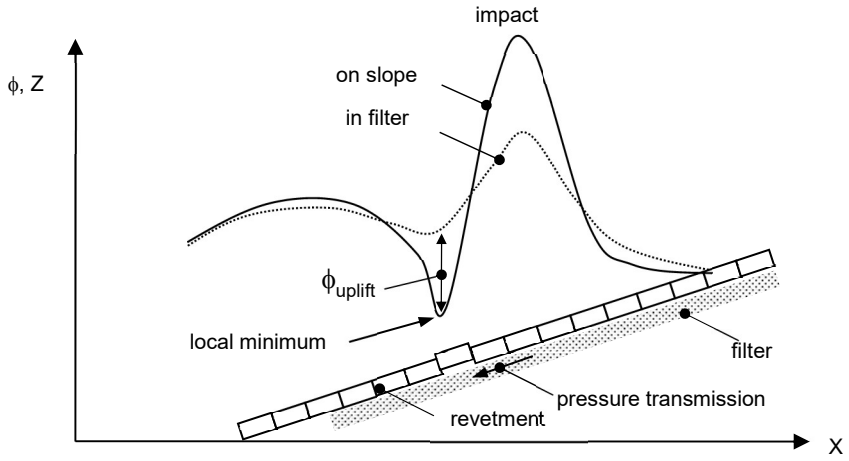

Figure 37. Pressures on the slope and under the revetment induced by wave impacts.

The failure of a block revetment does not necessarily lead to flooding: the probability of flooding given the failure of a block revetment is not equal to one. This is because of the time to failure of the revetment, the base and filter layers, geotextiles and the remainder of the levee. The time to failure of these layers is commonly referred to as "residual strength" in the Netherlands.

Figure 38 shows how the failure of a block revetment and subsequent erosion may lead to flooding. The events associated with levee failures due to the failure of block revetments under wave attack ('toetsspoor ZTG') have been highlighted. The other events/failure mechanisms are covered by different assessment rules.

For further details about this failure mechanism, the reader is referred to the WBI2017 phenomenological report ('t Hart, De Bruijn and De Vries, 2016).

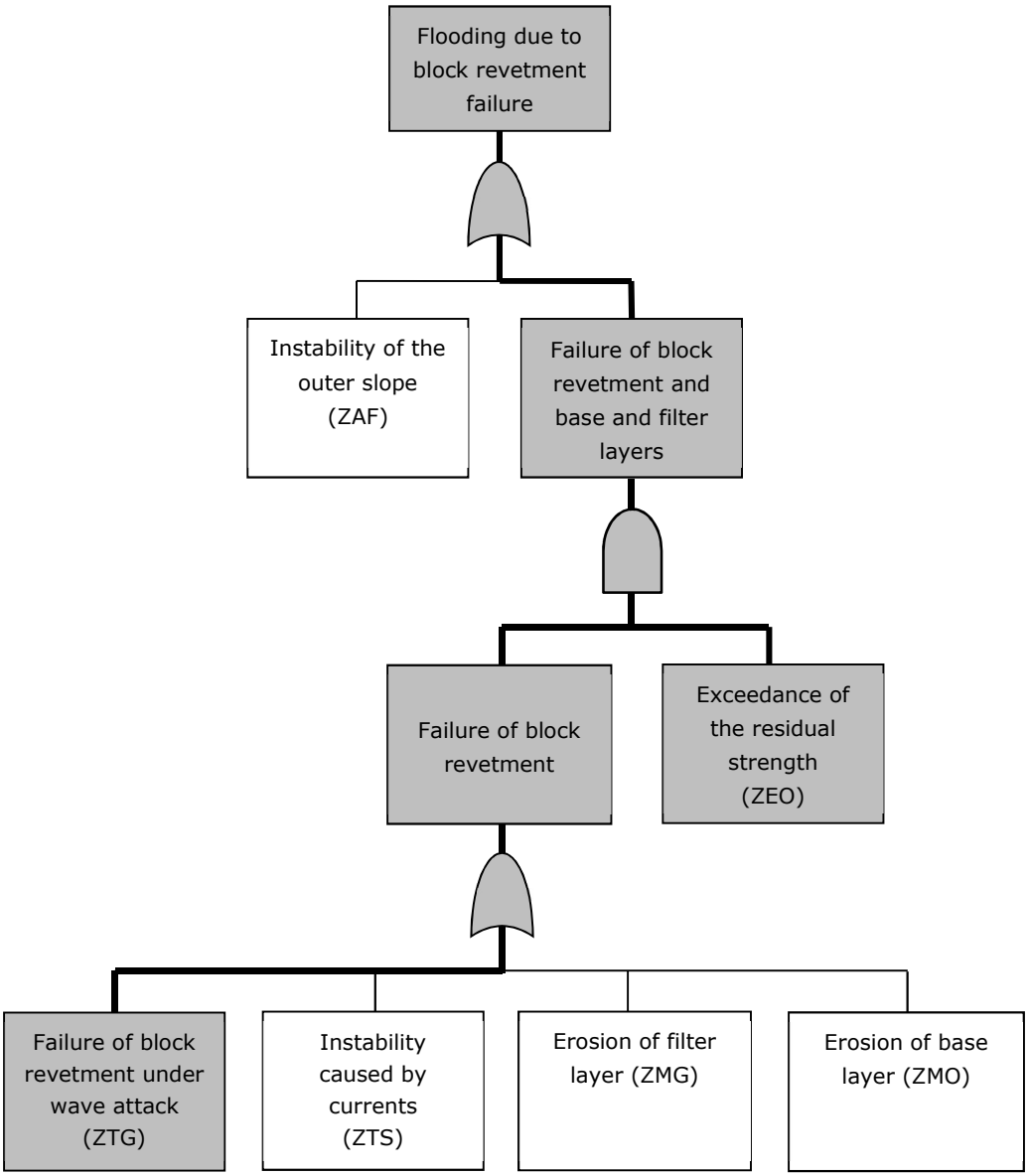

Figure 38. A fault tree for flooding due to revetment failure (former Dutch acronyms between brackets).

10.1.2 Failure mechanism model

The C#-version of Steentoets[12] would have been the ideal basis for the development of probabilistic assessment procedures for the stability of block revetments. At the time of the calibration study, only a probabilistic prototype based on this Steentoets version was available. Since the prototype was not yet sufficiently robust or efficient for large-scale application, response surfaces (also named proxy functions) were used for calibrating safety factors. A detailed discussion of the available models at the time of the calibration study is given by Jongejan et al. (2013).

[12] Steentoets is the name of a program for assessing the stability of various types of block revetments . It could be thought of as a repository of limit state functions for block revetments.

Response surfaces are available for three different types of block revetments: columns, blocks on their side, and "koperslakblokken". They are based on thousands of Steentoets calculations for three different types of block revetments. The response surfaces and the hydraulic loads are governed by relatively complex equations. This is why limit state functions are not presented here. For more details about the response surfaces, the reader is referred to Klein Breteler & Mourik (2014).

It is emphasized that the response surfaces are not part of the WBI2017. All semi-probabilistic assessments of block revetments should be carried out with Steentoets.

The impact of using a response surface rather than Steentoets in the calibration study has been investigated by comparing the outcomes of series of semi-probabilistic and probabilistic calculations with both models. The results of these calculations suggest that the use of response surfaces is slightly conservative yet unlikely to lead to noticeably higher partial safety factors: differences are smaller than 1%.

For quantifying the effect of residual strength, an experimental process-based erosion model was developed (Kaste and Klein Breteler, 2014). The model calculates, for each time step, the cumulative damage to the revetment and, following revetment failure, the erosion volume and resulting dike profile. The model is capable of dealing with a series of storms during a single storm season. The time to failure of geotextiles has been ignored.

Ideally, residual strength would have been an integral part of all probabilistic calculations. However, because of time constraints, the studies into the stability of blocks and the impact of residual strength on probabilities of failure had to be carried out in parallel. The results of these studies had to be integrated at a later stage, which is reflected in the step-wise handling of residual strength in the calibration procedure: residual strength has been included via safe estimates of conditional probabilities of failure, based on residual strength computations.

10.2 Reliability requirement

The cross-sectional reliability requirement for the stability of block revetments under wave attack is given by:

$$P_{T,cross} = \omega \cdot P_{max} \cdot \lambda_1 \cdot \lambda_2 \cdot \lambda_3 / N \cdot R \quad (82)$$

where

$P_{T,cross}$	Cross-sectional target failure probability
ω	Fraction of the maximum allowable probability of flooding that has been reserved for revetment failure
P_{max}	Maximum allowable probability of flooding, i.e. the standard of protection
λ_1	Maximum allowable contribution of failures of block revetments to the probability of flooding due to revetment failures (all types)
λ_2	Maximum allowable contribution of failures of block revetments and subsequent erosion (not slope instability, "ZAF") to the probability of flooding due to block revetment failure
λ_3	Maximum allowable contribution of failures of block revetments caused by wave attack to the overall probability of failure of a block revetment

R Reduction factor related to the correlation between revetment and overtopping failures.

The reduction factor R was introduced because of the exceptionally high relative importance of the uncertainty related to the hydraulic loading conditions (α_S<-0.9), combined with a relatively strict reliability requirement compared to the requirement for overtopping failures. The factor R follows from:

$$R = P(F_R) / P(F_R \cap \underline{F}_O) \quad (83)$$

where
F_R Failure of block revetment
$\underline{F}_O$ No overtopping failure

An overview of the values of the different parameters that determine the cross-sectional reliability requirement is given in Table 8. An overview of the contributors to the length effect is given in Figure 39.

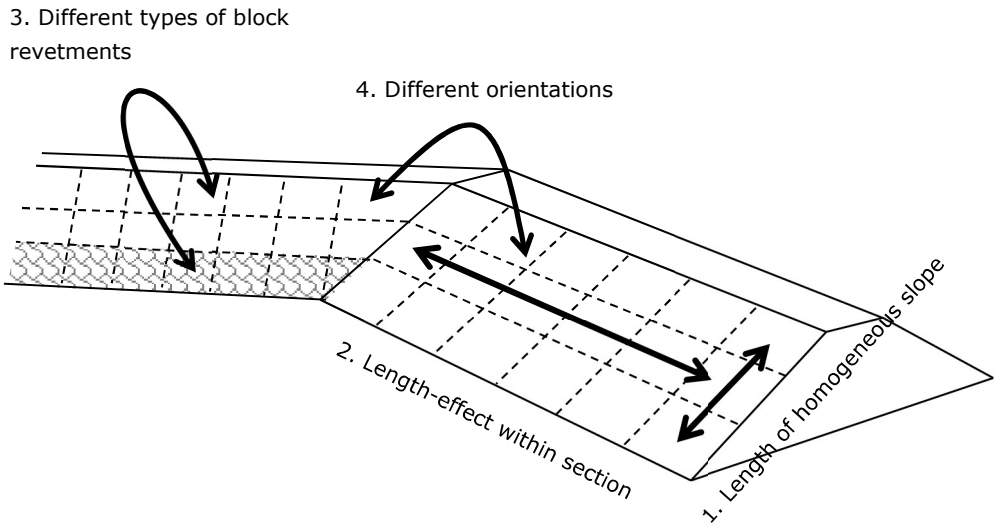

Figure 39. Schematic representation of the different contributors to the length effect.

Table 8. Parameter values pertaining to the cross-sectional reliability requirement for the stability of block revetments under wave attack.

Parameter		Motivation
N	4	The value is based on the expected importance of the various contributors to the length effect, see also Figure 39: 1. The length effect along the slope (vertical) is negligible because the scales of fluctuation of important stochastic variables are small relative to the length of a slope. Also, the critical zone is typically a fairly narrow band. 2. The length effect within a section (longitudinal) is small according to probabilistic calculations: the average length of equivalent, independent lengths is about 500m. 3. Model uncertainty parameters of different revetments are uncorrelated, giving rise to a length-effect. 4. A length effect may arise from cross sections having different orientations. The effects of contributors 3 and 4 are moderated by the fact that different revetments rarely have identical failure probabilities. Since the N-value is not predominantly related to the length of a segment, a fixed value of N=4 was chosen. The impact of variations has been evaluated in sensitivity analyses.
ω	0.1	Default value, see Table 1.
λ_1	0.5	The results of e.g. the VNK2-project indicate that block revetments are often reliable compared to grass and asphalt revetments. If λ_1 would be set equal to the average contribution of block revetments to revetment failures, λ_1 would get a (very) small value. Yet there may well be segments in which block revetments are relatively important. Choosing a relatively small value of λ_1 would lead to unduly stringent semi-probabilistic assessments for those cases. An intermediate value of λ_1=0.5 was therefore chosen.
λ_2	0.9	Failures of the outer slope due to slope instability ("ZAF") are assumed to be relatively improbable. A value of λ_2=0.9 was therefore assumed. Note that any value close to one would yield similar reliability requirements. Strictly speaking, the failure mechanisms "ZAF", "ZTS" and "ZMO" should be placed in the category "other" in Table 1. $\lambda_2=\lambda_3=1$ would then be appropriate. As discussed with and confirmed by the project management team of the WBI2017 (minutes of April 28, 2015, no. 1220077-000-HYE-0007), the failure mechanisms "ZAF", "ZTS" and "ZMO" have been treated as sub-failure mechanisms for "flooding due to revetment failure". Note that $\lambda_2=\lambda_3=1$ would hardly lead to different reliability requirements/safety factors.
λ_3	0.7	The outcomes of past statutory assessments suggest that instability of block revetments due to wave attack is a relatively important failure mechanism, suggesting that a relatively high value of λ_3 should be chosen.
R	2-4	These values rest on probabilistic calculations, see equation (83), with ω=0.24 for overtopping failure, see Table 1.

10.3 Safety format

10.3.1 Representative values

Representative values for wind and wave parameters have to be derived with an approximate probabilistic load model named "hydraulische-belastingen-bekledingen" (previously called "Q-variant") for an exceedance probability equal to the maximum allowable probability of flooding. The use of this exceedance probability facilitates comparisons between today's rules and the WBI2017-rules. An overview of the representative values of the other stochastic variables is given in Table 9.

Table 9. Stochastic variables and representative values for assessments of block revetments.

Symbol	**Unit**	**Description**	**Distribution**	**Representative value**
B	m	Width of blocks	Normal	50%-value
d_i	m	Thickness of filter layer i	Normal	50%-value
cot(α)	-	Cotangent of the slope of the revetment	Normal	50%-value
d_{klei}	-	Thickness of clay layer	Truncated normal	50%-value*
D	m	Thickness of top layer	Normal	50%-value
D_{f15}	m	15% quantile of the grain size distribution of the filter layer	Normal	50%-value
D_{f50}	m	50% quantile of the grain size distribution of the filter layer	Normal	50%-value
D_{i15}	m	Grain size of the infilling material	Normal	50%-value
L	m	Length of blocks	Normal	50%-value
n_{f1}	-	Porosity of filter material	Normal	50%-value
s_l	m	Width of horizontal joints	Normal	50%-value
s_s	m	Width of vertical joints	Normal	50%-value
tan(α)	-	Tangent of the outer slope	Normal	50%-value
$\tan(\alpha_{bottom})$	-	Tangent of the slope of the foreland	Normal	50%-value
Z_b	m	Upper boundary of the block revetment relative to NAP	Normal	50%-value
h_{berm}	m	level of the berm relative to NAP	Normal	50%-value
$Z_{voorland}$	m	Level of toe of the dike relative to NAP	Normal	50%-value
Z_0	m	Lower boundary of the block revetment relative to NAP	Normal	50%-value
ρ_S	kg/m^3	Block density	Normal	5%-value
Ω	-	Relative open surface of the revetment	Normal	50%-value
m_{br}	-	Model factor (different for each revetment type)	Lognormal	1.0 (see section 5.2)

* Median value of a normal distribution without truncation

The representative values of all model factors are equal to one. This effectively means that analysts do not have to determine representative values for model uncertainties.

The block densities that are currently used in safety assessments and design are close to 5%-quantile values. This quantile also fits with calculated influence coefficients. This is why the 5% quantile was chosen as the representative value for the block density.

The representative values of all stochastic variables in Table 9 are average values. The use of average values for these stochastic variables fits with calculated influence coefficients. It is also practical. Because the number of stochastic variables in Steentoets is considerable and because some variables concern spatial averages rather than point values, calculating e.g. 5% quantiles for some of these variables would be tedious and error-prone. Also, the values of these stochastic variables that are currently used in safety assessments and design are close to average values.

10.3.2 Partial safety factors

The dominant sources of uncertainty are the hydraulic load (α_S is typically smaller than -0.9), the block density and the model uncertainty (α_m is typically 0.1-0.3). This implies that the design point values of the other variables are close to their 50%-quantile values. Appropriate partial safety factors for these variables are thus close to 1. Hence, only the following two safety factors were considered:

1. A model factor (derived for a fixed target reliability), applied to the representative value of the model uncertainty parameter.
2. A β_T-dependent safety factor, applied to the block thickness.

These two factors have been combined into a single, overall safety factor to simplify the safety format (see also section 5.4).

10.3.3 Residual strength

In theory, the target reliability for the stability of a block revetment under wave attack could be written as a continuous function of the design values of residual strength variables. Safety factors that depend on elaborate residual strength computations would strongly complicate semi-probabilistic assessments however. Developing such sophisticated rules was also not feasible within the timeframe of the WBI2017-project. Three easily identifiable residual strength classes have therefore been defined. Safe estimates of conditional probabilities of flooding have been assigned to each class. With these conditional probabilities, semi-probabilistic assessments can be carried out as follows:

1. select the residual strength class to which the cross section belongs,
2. divide the cross-sectional target failure probability for the stability of the block revetment by the (safe estimate of the) conditional probability of flooding associated with the residual strength class from step 1,
3. calculate the β_T-dependent safety factor for the adjusted reliability requirement,
4. carry out the semi-probabilistic assessment for the stability of (only) the block revetment under wave attack with the β_T-dependent safety factor from step 3.

The abovementioned procedure rests on two conservative assumptions (i.e. assumptions that create a bias towards the safe side):

1. Within each residual strength class, the highest conditional probability of flooding is used for all cross-sections that belong to that class.

2. Only the reliability requirement is adjusted. The impact of the uncertainty related to residual strength on the influence coefficients of the other stochastic variables is ignored.

Using an advanced prototype model, Kaste & Klein Breteler (2014) carried out a series of probabilistic calculations for the stability of concrete columns and subsequent erosion. Based on the insights obtained from these calculations, they proposed the following residual strength classes (Klein Breteler, 2015):

1. Small residual strength, if:
   – $H_s > 2.0$ m or
   – $d_c/H_s < 0.6$ and $B_{dike}/H_s < 20$
2. Large residual strength, if:
   – $H_s < 1.5$ m and $d_c/H_s > 0.8$
   – $H_s < 1.5$ m and $B_{dike}/H_s > 30$
3. Medium residual strength, if the residual strength is neither small nor large

where

H_s Significant wave height at the toe of the structure as used for the simple safety assessment

d_c Thickness of the clay layer

B_{dike} Width of the dike at the assessment water level as used for the simple safety assessment

10.4 Calibrated safety factors

10.4.1 Computational results

The calculated β_T-dependent safety factors, including the effect of residual strength, are shown in Table 10. Results for the default length effect factor N=4 are shown in bold. Results for non-existing standards of protection are shown in grey.

Table 10. β_T-dependent safety factors including the effect of residual strength, for different length effect factors.

Block type	Water system	P_{max} (per year)	β_T-dependent safety factor								
			Small residual strength			Medium residual strength			High residual strength		
			N=2	**N=4**	N=8	N=2	**N=4**	N=8	N=2	**N=4**	N=8
Columns	Western Scheldt	1/300	1,02	**1,06**	1,09	0,90	**0,94**	0,98	0,78	**0,83**	0,88
		1/1000	1,01	**1,05**	1,08	0,90	**0,94**	0,98	0,79	**0,84**	0,88
		1/3000	1,01	**1,04**	1,07	0,91	**0,94**	0,98	0,81	**0,85**	0,89
		1/10000	1,00	**1,03**	1,06	0,91	**0,94**	0,97	0,82	**0,85**	0,89
		1/30000	1,00	**1,03**	1,06	0,91	**0,94**	0,97	0,82	**0,86**	0,89
	Wadden Sea	1/300	1,03	**1,06**	1,09	0,91	**0,95**	0,98	0,79	**0,84**	0,88
		1/1000	1,01	**1,04**	1,07	0,90	**0,94**	0,97	0,80	**0,84**	0,88
		1/3000	1,00	**1,03**	1,06	0,90	**0,93**	0,96	0,81	**0,84**	0,88
		1/10000	0,99	**1,02**	1,04	0,90	**0,93**	0,95	0,81	**0,84**	0,87
		1/30000	0,99	**1,01**	1,04	0,90	**0,92**	0,95	0,81	**0,84**	0,87
	Lake IJssel	1/300	1,12	**1,18**	1,23	0,98	**1,05**	1,11	0,85	**0,92**	0,99
		1/1000	1,09	**1,14**	1,20	0,96	**1,02**	1,08	0,85	**0,91**	0,97
		1/3000	1,06	**1,11**	1,16	0,94	**1,00**	1,05	0,84	**0,90**	0,95
		1/10000	1,04	**1,09**	1,14	0,93	**0,98**	1,03	0,83	**0,89**	0,94
		1/30000	1,02	**1,07**	1,11	0,92	**0,97**	1,01	0,82	**0,87**	0,92

Block type	Water system	P_{max} (per year)	β_T-dependent safety factor								
			Small residual strength			Medium residual strength			High residual strength		
			N=2	**N=4**	N=8	N=2	**N=4**	N=8	N=2	**N=4**	N=8
Blocks on their side	Western Scheldt	1/300	0,99	**1,04**	1,08	0,86	**0,91**	0,96	0,74	**0,80**	0,86
		1/1000	0,99	**1,03**	1,07	0,87	**0,92**	0,97	0,77	**0,82**	0,87
		1/3000	0,99	**1,03**	1,07	0,88	**0,92**	0,97	0,78	**0,83**	0,87
		1/10000	0,99	**1,03**	1,07	0,89	**0,93**	0,97	0,80	**0,84**	0,88
		1/30000	0,99	**1,03**	1,06	0,89	**0,93**	0,97	0,81	**0,85**	0,89

The effect of residual strength rests on a careful interpretation of the outcomes of residual strength calculations. While the impact of residual strength could be far greater in some cases, more daring conclusions would require further study. Such studies could also be tailored to site-specific conditions in advanced assessments (in Dutch: "beoordeling op maat"). The cautious handling of residual strength is in line with Rijkswaterstaat's position on this topic. The calibration procedure itself can easily accommodate future refinements.

10.4.2 Interpretation and proposal

Based on the computational results presented in Table 10, it was proposed to adopt partial safety factors on the block thickness that only depend on the residual strength classification:

- Small residual strength: $\gamma = 1.1$
- Medium residual strength: $\gamma = 1.0$
- Large residual strength: $\gamma = 0.9$

The proposal rests on the following considerations:

- Differences in safety factors of less than e.g. 5% lie within the uncertainty bandwidth surrounding the results presented in Table 10. Such small differences would also be of little practical relevance: a 5% difference corresponds to a 1 cm difference for a block thickness of 20 cm, or 2 cm for a block thickness of 40 cm.
- The calibrated partial safety factor for the block thickness is virtually independent of the flood protection standard. This can be explained by the fact that the representative value of the hydraulic load is tied to the flood protection standard, see also Figure 23. A more stringent flood protection standard therefore leads to a higher representative load. Because of the dominance of the uncertainty related to the hydraulic load, the change in the representative load is sufficient to account for the effect of a more stringent flood protection standard.
- Differentiating between Lake IJssel and the other water systems would lead to partial safety factors that are about 5% to 10% greater along Lake IJssel than elsewhere (see Table 10). The greatest differences would be found for the lowest residual strength class and the highest maximum allowable probabilities of flooding: 1/300 and 1/1000 per year. The associated representative hydraulic loads are significantly lower than the representative loads for today's flood protection standards (exceedance probabilities of 1/4,000 and 1/10,000 per year along Lake IJssel). It therefore seems unlikely that a 5% to 10% higher safety factor along Lake Ijssel would make a difference. Because of this, no distinctions are made between Lake IJssel and the other water systems.

- The impact of residual strength is sufficient to warrant a dependence of the safety factor on the residual strength classification.

10.5 Comparison with former assessment rule

The proposed new partial safety factors for the WBI2017 range from 0.9 to 1.1. The older WTI2011-assessment rule contains a partial safety factor of 1.0, independent of the amount of residual strength. Representative values are defined similarly. This implies that the implementation of the proposed new safety factors will not lead to a radical departure from status quo. Changes in probabilistic load models are likely to have greater consequences.

The integration of (1) assessments of the stability of blocks and (2) the residual strength of base and filter layers is an important improvement over the conservative, step-wise procedure of the past. The integrated procedure makes it possible to take residual strength into account in a less conservative manner. While the handling of residual strength in the newly calibrated rule still rests on cautious estimates of the effect of residual strength, the procedure itself can easily accommodate future refinements.

10.6 Discussion

The calibrated safety factors rest on code calibration studies for two most common types of block revetments in the Netherlands and a study into the effect of residual strength. While not all types of blocks have been considered, the calibrated partial safety factors are believed to be more broadly applicable. This is because the models for other block types rest on similar theories and conservative assumptions. Also, the results for columns and blocks on their side are very similar, despite the very different behaviors of these blocks under wave attack.

The safety factors can only be used in assessments of block revetments in the Netherlands with Steentoets as implemented in the WBI2017. Significant changes to Steentoets or the residual strength model could necessitate changes to the calibrated safety factors.

The impact of residual strength on failure probabilities can be analyzed in greater detail in future studies, possibly within the context of advanced assessments (the “beoordeling op maat”). The results can then be used to update the semi-probabilistic rule.

11 Asphalt revetment failure caused by wave impacts

This chapter gives a summary of the WBI2017 code calibration study for the failure of asphalt revetments due to wave impacts (see Klerk & Kanning 2014). For further details about assessments of asphalt revetments, the reader is referred to the WBI2017 schematization guideline (Ministry of Infrastructure and the Environment, 2016e).

11.1 Failure mechanism

11.1.1 Qualitative description

Asphalt revetments are usually constructed directly on a sandy dike body. Fatigue, caused by wave impacts, may lead to the failure of an asphalt revetment. Progressive erosion may then lead to flooding, see Figure 40. The events associated with wave attack ('toetsspoor AGK') have been highlighted. The other events/failure mechanisms are covered by different assessment rules. For further details about this failure mechanism, the reader is referred to the WBI2017 phenomenological report ('t Hart, De Bruijn and De Vries, 2016).

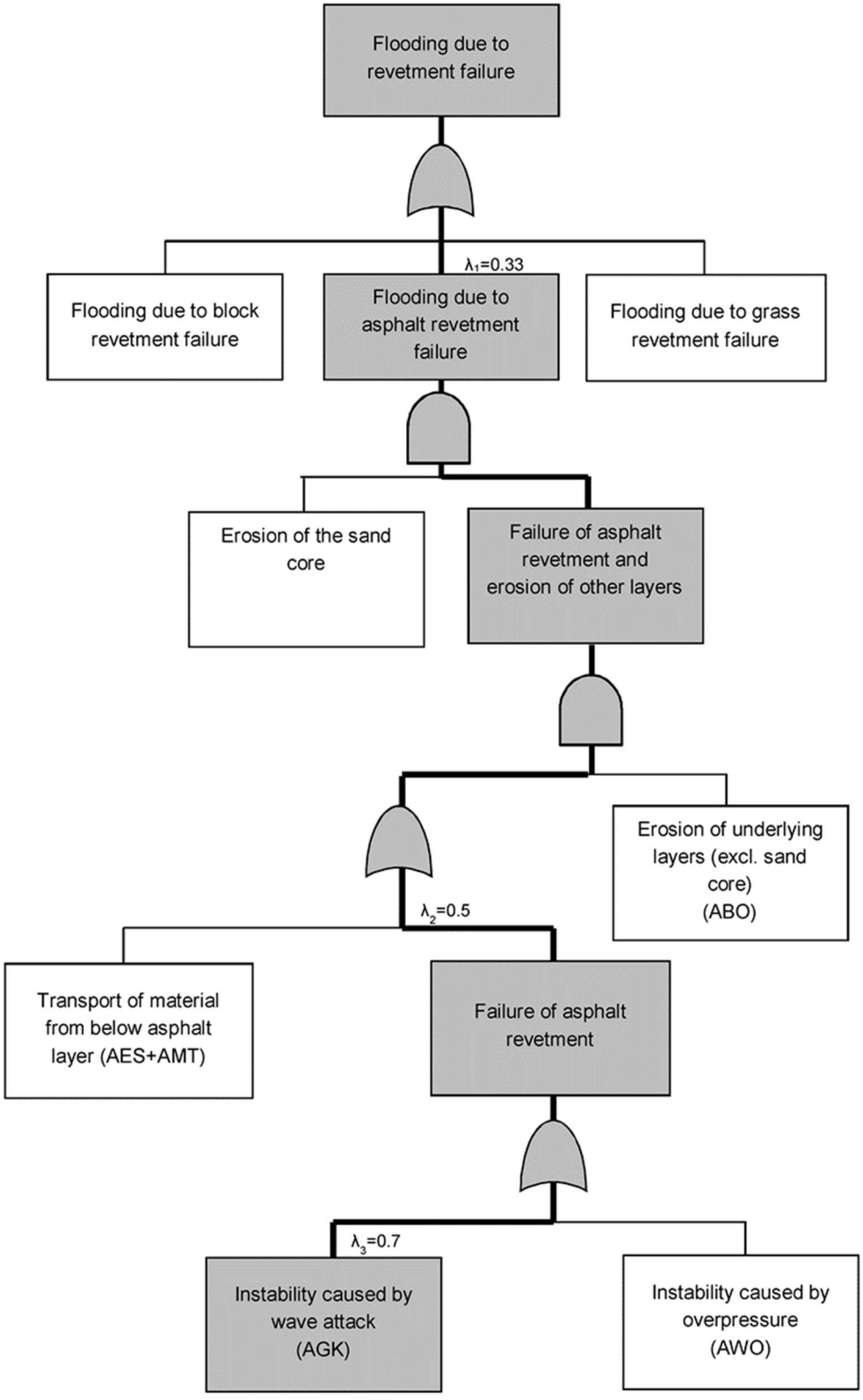

Figure 40. A fault tree for flooding due to asphalt failure caused by wave impacts (former Dutch acronyms between brackets).

11.1.2 Failure mechanism model

A fatigue model has been implemented in WaveImpact. WaveImpact compares the stresses that occur in the asphalt during a storm event due to wave impacts to the asphalt's resistance against fatigue. To that end, each storm event is divided into small time steps and the cross-section is divided into parts. For each time step, the model calculates the stresses that occur in the different parts of the revetment. For each part, the model calculates the Miner sum and compares it to the maximum or critical value of the Miner sum. For more information on WaveImpact, the reader is referred to KOAC-NPC (2009).

11.2 Reliability requirement

The cross-sectional reliability requirement for the stability of an asphalt revetment under wave attack is given by:

$$P_{T,cross} = \omega \cdot P_{max} \cdot \lambda_1 \cdot \lambda_2 \cdot \lambda_3 / N \cdot R \quad (84)$$

where

$P_{T,cross}$	Cross-sectional target failure probability
ω	Fraction of the maximum allowable probability of flooding that has been reserved for revetment failure
P_{max}	Maximum allowable probability of flooding, i.e. the standard of protection
λ_1	Maximum allowable contribution of failures of asphalt revetments to the probability of flooding due to revetment failure (all revetment types)
λ_2	Maximum allowable contribution of failures of asphalt revetments due to damages that occur during storms (AGK and AWO). AES and AMT concern damages that occur before/between storms.
λ_3	Maximum allowable contribution of AGK to failures of asphalt revetments due to caused either AGK or AWO.
R	Reduction factor related to the correlation between revetment and overtopping failures.

The spatial scale to which the outcomes of (2-dimensional) WaveImpact-calculations apply is uncertain. If WaveImpact were interpreted as an unbiased model for truly cross-sectional evaluations, the length of equivalent, independent stretches would be in the order of 10m due to the strong spatial variability of relatively uncertain resistance parameters. This, however, would lead to highly unrealistic probabilities of failure for longer stretches. Revetment specialists believe the results of cross-sectional probabilistic calculations with WaveImpact on the basis of the statistics of point values to relate to lengths of about 1 kilometer. The length effect factor N is therefore given by:

$$N = \max\{ 1 , a \cdot L / 1000\ m \} \quad (85)$$

where

a	Fraction of the length of the segment with an asphalt revetment
L	Length of the segment

An overview of the values of the parameters that determine the cross-sectional reliability requirements is given in Table 11.

Table 11. Parameter values pertaining to the cross-sectional reliability requirement for the stability of asphalt revetments under wave attack.

Parameter		Motivation
ω	0.1	Default value, see Table 1.
λ_1	0.33	Asphalt revetments are often combined with other types of revetments.
λ_2	0.5	Revetment specialists believe that initial damages (unnoticed or not yet repaired) contribute strongly to the failure probabilities of asphalt revetments, which would imply a very small value of λ_2. Improvements in inspection and maintenance are expected to reduce the probability of damages prior to storms. This is why revetment specialists have suggested a value of 0.5.
λ_3	0.7	The failure of an asphalt revetment failure due to wave impact (AGK) is considered more likely than failure due to overpressure (AWO)
R	1	Because the influence coefficient of the hydraulic load is around -0.5 to -0.8 for failures of asphalt revetments, the correlation between failures of asphalt revetments and overtopping failures is small.

11.3 Safety format

11.3.1 Representative values

The representative values for water level and wave parameters are to be derived from an approximate probabilistic load model named "hydraulische-belastingen-bekledingen" (previously called "Q-variant") for an exceedance probability equal to the maximum allowable probability of flooding. This ensures consistency across failure mechanisms and facilitates comparisons between today's rules and the WBI2017-rules. An overview of the representative values of the other stochastic variables is given in Table 12.

Table 12. Stochastic variables and representative values for assessments of asphalt revetments.

Symbol	**Unit**	**Description**	**Distribution**	**Representative value**
c	MPa/m	Modulus of subgrade reaction	Lognormal	5%-value
d_l	m	Thickness of the asphalt layer	Lognormal	5%-value
E_l	MPa	Stiffness of the asphalt top layer	Lognormal	95%-value
$\sigma_{b,l}$	MPa	Strength in bending of the asphalt top layer	Lognormal / Student-t	5%-value
m	-	Model uncertainty	Lognormal	1.0*

* In the calibration report, the design value of the model uncertainty parameter is presented as a β_T-invariant safety factor equal to 1.77. This implies a representative value equal to 1.0, see also see section 5.2. Note that the combination of a representative value of m equal to its expected value (μ_m=1.77) and a partial factor of 1.0 gives the same end-result, namely a design value m_d equal to 1.77.

11.3.2 Partial safety factors

The safety format is such that a revetment passes the semi-probabilistic assessment when the following condition is met:

$$-\text{Log10}(\gamma_m \cdot \text{Miner}) > \gamma_{\beta T} \quad (86)$$

where

γ_m Model factor (see discussion in section 11.3.1 on the meaning of this parameter)

$\gamma_{\beta T}$ β_T-dependent safety factor

Miner Miner-sum as calculated by WaveImpact

The following safety format may seem more intuitive:

$$\gamma_{\beta T}^* \cdot \gamma_m \cdot \text{Miner} < 1 \quad (87)$$

A disadvantage of such a safety format is that values of $\gamma_{\beta T}^*$ would have to range from 1 to more than 30. Safety factors that vary over such a range would be most unusual. This can be avoided with the safety format given by equation (86). Note that $\gamma_{\beta T} = \log10(\gamma_{\beta T}^*)$ and $\gamma_{\beta T}^* = 10^{\gamma \beta T}$.

11.4 Calibrated safety factors

From field observations and the results of previous safety assessments, the distinction between the characteristics of old (>40 years) and young asphalt appears to be important, especially with respect to the coefficient of variation for the cracking strength. This leads to very different β_T-dependent safety factors for old and young asphalt. Because the coefficient of variation of the cracking strength is not only influenced by ageing but also by construction quality, β_T-dependent safety factors were calibrated for coefficients of variation of 0.2 and 0.35. β_T-dependent safety factors for intermediate coefficients of variation can be derived via linear interpolation.

Because of significant differences between the calibrated β_T-dependent safety factors for different water systems, different factors were defined for the Wadden Sea, Lake IJssel, the Western Scheldt and the coast. An overview of the calibrated β_T-dependent safety factors is given in Table 13.

Table 13. β_T-dependent safety factor for assessing the stability of asphalt revetments under wave attack.

Water system	CoV cracking strength	β_T-dependent safety factor
Western Scheldt/ Coast	0.2 (young asphalt)	$\gamma_{\beta T} = 0.52\ (\beta_{T,cross}\text{-}1.97) - 0.33\ \beta_{max}$
	0.35 (old asphalt)	$\gamma_{\beta T} = 0.61\ (\beta_{T,cross}\text{-}1.99) - 0.34\ \beta_{max}$
Wadden sea	0.2 (young asphalt)	$\gamma_{\beta T} = 0.57\ (\beta_{T,cross}\text{-}2.37) - 0.29\ \beta_{max}$
	0.35 (old asphalt)	$\gamma_{\beta T} = 0.68\ (\beta_{T,cross}\text{-}2.47) - 0.26\ \beta_{max}$
Lake IJssel	0.2 (young asphalt)	$\gamma_{\beta T} = 0.74\ (\beta_{T,cross}\text{-}1.28) - 0.66\ \beta_{max}$
	0.35 (old asphalt)	$\gamma_{\beta T} = 0.82\ (\beta_{T,cross}\text{-}1.37) - 0.68\ \beta_{max}$

Values of $\gamma_{\beta T}$ range from about 0.3 to 0.7 for young asphalt, depending on the standard of protection, the length of the segment and loading characteristics. For old asphalt, values of $\gamma_{\beta T}$ range from about 0.5 to 1.1.

11.5 Comparison with former assessment rule

In the WTI2006, no safety factors were used for assessments of the stability of asphalt revetments under wave attack (Rijkswaterstaat, 2007). This means that the newly calibrated assessment rule marks an important departure from status quo. For $\gamma_m \cdot \gamma_{\beta T}^* > 1$ or, equivalently, $\gamma_m \cdot 10^{\gamma_{\beta T}} > 1$, the new rule is stricter than the WBI2006 rule when the old and new standards are numerically the same. For instance, for $\gamma_m = 1.77$ and $\gamma_{\beta T} = 0.3$, the newly calibrated rule requires the Miner-sum to be a factor $1.77 \cdot 10^{0.3} = 3.5$ times greater than before. For $\gamma_{\beta T} = 1{,}1$, the difference is a factor $1.77 \cdot 10^{1.1} = 22$. Changes to WaveImpact and the probabilistic load model may also lead to differences between assessments based on the WBI2017 and assessments according to the WTI2006 and the WTI2011.

11.6 Discussion

The calibrated semi-probabilistic assessment rule for the stability of asphalt revetments under wave attack can be used for most water systems in the Netherlands. No safety factors were calibrated for the Eastern Scheldt. This is because the relatively complex water level and wave statistics in this estuary, since these are influenced by the possible closure and failure of the Eastern Scheldt Barrier. Also, the vast majority of asphalt revetments along the Eastern Scheldt concerns "open steen asfalt", rather than the more common "waterbouwasfaltbeton".

Because of limits to parameter values in WaveImpact, all calculations were carried out with wave heights H_{m0} smaller than 3 m, slopes between 1:2 and 1:7, asphalt thicknesses (top layer thicknesses) of at least 0.1 m and a Young's modulus not greater than 25,000 MPa. These limits also exist within the version of WaveImpact that has been implemented in the WBI2017.

The calibrated WBI2017 assessment rule is stricter than the former WTI2006 assessment rule when the maximum allowable probability of flooding is equal to the former exceedance probability standard. This is mainly because the calibration study led to awareness of the effects of spatial variability (length effects) and model uncertainties.

The calibration study revealed the importance of a better understanding of the way in which the spatial variability of input parameters should be dealt with in WaveImpact calculations. A closely related issue concerns the spatial scale to which the outcomes of WaveImpact calculations apply. These issues are important for quantifying length effects, for being able to specify model uncertainties and for validating the WaveImpact model against field observations and/or full scale tests. With an improved failure mechanism model, a semi-probabilistic rule could again be calibrated along the lines set out by Klerk and Kanning (2014).

12 Grass revetment failure caused by wave impacts

This chapter gives a summary of the WBI2017 code calibration study for the failure of grass revetments on a levee's outer slope caused by wave impacts (Klerk and Jongejan, 2016). For further details about assessments of grass revetments, the reader is referred to the WBI2017 schematization guideline (Ministry of Infrastructure and the Environment, 2016f).

12.1 Failure mechanism

12.1.1 Qualitative description

Wave impacts can cause damage to the grass cover of a levee's outer slope. The subsequent erosion of base layers and the dike body may lead to flooding. An overview of this failure mechanism is given in Figure 41. For further details, the reader is referred to the WBI2017 phenomenological report ('t Hart, De Bruijn and De Vries, 2016). The part of the failure mechanism that is considered in WBI2017 assessment is shown in the top part of Figure 41.

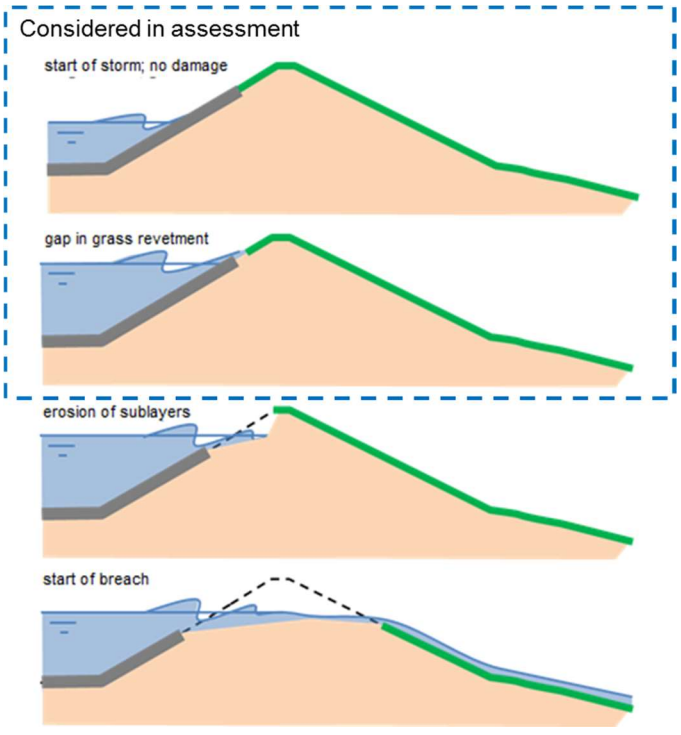

Figure 41. Levee failure caused by grass revetment failure (due to wave impact or wave run-up).

Figure 40 shows how wave impact may lead to flooding. The events associated with this failure mechanism ('toetsspoor GEBU') have been highlighted. The other events/failure mechanisms are covered by different assessment rules. It should be noted that "GEBU" covers failures of grass revetments caused by both wave run-up and wave impacts. The wave run-up mechanism is discussed separately in chapter 13.

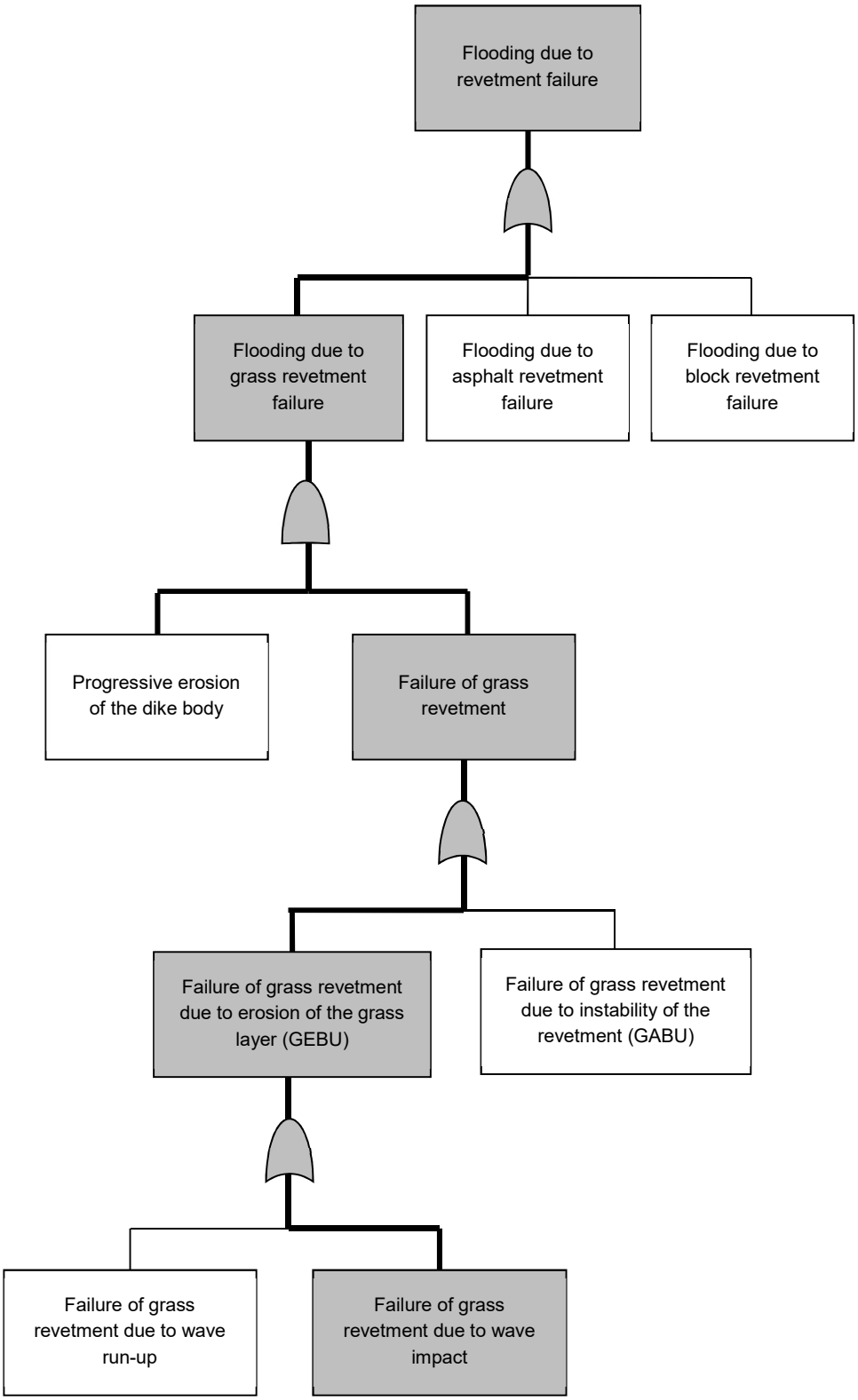

Figure 42. A fault tree for flooding due to grass revetment failure caused by wave impact (former Dutch acronyms between brackets). The events that are considered in WBI2017 assessments of the stability of grass revetments under wave impacts are shown in grey.

12.1.2 Failure mechanism model

The failure of a grass revetment due to wave impact is modelled on the basis of a relationship between critical significant wave height and the load duration:

$$H_{m0,crit} = a \cdot \exp(-b \cdot T) + c \quad (88)$$

where

$H_{m0,crit}$ Critical value of the significant wave height (m)
T Load duration (s)
a Stochastic variable (m)
b Deterministic constant (s^{-1}); b = 0.035 s^{-1} for an closed grass cover, b = 0.07 s^{-1} for an open grass cover
c Deterministic constant (m); c = 0.25 m

Note that the abovementioned relationship can also be used inversely to compute the time to failure for a given significant wave height. The distributions of the constant "a" for closed and open sods is given in Table 14. They are based on an interpretation of the outcomes of flume experiments and field observations.

Table 14. The distributions of the constant a in equation (88).

Parameter	Distribution type	Mean value (m)	Standard deviation (m)
Closed sod	Lognormal	1.82	0.62
Open sod	Lognormal	1.40	0.50

The highest wave impacts on grass revetments take place around the water line. The water level during a storm event may vary, exposing different parts of a grass slope to different wave impacts with different durations. The grass revetment fails when $H_{mo,crit}$ is exceeded somewhere along the outer slope.

12.2 Reliability requirement

The cross-sectional reliability requirement for grass revetment failures caused by impacts is given by:

$$P_{T,cross} = \omega \cdot P_{max} \cdot \lambda_1 \cdot \lambda_2 \cdot \lambda_3 / N \cdot R \quad (89)$$

where

$P_{T,cross}$ Cross-sectional target failure probability
ω Fraction of the maximum allowable probability of flooding that has been reserved for revetment failure
P_{max} Maximum allowable probability of flooding, i.e. the standard of protection
λ_1 Maximum allowable contribution of failures of grass revetments to the probability of flooding due to revetment failures (all revetment types)
λ_2 Maximum allowable contribution of failures of grass revetments due to erosion ("GEBU"), not sliding ("GABU").
λ_3 Maximum allowable contribution of wave impact, not wave run-up.
R Reduction factor related to the correlation between revetment and overtopping failures.

An overview of the values of the parameters that determine the cross-sectional reliability requirements is given in Table 15.

Table 15. Parameter values pertaining to the cross-sectional reliability requirement for grass revetment failures caused by wave impacts.

Parameter		Motivation
N	3	The length effect for this failure mechanism is expected to be dominated by variations in the orientation of the levee, just like the length effect for overtopping failures. N=3 is the highest value used in probabilistic cross-sectional overtopping assessments in the WBI2017.
ω	0.1	Default value, see Table 1.
λ_1	0.5	Grass revetments are generally present alongside other types of revetments. Note that the values of λ_1 for grass, asphalt and block revetments add up to a value greater than one. This is because it is believed to be too conservative to assume that they are equally reliable.
λ_2	1	Revetment specialists believe erosion to be a considerably more important failure mechanism ("GEBU") than sliding ("GABU"). This implies a value of λ_2 close to 1. For reasons of simplicity, a value of 1.0 has been chosen.
λ_3	1	Erosion caused by wave impact and erosion caused by wave run-up are strongly correlated failure mechanisms
R	1	The conditions that are relevant for this failure mechanism may be different from the ones that are most relevant for overtopping failures when water levels and wave heights are not strongly correlated.

12.3 Safety format

The design value of the hydraulic load is defined by an exceedance probability equal to the cross-sectional target failure probability, not an exceedance probability equal to the standard of protection. This rests on the following considerations:

1. The uncertainty related to the hydraulic load is relatively important. Defining the design value of the hydraulic load by a relatively small exceedance probability leads to a relatively strong link between probabilistic and semi-probabilistic assessments.
2. To be able to identify where grass can safely be applied along a slope, the reliability of a grass revetment has to be evaluated at different levels. When the water level and wave height are strongly correlated, it is likely that the reliability requirement can only be satisfied when the transition from a hard (block, asphalt) revetment to a grass revetment lies at a level where the probability of observing a (severe) wave impact is smaller than the cross-sectional target failure probability. Defining the design value of the hydraulic load by an exceedance probability that is greater than the cross-sectional failure probability might make it impossible to determine the required level of the transition correctly.

The only other stochastic variable in the limit state function concerns the variable "a" that describes the uncertainty related to $H_{m0,crit}$, see equation (88). Its design value is a constant. It has not been split into a representative value and a safety factor.

12.4 Calibrated safety factors

With a design value of the hydraulic load that is defined as a function of the cross-sectional target reliability, there is no need for a β_T-dependent safety factor.

From probabilistic analyses for coastal areas, it appears that the importance of the uncertainty related to resistance is insignificant ($\alpha_a \approx 0$) compared to the uncertainty related to the loading conditions. For such cases, the use of a median resistance-duration curve in semi-probabilistic assessments would be appropriate.

For riverine areas, where water levels and wave heights are largely independent, the influence coefficients of stochastic variable "a" are typically in the order of 0.3 to 0.5. In such cases, a design value with a cumulative probability of about 1-5% would be appropriate.

Rather than specifying different design values (or partial safety factors) for "a" for coastal and riverine areas, it was decided to consistently adopt a design value with a cumulative probability of 5%. This rests on the following considerations:

1. Sheltered locations along the coast (or a lake) may more closely resemble a riverine location than a coastal location.
2. The design value of "a" is largely irrelevant for wind-dominated regimes. In such cases, grass revetments will only pass an assessment at a level where the probability of a wave impact is smaller than the cross-sectional target failure probability. Using e.g. a 5% or a 50% quantile value for "a" will not significantly change the outcome of an assessment.
3. For riverine areas, the exceedance probability of the design load is somewhat conservative. This is because it rests on $\alpha_{Hs} \approx -1$ instead of e.g. $\alpha_{Hs} = -(1-0.3^2) = -0.91$. It was therefore decided to define the design value of "a" by a cumulative probability of 5% rather than 1%.

12.5 Comparison with former assessment rule

The former assessment rule focused on wave impacts within a clearly defined impact zone. The fact that, in reality, there is no such thing as a fixed/deterministic impact zone is recognized by the newly developed assessment procedure. The new procedure requires assessments at different levels, as the critical level cannot always easily be identified without such assessments.

The exceedance probability of the representative load in the newly calibrated assessment rule is significantly smaller than the standard of protection. This is different from the past, when standards were defined in terms of exceedance probabilities of design loads.

Although the exceedance probability of the design loads are very different from the ones used in the past, the design values of $H_{m0,crit}$ for different load durations are broadly similar to the ones proposed by Rijkswaterstaat (2012), see Figure 43 and Figure 44.

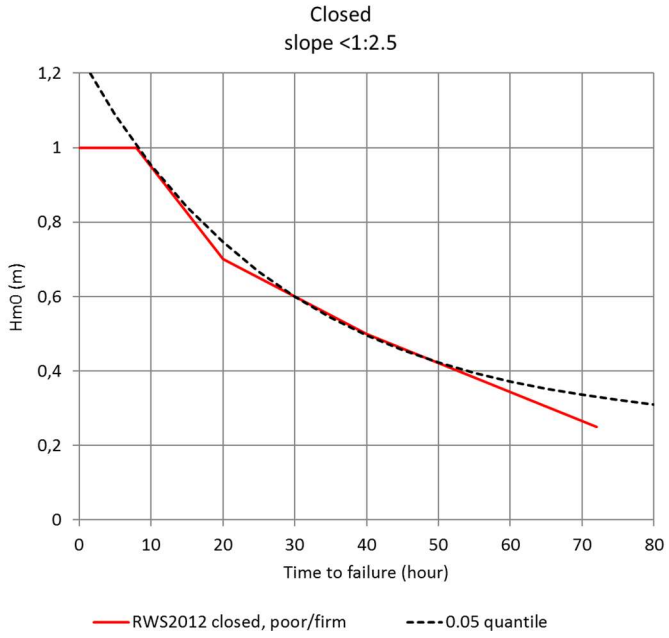

Figure 43. Relationship between the critical significant wave height and the load duration for a closed sod.

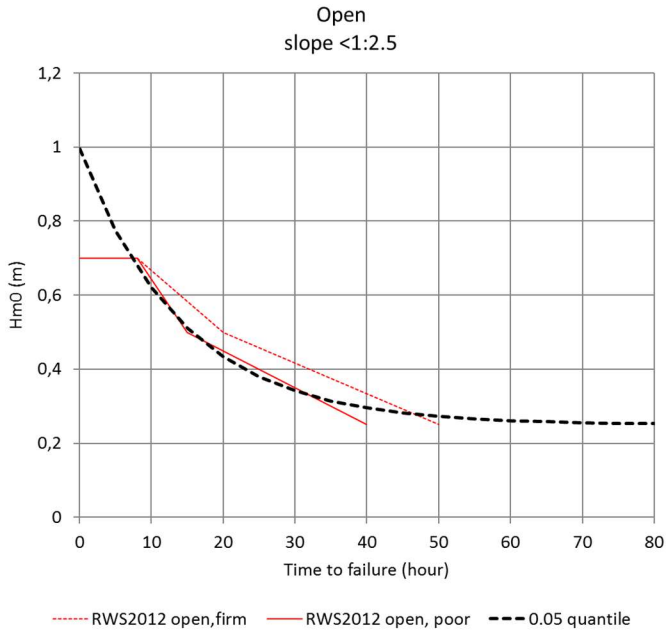

Figure 44. Relationship between the critical significant wave height and the load duration for an open sod.

The above shows that the design values of $H_{m0,crit}$ for the newly calibrated rule are broadly similar to the ones proposed by Rijkswaterstaat (2012). This, combined with the lower exceedance probabilities of the hydraulic loads, suggests the newly calibrated rule is more conservative than the 2012-assessment rule.

12.6 Discussion

Considering the fact that the newly calibrated rule appears to be stricter than the existing rule, a careful evaluation of its consequences is recommended. When these are unexpected, assumptions concerning the distributions of input parameters could be revisited. Also, the residual strength of base layers could be included in assessments. Scrutinizing the modelling of the hydraulic loads should be a priority however. The hydraulic loads are calculated with approximate probabilistic load model named "hydraulische-belastingen-bekledingen" (previously called "Q-variant"). This is because a probabilistic load model that is capable of providing time-dependent information, not just level crossing statistics, is unavailable at present.

The residual strength of the dike body is not considered in reliability assessments of grass revetments in the WBI2017. This is conservative, particularly in riverine areas. In these areas, the correlation between water levels and wave heights is typically small, so that high wave impacts are most likely at relatively low water levels where the dike is relatively wide. Whether this conservatism will have to be addressed in future updates of the WBI2017 will strongly depend on the practical implications of ignoring residual strength in riverine areas.

13 Grass revetment failure caused by wave run-up

This chapter gives a summary of the WBI2017 code calibration study for the failure of grass revetments on a levee's outer slope caused by wave run-up (Klerk and Jongejan, 2016). For further details about assessments of grass revetments, the reader is referred to the WBI2017 schematization guideline (Ministry of Infrastructure and the Environment, 2016f).

13.1 Failure mechanism

13.1.1 Qualitative description

Wave run-up can cause damage to the grass cover of a levee's outer slope. The subsequent erosion of base layers and the dike body may lead to flooding. The lowest resistance to wave run-up is generally found at the transition between a hard revetment (e.g. block or asphalt) and grass. This is usually the starting point of erosion. For further details, the reader is referred to the WBI2017 phenomenological report ('t Hart, De Bruijn and De Vries, 2016).

In the WBI2017, the residual strength of base layers and the dike body is not considered. The part of the failure mechanism that is considered in the assessment is shown in the first two figures in Figure 41 in chapter 12.

Figure 45 shows how wave run-up may lead to flooding. The events associated with this failure mechanism ('toetsspoor GEBU') have been highlighted. The other events/failure mechanisms are covered by different assessment rules. It should be noted that "GEBU" covers failures of grass revetments caused by both wave-up and wave impacts. The wave impact mechanism has already been discussed in chapter 12.

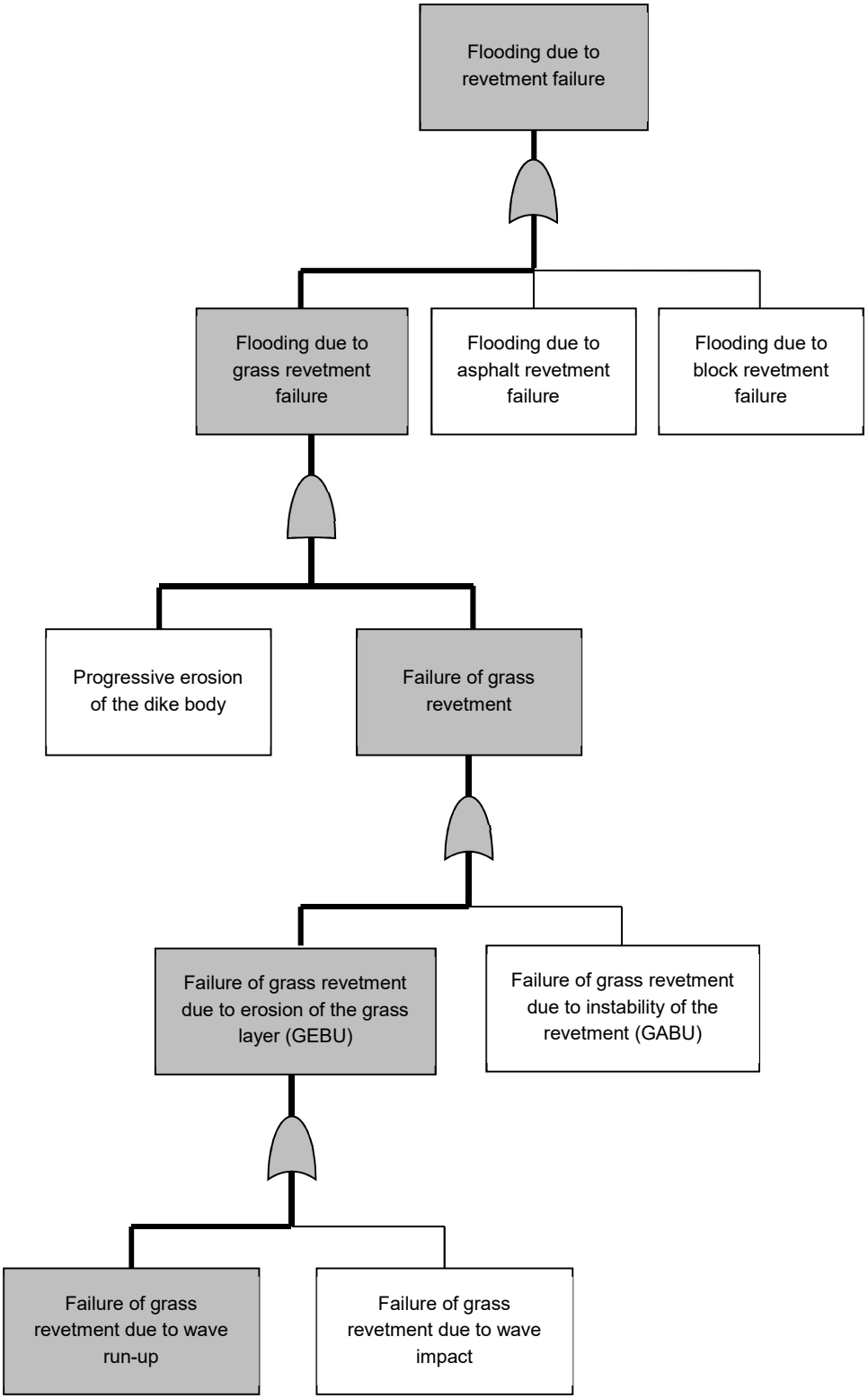

Figure 45. A fault tree for flooding due to grass revetment failure caused by wave run-up (former Dutch acronyms between brackets). The events that are considered in WBI2017 assessments of the stability of grass revetments under wave run-up are shown in grey.

13.1.2 Failure mechanism model

The failure of a grass revetment due to wave run-up is modelled using a cumulative overload approach (Van der Meer *et al.*, 2010; Van der Meer, Steendam and Van Hoven, 2015). The cumulative overload is given by:

$$D = \sum_{i=1..N} (\max\{ \alpha_m \cdot U_i^2 - \alpha_s \cdot U_c^2 \ ; \ 0\}) \quad (90)$$

where
- D Cumulative overload (m^2/s^2)
- N Number of waves (-)
- U_i Velocity of wave front of running up wave i out of N (m/s)
- U_c Critical flow velocity of a wave front (m/s)
- α_s Strength reduction factor in case of a transition (-)
- α_m Load increase factor in case of a transition (-)

The limit state function is given by:

$$Z = D_{crit} - D \quad (91)$$

where
- D Cumulative overload (m^2/s^2)
- D_{crit} Critical cumulative overload (m^2/s^2)

Experiments have shown that the critical cumulative overload is around 7000 m^2/s^2. The cumulative overload is evaluated at the most critical level, which is usually the transition between a 'hard' revetment (e.g. block, asphalt) and a grass revetment. For more details on the software implementation of the cumulative overload model, see Van Hoven and De Waal (2015).

13.2 Reliability requirement

The cross-sectional reliability requirement for the stability of a grass revetments under wave run-up is the same as the cross-sectional reliability requirement for the stability of a grass revetments under wave impact, see section 12.2.

13.3 Safety format

An overview of representative values is given in Table 16. The representative value of the hydraulic load is defined by an exceedance probability equal to the cross-sectional target failure probability. This was mostly done for reasons of consistency with the wave impact mechanism for grass revetments, for which the same exceedance probability is considered in semi-probabilistic assessments (see section 13.3). Using an exceedance probability equal to the standard of protection would lead to higher safety factors.

Table 16. Stochastic variables and representative values for assessments of grass revetments subject to wave run-up.

Symbol	Unit	Description	Distribution	Representative value
U_i		Velocity of wave front of wave i out of N		Value with an exceedance probability equal to the cross-sectional target failure probability
U_c	m/s	Critical flow velocity of a wave front	Lognormal	5%-value
D_{crit}	m^2/s^2	Critical value of cumulative overload	Lognormal	50%-value
α_m	-	Factor for increased load at transitions and objects*	Deterministic** (α_m=1)	-
α_s	-	Factor for decreased strength at transitions and objects*	Deterministic** (α_s=1)	-

* While these are stochastic variables in principle, they are treated as deterministic in the WBI2017.

13.4 Calibrated safety factors

The β_T-dependent safety factor was code calibrated using the cumulative overload approach and a simplified probabilistic load model, for three different water systems and a broad range of standards of protection. Results are shown Table 17.

Table 17. Values of the calibrated β_T-dependent safety factor for the default failure probability budget.

P_{max} (yr^{-1})	β_T	Lake IJssel	Wadden Sea	Western Scheldt
1/300	3.86	0.92	0.96	0.95
1/1,000	4.15	0.93	0.97	0.96
1/3,000	4.39	0.93	0.98	0.97
1/10,000	4.65	0.94	1.00	0.98
1/30,000	4.87	0.95	1.01	0.98
1/100,000	5.10	0.96	1.02	0.99

The value of the β_T-dependent safety factor is consistently close to 1.0, regardless of the water system or standard of protection. This is why a fixed value of 1.0 was chosen, for use in combination with the default failure probability budget from Table 1. The WBI2017 refers to the relationships shown in Table 18 for deriving β_T-dependent safety factors for different failure probability budgets.

Table 18. β_T-dependent safety factor for assessing wave run-up.

Water system	β_T-dependent safety factor
Western Scheldt	$\gamma_{\beta T} = 0.245\ (\beta_{T,cross} + 3.10) - 0.157\ \beta_{max}$
Wadden sea	$\gamma_{\beta T} = 0.235\ (\beta_{T,cross} + 3.27) - 0.142\ \beta_{max}$
Lake IJssel	$\gamma_{\beta T} = 0.303\ (\beta_{T,cross} + 2.76) - 0.257\ \beta_{max}$

In practice, the use of the relationships shown in Table 18 is unlikely to lead to values of $\gamma_{\beta T}$ that differ significantly from 1.0. In general, there is little benefit in optimizing the default value of ω=0.1 for revetment failures: increasing ω will hardly influence the assessment rules for revetments (not just wave run-up), while decreasing ω will hardly give more room to other failure mechanisms since ω=0.1 is already a relatively small value.

13.5 Comparison with former assessment rule

The failure mechanism model underlying the WTI2006-rule for wave run-up assessments (Rijkswaterstaat, 2007) differs in various respects from the one underlying the newly calibrated WBI2017-assessment rule. This hinders a direct comparison of the calibrated assessment rule with the WTI2006-rule.

First, the WTI2006 rule for wave run-up assessments rests on an erosion model based on the CIRIA-curves (Hewlett, Boorman and Bramley, 1987). These curves were developed for the design of waterways and are based on experiments in which young grass (1-2 growing seasons old) was subjected to stationary flow. In writing the VTV2006, it was recognized that both the erosive load in the wave run-up zone and the strength of a fully developed grass sod are quite different from the conditions in the CIRIA-experiments.

Second, the grass quality description differs in the WTI2006 and the WBI2017. In the WTI2006, the classifications were ‘good’, ‘moderate’ and ‘bad’. In the WBI2017, they are ‘closed’, ‘open’ or ‘fragmented’, the latter having no erosion resistance at all. The sod descriptions now rest on the presence of open spots in the root system. Previously, the root density was considered more important than the presence of open spots.

Third, the WTI2006-load model gave constant flow velocities in the run-up zone. The WBI2017-model takes the maximum front velocity for each wave during a storm event.

13.6 Discussion

The development of the WBI2017-assessment rule for wave run-up failures of grass revetments took place under significant time pressure. Various pragmatic choices had to be made. These primarily relate to the inputs of the failure mechanism model and the model itself. The cumulative overload model that underlies the assessment rule is based on the results of large-scale overtopping experiments. It has primarily been developed for assessments of the inner slopes of dikes. Not all wave run-up experiments led to failures of the grass sod, implying the model may be conservative. Still, the model is believed to be an improvement compared to the CIRIA-model. For other items related to grass revetments that should be considered in future updates of the WBI2017, see section 12.6.

14 Concluding remarks

To more efficiently manage the risk of flooding in the Netherlands, new flood protection standards have been introduced in 2017. These are defined in terms of maximum allowable probabilities of flooding. Safety assessments on the basis of the new standards require clear distinctions between:

1. reliability requirements,
2. the modelling of physical processes or phenomena ("pure" physics, no implicit safety margins), i.e.
    a. load and failure mechanism models including model uncertainties
    b. model inputs and their uncertainties.
3. methods for evaluating whether the reliability requirements are met.

There are essentially two methods for assessing whether a flood defense complies with a flood protection standard:

1. Probabilistic (using e.g. Monte Carlo, Directional sampling, FORM)
2. Semi-probabilistic (using a partial factor or load and resistance factor design approach)

To ensure consistency between probabilistic and semi-probabilistic assessments, the former safety assessment rules for levees and hydraulic structures had to be (re)calibrated. A standardized code calibration procedure was developed for reasons of consistency, efficiency and transparency. This procedure was applied successfully to various failure mechanisms.

Design values, and hence partial factors, depend on cross-sectional target reliability indices. These vary throughout the Netherlands because of variations in the standards of protection and the length effect. It would be impractical, however, if all partial factors were to vary from segment to segment. This is why it was decided to derive the values of all but one partial factor for a fixed reliability index, β_{basis}, and to include a factor ($\gamma_{\beta T}$) that corrects for the difference between β_{basis} and that actual target reliability β_T. For dune erosion and grass revetment failure, the design loads were defined as a function of β_T. While these design loads could have been split into representative values and β_T-dependent partial factors, doing so would have only made the semi-probabilistic assessment rules for these mechanisms more complex and less accurate.

In future updates of the WBI2017, the semi-probabilistic assessment rules presented herein could be improved in various ways, by considering more test cases, by using more refined load models or by applying more advanced fitting procedures. Improving models and revisiting the distributions of input parameters is likely to be more important, however, than investing in more refined code calibration studies.

For geotechnical failure mechanisms such as piping and slope instability, obtaining a close relationship between semi-probabilistic and probabilistic assessments proved to be relatively difficult. This is because soil properties are highly variable throughout the country. It is impossible to accurately cover such variability with a single set of safety factors. While the ensuing conservatism could, in theory, be reduced by specifying different sets of safety factors for different conditions, it may not be straightforward to clearly define these conditions. Furthermore, variability

within easily identifiable groups of cases may still be significant. Rather than attempting to refine semi-probabilistic methods, moving towards to a truly probabilistic approach may well be easier.

Although the presentation of material in this report may suggest otherwise, engineering judgment played a vital role in the code calibration studies. Sensitivity analyses triggered valuable discussions on input parameters and modelling assumptions. While this report only shows final results, the importance of the several rounds of calculations and discussions that preceded them should not be overlooked. A mechanical approach to code calibration, in which computational results are simply taken at face value, is strongly advised against. This is because modelling inevitably involves simplification. Engineering models have not always been developed with a probabilistic application in mind, meaning they may contain safe biases. These have to be addressed to avoid unnecessary conservatism.

The calibration studies gave early insight into the likely outcomes of (semi-)probabilistic assessments, created awareness of model biases and the importance of model and parameter uncertainties, helped identify bugs in software models developed for the WBI2017 and raised questions related to schematization guidelines and the precise definitions of input parameters when conditions are spatially variable. As such, the calibration studies have helped the move towards a truly probabilistic approach to flood protection, a move that will take many more years to complete.

An overview of the code calibrated semi-probabilistic assessment rules can be found in Appendix 3 of the WBI2017 (Ministry of Infrastructure and the Environment, 2016c). A primary flood defense that complies with these assessment rules complies with statutory requirements.

References

't Hart, R., De Bruijn, H. and De Vries, G. (2016) *Fenomenologische beschrijving Faalmechanismen WTI*. Deltares, report no. 1220078-000-GEO-0010, version 3, 18 February 2016, final.

Alkyon, Delft Hydraulics | WL and Delft University of Technology (2007) *Dune erosion. Product 3: Probabilistic dune erosion prediction method*.

Allen, T. M., Nowak, A. S. and Bathurst, R. J. (2005) 'Calibration to determine load and resistance factors for geotechnical and structural design', *Transportation Research E-Circular*, (E-C079).

Arnold, P., Fenton, G. A., Hicks, M. A., Scheckendiek, T. and Simpson, B. (eds) (2013) *Modern Geotechnical Design Codes of Practice, Implementation, Application and Development*. Amsterdam: IOS Press.

Van Balen, W., Diermanse, F., Wojciechowska, K., Roscoe, K., Lopez de La Cruz, J., Steenbergen, H. and T., V. (2016) *Hydra-Ring 2.0, Probabilistics toolbox for the WTI2017, Technical Reference Manual*. Deltares, report no. 1230088-DSC-0072.

Bazzurro and Cornell (2004) 'Nonlinear Soil-Site Effects in Probabilistic Seismic-Hazard Analysis', *Bulletin of the Seismological Society of America*, 94(6), pp. 2110–2123.

Bedford, T. and Cooke, R. (2001) *Probabilistic Risk Analysis: Foundations and Methods*. Cambridge: Cambridge University Press.

Bishop, A. W. (1955) 'The use of the slip circle in the stability analysis of slopes', *Geotechnique*, 5, pp. 7–17.

Boulanger, R. W. and Montgomery, J. (2016) 'Nonlinear deformation analyses of an embankment dam on a spatially variable liquefiable deposit', *Soil Dynamics and Earthquake Engineering*, 91, pp. 222–233. doi: 10.1016/j.soildyn.2016.07.027.

Calle, E. O. F. (1985) 'Probabilistic analysis of stability of earth slopes', in *Proceedings of the Eleventh International Conference on Soil Mechanics and Foundation Engineering*. San Francisco, 12-16 August 1985, pp. 809–812.

Calle, E. O. F. (2007) 'Statistiek bij Regionale Proevenverzamelingen deel 1', *Geotechniek*, July.

Calle, E. O. F. (2008) 'Statistiek bij Regionale Proevenverzamelingen deel 2', *Geotechniek*, Januari.

Calle, E. O. F. and Barends, F. B. J. (1990) *PROSTAB een computerprogramma voor probabilistische analyse van stabiliteit van taluds*. Grondmechanica Delft, CO-266484/32.

Calle, E. O. F. and Van der Meer, M. T. (1997) *Probabilisme in de Geotechniek. Onderdeel ruimtelijke variabiliteit, Fase A.III. E*. Rapport Grondmechanica Delft,

report no. 361410/95, December 1997.

CIRIA (1977) *Rationalisation of safety and serviceability factors in structural codes*. CIRIA Report 63, London.

CUR (2002) *CUR190 Kansen in de civiele techniek. Deel 1: probabilistisch ontwerpen in theorie*. Civieltechnisch Centrum Uitvoering Research en Regelgeving.

Deltares (2016) *D-Geo Stability - Slope stability software for soft soil engineering – User manual*. version 16.1.1, Deltares, the Netherlands.

Diermanse, F. (2017) *WBI - Onzekerheden Overzicht van belasting- en sterkteonzekerheden in het wettelijk beoordelingsinstrumentarium*. Deltares, report no. 1220080-001-ZWS-0004-r, final.

Diermanse, F. and Van Geer, P. (2016) *Semi-probabilistisch toetsvoorschrift voor duinen ten behoeve van WTI2017*. Deltares, report no. 1220080-008-ZWS-0002.

Van Duinen, A. (2014) *Modelonzekerheidsfactoren Spencer-Van der Meij model en ongedraineerde schuifsterkte*. Deltares, report. no. 1207808-001-GEO-0005, version 2, 17 December 2014.

EN1990 (2002) *Eurocode - Basis of structural design*.

ENW (2007a) *Addendum op het technisch rapport waterkerende grondconstructies*. Expertise Netwerk Waterveiligheid.

ENW (2007b) *Technisch rapport Duinafslag (in Dutch)*. Expertise Netwerk Waterveiligheid.

ENW (2012) *Technisch Rapport Grondmechanisch Schematiseren bij Dijken (in Dutch)*. Expertise Netwerk Waterveiligheid.

ENW (2017) *Fundamentals of Flood Protection*. Expertise Netwerk Waterveiligheid, Ministry of Infrastructrure and the Environment.

Faber, M. H. and Sørensen, J. D. (2002) *Reliability based code calibration*. Zurich, Switzerland: Joint Committee on Structural Safety.

Fenton, G. A. and Naghibi, F. (2014) 'Reliability-Based Geotechnical Design Code Development', in *Vulnerability, Uncertainty, and Risk*. Reston, VA: American Society of Civil Engineers, pp. 2468–2477. doi: 10.1061/9780784413609.248.

Förster, U., De Visser, M., De Bruijn, H., Kruse, G., Hijma, M. and Vonhögen-Peeters, L. (2015) *Schematiseringshandleiding Piping bij dijken WTI 2017 (in Dutch)*. Deltares, report no. 1220084-006-GEO-0001.

Griffiths, D. V. and Fenton, G. A. (2004) 'Probabilistic Slope Stability Analysis by Finite Elements', *Journal of Geotechnical and Geoenvironmental Engineering*, 130(5), pp. 507–518. doi: 10.1061/(ASCE)1090-0241(2004)130:5(507).

Hasofer, A. M. and Lind, N. C. (1974) 'Exact and Invariant Second-Moment Code Format', *Journal of the Engineering Mechanics Division, ASCE*, 100, pp. 111–121.

Hewlett, H. W. M., Boorman, L. A. and Bramley, M. E. (1987) *Design of reinforced grass waterways*. CIRIA Report 116, London.

HKV (2015) *Afleiden lengtefactoren (N-waarden) golfoverslag en duinafslag*. PR3085.10.

Van Hoven, A. and De Waal, H. (2015) *Failure Mechanism Module Grass Wave Runup Zone Requirements and Functional Design*. Deltares: Deltares, report no. 1220043-002-HYE-0004.

JCSS (2001) *Probabilistic Model Code*. Joint Committee on Structural Safety.

Jongejan, R. B. (2012) *Het lengte-effect in een statistisch homogeen vak*. Memorandum, 11 February 2012, Jongejan RMC.

Jongejan, R. B. and Calle, E. O. F. (2013) 'Calibrating semi-probabilistic safety assessments rules for flood defences', *Georisk: Assessment and Management of Risk for Engineered Systems and Geohazards*, 7(2), pp. 88–98. doi: 10.1080/17499518.2013.790731.

Jongejan, R. B., Den Hengst, S., Kaste, D., 't Hart, R. and Klein Breteler, M., Diermanse, F. (2013) *Probabilistic assessments of block revetments in the WTI2017. Alternatives and proposed course of action*. Deltares, report no. 1207805-006.

Jongejan, R. B. and Klein Breteler, M. (2015) *A semi-probabilistic assessment rule for the stability of block revetments under wave attack*. Deltares, report no. 1220080-004-ZWS-0002.

Jongejan, R. B. and Maaskant, B. (2015) 'Quantifying Flood Risks in the Netherlands', *Risk Analysis*, 35(2), pp. 252–264. doi: 10.1111/risa.12285.

Jongejan, R. B. and De Visser, M. (2017) *Voorstel t.a.v. beoordeling macrostabiliteit incl. golfoverslag*. Kennisplatform Risicobenadering, memorandum 14 March 2017.

Jonkman, S. N., Jongejan, R. and Maaskant, B. (2011) 'The use of individual and societal risk criteria within the Dutch flood safety policy--nationwide estimates of societal risk and policy applications.', *Risk analysis*, 31, pp. 282–300. doi: 10.1111/j.1539-6924.2010.01502.x.

Kanning, W., Teixeira, A., Van der Krogt, M. and Rippi, K. (2017) *Derivation of the semiprobabilistic safety assessment rule for inner slope stability*. Deltares, report no. 1230086-009-GEO-0030, 28 April 2017.

Kanning, W. and Van der Krogt, M. (2016) *Pore water pressure uncertainties*. Deltares memorandum 1230090-034.

Kaste, D. and Klein Breteler, M. (2014) *Sensitivity study into residual strength of dikes after block revetment failure, given as preliminary safety factor*. Deltares, report no. 1207811-010-HYE-0005.

Kind, J. M. (2014) 'Economically efficient flood protection standards for the Netherlands', *Journal of Flood Risk Management*, 7(2), pp. 103–117. doi: 10.1111/jfr3.12026.

Der Kiureghian, A. and Ditlevsen, O. (2009) 'Aleatory or epistemic? Does it matter?', *Structural Safety*, pp. 105–112. doi: 10.1016/j.strusafe.2008.06.020.

Klein Breteler, M. (2015) *Detailed safety assessment method for block revetments WTI-2017 Cluster 5*. Deltares, report no. 1209437-016-HYE-0003.

Klein Breteler, M. and Mourik, G. C. (2014) *Vereenvoudiging van Steentoets tot enkele eenvoudige formules: geklemde rechthoekige blokken, zuilen, blokken op hun kant.* Deltares, report no. 1208045-015-HYE-0004.

Klerk; W.J. Kanning; W. (2014) *Calibration of Safety Factors for wave impact on Hydraulic Asphalt Concrete Revetments WTI Cluster C*. Deltares, report no. 1209431-010-ZWS-0002.

Klerk, W. J. and Jongejan, R. B. (2016) *Semi-probabilistic assessment of wave impact and runup on grass revetments*. Deltares, report no. 1220080-005-ZWS-0003, preliminary.

KOAC-NPC (2009) *GOLFKLAP - Gebruikershandleiding bij versie 1.3*. Lelystad, the Netherlands: Rijkswaterstaat Waterdienst.

Ladd, C. C. and Foot, R. (1974) 'New design procedure for stability of soft clays', *International Journal of Rock Mechanics and Mining Sciences & Geomechanics*, 11(11), pp. 763–786.

Lind, N. C. (1971) 'Consistent Partial Safety Factors', *Journal of the Structural Division*, 97(6), pp. 1651–1669.

Lopez de La Cruz, J., Schweckendiek, T., Mai Van, C. and Kanning, W. (2010) *SBW Piping - HP8b Kalibratie van de veiligheidsfactoren*. Deltares, report no. 1202123-002-GEO-0005.

Van der Meer, J. W., Hardeman, B., Steendam, G. J., Schüttrumpf, H. and Verheij, H. (2010) 'Flow depths and velocities at crest and inner slope of a dike, in theory and with the wave overtopping simulator', in *Proceedings of the International Conference on Coastal Engineering*. Shanghai: ASCE.

Van der Meer, J. W., Steendam, G. J. and Van Hoven, A. (2015) 'Validation of Cumulative Overload Method based on Tests by the new Wave Run-up Simulator', in *Proceedings of Coastal Structures*. Boston: ASCE.

Van der Meij, R. and Sellmeijer, J. B. (2010) 'A Genetic Algorithm for Solving Slope Stability Problems: from Bishop to a Free Slip Plane.', in Benz and Nordal (eds) *Numerical Methods in Geotechnical Engineering*, pp. 345–350.

Ministry of Infrastructure and the Environment (2016a) *Regeling veiligheid primaire waterkeringen 2017, Bijlage I Procedure (in Dutch)*. Ministerie van Infrastructuur en Milieu.

Ministry of Infrastructure and the Environment (2016b) *Regeling veiligheid primaire waterkeringen 2017, Bijlage II Hydraulische belastingen (in Dutch)*. Ministerie van Infrastructuur en Milieu.

Ministry of Infrastructure and the Environment (2016c) *Regeling veiligheid primaire waterkeringen 2017, Bijlage III Sterkte en veiligheid (in Dutch)*. Ministerie van Infrastructuur en Milieu.

Ministry of Infrastructure and the Environment (2016d) *Regeling veiligheid primaire waterkeringen 2017, IENM/BSK-2016/283517*. Netherlands.

Ministry of Infrastructure and the Environment (2016e) *Schematiseringshandleiding duinafslag WBI2017 (in Dutch)*. version 2.0, 1 December 2016.

Ministry of Infrastructure and the Environment (2016f) *Schematiseringshandleiding grasbekleding WBI2017 (in Dutch)*. version 2.0, 1 December 2016.

Ministry of Infrastructure and the Environment (2016g) *Schematiseringshandleiding macrostabiliteit WBI2017 (in Dutch)*. version 2.1, 1 December 2016.

Ministry of Infrastructure and the Environment (2016h) *Schematiseringshandleiding piping WBI2017 (in Dutch)*. version 2.2, 2 January 2017.

Ministry of Infrastructure and the Environment (2016i) *Schematiseringshandleiding steenzetting WBI2017 (in Dutch)*. version 2.0, 1 December 2016.

Van der Most, H., Tanczos, I., De Bruijn, K. M. and Wagendaar, D. (2014) 'New risk-based standards for flood protection in the Netherlands', in *6th International Conference on Flood Management*. Sao Paulo, Brazil, September 2014.

National Research Council (2007) *Load and resistance factor design (LRFD) for deep foundations*, *507*. Transportation Research Board.

Nowak, A. S. and Lind, N. C. (1979) 'Practical code calibration procedures', *Canadian Journal of Civil Engineering*, 6(1), pp. 112–119. doi: 10.1139/l79-012.

Ravindra, M. K. and Galambos, T. V. (1978) 'Load and resistance factor design', *Journal of Structural Devision, ASCE*, 104(ST9), pp. 1337–1353.

Rijkswaterstaat (2007) *Voorschrift Toetsen op Veiligheid Primaire Waterkeringen, Bijlage II, bedoeld in artikel 2 van de Regeling veiligheid primaire waterkeringen (in Dutch)*.

Rijkswaterstaat (2012) *Handreiking Toetsen Grasbekledingen op Dijken t.b.v. het opstellen van het beheerdersoordeel (BO) in de verlengde derde toetsronde*. Ministry of Infrastructure and the Environment.

Rijkswaterstaat (2016) *Scherper toetsen voor piping bij dijken WBI2017 Informatie t.b.v. ENW-Voorbereidingsgroep april 2016 (in Dutch)*. version 2, April 2016.

Rijkswaterstaat VNK Project Office (2014) *The National Flood Risk Analysis for the Netherlands, Final Report*.

Roscoe, K. L. and Diermanse, F. (2011) 'Effect of surge uncertainty on probabilistically computed dune erosion', *Coastal Engineering*, 58(11), pp. 1023–1033. doi: 10.1016/j.coastaleng.2011.05.014.

Schofield, A. N. and Wroth, C. P. (1968) *Critical State Soil Mechanics*. McGraw Hill, Maidenhead.

Schweckendiek, T. and Kanning, W. (2016) *Reliability updating for slope stability of dikes Approach with fragility curves (background report)*. Deltares, report no. 1230090-033-GEO-0001, version 02, 26 August 2016, draft.

Sellmeijer, H., López de la Cruz, J., Van Beek, V. M. and Knoeff, H. (2011) 'Fine-tuning of the backward erosion piping model through small-scale, medium-scale and IJkdijk experiments', *European Journal of Environmental and Civil Engineering*, 15(8), pp. 1139–1154.

Slomp, R., Knoeff, H., Bizzarri, A., Bottema, M. and Vries, W. de (2016) 'Probabilistic Flood Defence Assessment Tools', in Lang, M., Klijn, F., and Samuels, P. (eds) *Proceedings of the 3rd European Conference on Flood Risk Management (FLOODrisk 2016)*. Lyon: E3S Web of Conferences.

Spencer, E. (1967) 'A method of analysis of the stability of embankments assuming parallel inter-slice forces', *Geotechnique*, 17(1), pp. 11–26.

TAW (1989) *Leidraad voor het ontwerpen van rivierdijken deel 2 benedenrivierengebied (in Dutch)*. Technische Adviescommissie voor de Waterkeringen.

TAW (1999) *Technisch Rapport: Zandmeevoerende wellen (in Dutch)*. Technische Adviescommissie voor de Waterkeringen.

TAW (2001) *Technisch Rapport Waterkerende Grondconstructies; Geotechnische aspecten van dijken, dammen en boezemkaden (in Dutch)*. Technische Adviescommissie voor de Waterkeringen.

TAW (2004) *Technisch Rapport Waterspanningen bij dijken (in Dutch)*. Technische Adviescommissie voor de Waterkeringen, ISBN-90-369-5565-3, DWW-2004-057.

Teixeira, A., Wojciechowska, K. and Ter Horst, W. (2016) *Derivation of the semiprobabilistic safety assessment for piping WTI 2017: Cluster C, piping failure mechanism*. Deltares, report no. 1220080-002-ZWS-0006; version 4.1, 29 February 2016.

Terzaghi, K. (1929) 'Effect of minor geologic details on the safety of dams', *Bulletin of the American Institute of Mining and Metallurgical Engineers*, 215, pp. 31–44.

USACE (2013) *Engineering and design of I-Walls*. Washington, DC.

Van, M. A. (2001) 'New approach for uplift induced slope failure', in *XVth International Conference on Soil Mechanics and Geotechnical Engineering*. Istanbul, pp. 2285–2288.

Vanmarcke, E. (2011) 'Risk of Limit-Equilibrium Failure of Long Earth Slopes: How It Depends on Length', in *Georisk 2011*. Reston, VA: American Society of Civil Engineers, pp. 1–24. doi: 10.1061/41183(418)1.

VanMarcke, E. . (1977) 'Reliability of Earth Slopes', *Journal of the Geotechnical*

Engineering Division, 103(11), pp. 1247–1265.

Vrijling, J. K. (2001) 'Probabilistic design of water defense systems in The Netherlands', *Reliability Engineering & System Safety*, 74(3), pp. 337–344. doi: 10.1016/S0951-8320(01)00082-5.

Vrouwenvelder, T. (2006) 'Spatial effects in reliability analysis of flood protection systems', in *Second IFED Forum*. Lake Louise, Canada.

Vrouwenvelder, T. and Calle, E. (2003) 'Measuring Spatial Correlation of Soil Properties', *Heron*, 48(4).

De Waal, H. (2016) *Basisrapport WBI 2017 (in Dutch)*. Deltares, report no. 1230086-002-GEO-0003, 14 September 2016, version 1.1, final.

Winkler, R. L. (1996) 'Uncertainty in probabilistic risk assessment', *Reliability Engineering & System Safety*, 54(2–3), pp. 127–132.

Appendix A System reliability and the length effect

A.1 A method for quantifying system reliability

A system failure probability for a particular failure mechanism can be calculated on the basis of (Vrouwenvelder, 2006; Jongejan and Maaskant, 2015):

1. cross-sectional failure probabilities (identical throughout each section because sections are homogeneous),
2. the spatial correlations within each section and
3. the correlations between sections.

This is illustrated in Figure 46. Note that cross-sectional lengths could also be treated like sections when calculating a segment's failure probability, thus sidestepping step 2 in Figure 46. The reason for treating cross-sectional lengths differently is that the identical statistical properties of the cross-sectional lengths within each section allows for the use of relatively efficient computational techniques. The failure probability of a section can be calculated on the basis of the outcrossing method. Using this method, which is discussed in greater detail in section A.2, the failure probability for a single cross-sectional length can be scaled directly to the failure probability of an entire section.

0. Divide segments into sections
(example with 2 sections)

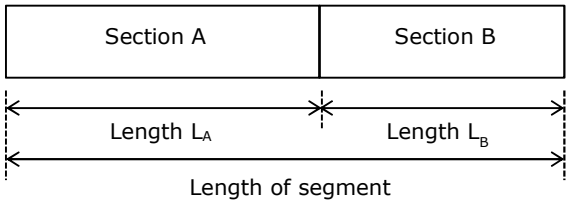

1. Calculate cross-sectional failure probabilities
(example for section A only)

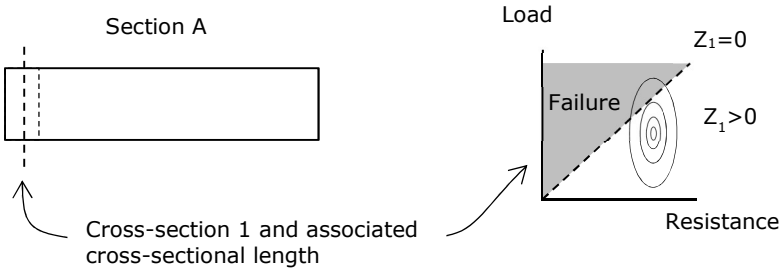

2. Calculate each section's failure probability, based on spatial correlations and cross-sectional reliabilities

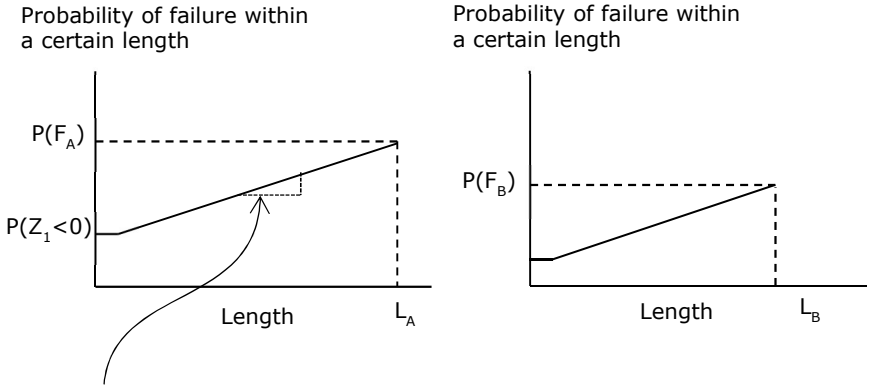

The steepness of this line depends on the (spatial) autocorrelation function of the limit state function Z_1

3. Combine the sections, taking their correlations and varying reliabilities into account

$$P(F_{system}) = P(F_A \cup F_B) = P(Z_A<0 \cup Z_B<0)$$

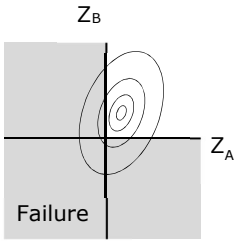

Figure 46. Schematic overview of a system reliability analysis for a segment that consists of two sections.

A.2 The length-effect within statistically homogenous sections

The length-effect within a (statistically homogenous) section can be quantified on the basis of the following inputs (after Calle & Barends 1990; Vrouwenvelder & Calle 2003):

1. the autocorrelation functions of the different stochastic variables and
2. their FORM-influence coefficients.

Together, these factors determine the spatial variability of a linearized and normalized limit state function. The more spatially variable the limit state function, the greater the probability that it will drop below zero somewhere within a section, see Figure 47.

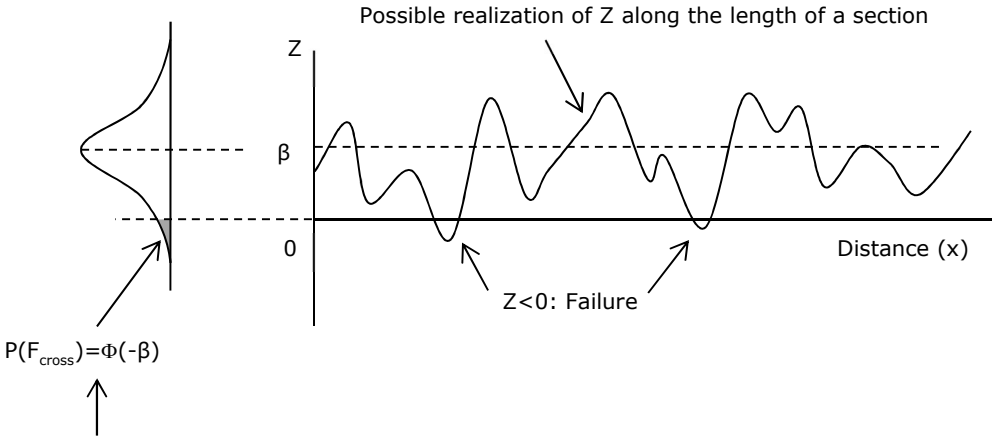

Figure 47. Cross-sectional failure probability and a possible realization of a spatially variable limit state function within a statistically homogenous section.

The variability of the limit state function within a section can be described by its autocorrelation function. The autocorrelation function of a limit state function $Z=f(X_1, X_2,\ldots, X_n)$ can be approximated by the sum of the autocorrelations functions of the different stochastic variables, weighted by their squared influence coefficients:

$$\rho_Z(\Delta h) = \Sigma \alpha_X^2 \, \rho_{Xi}(\Delta h) \qquad (92)$$

The functional form of the autocorrelation functions in Hydra-Ring is as follows (Van Balen et al. 2016):

$$\rho_i(\Delta h) = \rho_{i,\infty} + (1-\rho_{i,\infty}) \cdot \exp(-\Delta h^2/d_i^2) \qquad (93)$$

where

Δh distance between two cross-sections

$\rho_{i,\infty}$ lower limit of the autocorrelation function ('residual correlation') for stochastic variable X_i

d_i correlation distance for stochastic variable X_i

Examples of such autocorrelation functions are given in Figure 48.

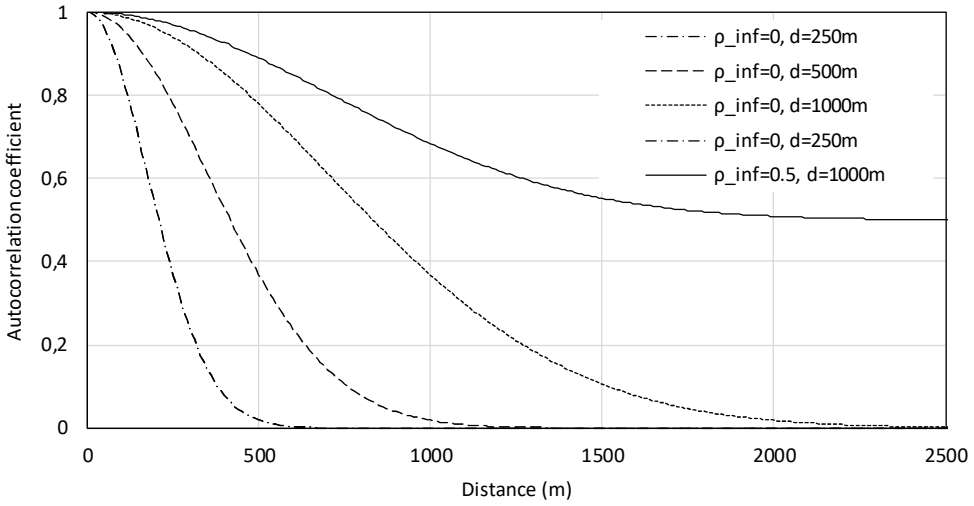

Figure 48. Examples of autocorrelation functions.

The failure probability of a section ($L_{section}$) can now be approximated by (e.g. Jongejan 2012):

$$P(F_{section}) = 1-(1-P(F_{cross})) \cdot \exp(-L_{section} / (2\pi) \cdot \text{sqrt}(-d^2\rho_Z(0)/d\Delta h^2) \cdot \exp(-\beta_{cross}^2/2)) \quad (94)$$

Where:

P(F)	Failure probability of a section, i.e. the failure probability of a statistically homogenous length
$P(F_{cross})$	Cross-sectional probability of failure
β_{cross}	Cross-sectional reliability index

From the above, it follows that a section could be thought of, approximately, as a series system of independent equivalent lengths (Δl):

$$\Delta l = P(F_{cross}) \cdot 2\pi / \text{sqrt}(-d^2\rho_Z(0)/d\Delta h^2) \cdot \exp(\beta_{cross}^2/2) \quad (95)$$

which may be approximated as follows for sufficiently high reliability indices, e.g. $\beta_{cross}>2$ (Vrouwenvelder and Calle, 2003):

$$\Delta l = \sqrt{\pi} / (\text{sqrt}(-d^2\rho_Z(0)/d\Delta h^2) \cdot \beta_{cross}) \quad (96)$$

Assuming an autocorrelation of the limit state function of the form given by equation (93), this can be simplified to:

$$\Delta l \approx d_Z \sqrt{\pi} / \beta_{cross} / \sqrt{(1-\rho_{Z,\infty})} \quad (97)$$

where

Δl	Independent equivalent length
β_{cross}	Cross-sectional reliability index

Using these equations, estimates can be obtained of the length-effect within statistically homogeneous sections.

A.3 From system-level reliability requirements to cross-sectional requirements

A system failure probability will be higher than the highest cross-sectional failure probability in case of imperfect spatial correlations. In such cases, the cross-sectional reliability requirement will therefore have to be stricter than the system-level reliability requirement:

$$P_{T,cross} = P_T / N \qquad (\text{with } P_T = \omega \cdot P_{max}) \tag{98}$$

where

- $P_{T,cross}$ Cross-sectional target failure probability for the failure mechanism under consideration
- P_T Target failure probability for an entire segment for the failure mechanism under consideration
- N Length effect factor for the failure mechanism under consideration ($N \geq 1$)
- ω Fraction of the maximum allowable probability of flooding that has been reserved for the failure mechanism under consideration ($0 < f \leq 1$), see also Table 1
- P_{max} Maximum allowable probability of flooding or standard of protection

The length effect factor differs per failure mechanism and depends on:

1. *The length-effect within statistically homogenous sections*
   The length effect within sections depends on the spatial variability of the limit state function. For a failure mechanism such as overtopping, the length effect within a statistically homogenous section is relatively small. For geotechnical failure mechanisms, such as slope instability and internal erosion, the length effect is relatively strong. This is because the uncertainties related to strongly spatially variable soil properties are often relatively important.

2. *The correlations between sections*
   Even when correlations within statistically homogeneous sections are strong, adjacent sections could still be weakly correlated, giving rise to a length-effect. When, for instance, different sections have different orientations and the angle of wave incidence is an important stochastic variable, these sections may fail independently. This is the case for e.g. revetment failures.

3. *The differences between the reliabilities of different sections*
   Segments consist of various sections. Their reliabilities may vary. The weakest sections will disproportionately impact the failure probability of the entire segment. The assumption that all sections are equally reliable would lead to unnecessarily pessimistic cross-sectional reliability requirements.

The way in which these factors influence the difference between the reliability of individual cross-sections and the reliability of an entire segment is explained graphically in Figure 49.

The difference between cross-sectional and system-level reliabilities depends on…

1. … the length effect within statistically homogeneous sections

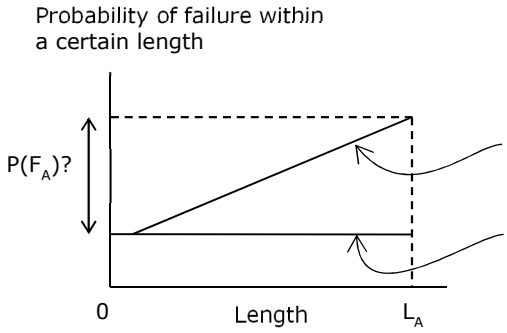

2. … the correlations between sections

No correlation ($\rho_{ZA,ZB}=0$)

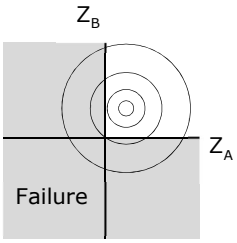

$P(Z_A<0 \cup Z_B<0) \approx P(Z_A<0) + P(Z_B<0)$

e.g. slope instability

Strong correlation ($\rho_{ZA,ZB}\approx1$)

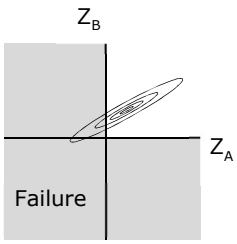

$P(Z_A<0 \cup Z_B<0) \approx P(Z_B<0)$

e.g. overtopping for sections with similar orientations

3. … the differences between the reliabilities of different sections

When $P(Z_B<0)$ is much greater than $P(Z_A<0)$, $P(Z_A<0 \cup Z_B<0) \approx P(Z_B<0)$ regardless of the correlation between Z_A and Z_B:

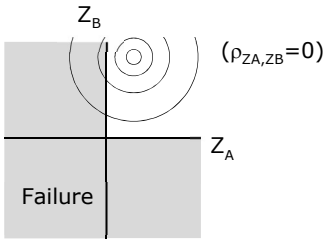

Figure 49. Three factors that influence the difference between cross-sectional and segment reliabilities, and that therefore determine the length effect factor N.

Appendix B Calibration criterion

This Appendix is based on a contribution by prof. A.C.W.M. Vrouwenvelder. It provides the basis for the calibration criterion that holds that a semi-probabilistic rule may be considered sufficiently safe when probabilities of failure are on average equal to or smaller than the target probability of failure (see section 6.2.2).

In case of an infinite time horizon, stationary conditions and the absence of correlation between subsequent years, the present value of total cost follows from:

$$C = I + P(F) \cdot D / \delta \quad (A1)$$

where
C Present value of total cost
I Investment cost
P(F) Annual probability of failure
D Potential damage
δ Discount rate

with:

$$I = I_f + I_v \cdot \gamma \quad (A2)$$

where
I_f Fixed cost
I_v Variable cost
γ Safety factor

For a system composed of i=1..n independent sections, the present value of the total cost is given by:

$$C = \Sigma(I_i + P(F_i) \cdot D_i / \delta) \quad (A3)$$

or:

$$C = \Sigma(I_{f,i} + I_{v,i} \cdot \gamma + P(F_i) \cdot D_i / \delta) \quad (A4)$$

When the relationship between the partial factor (or design value) and the probability of failure is exponential, i.e.:

$$P(F_i) = P_0 \cdot \exp(-\gamma \cdot b_i) \quad (A5)$$

equation (A4) can be expanded to:

$$C = \Sigma(I_{f,i} + I_{v,i} \cdot \gamma + P_0 \cdot \exp(-\gamma \cdot b_i) \cdot D_i / \delta) \quad (A6)$$

Differentiating the present value of the total cost with respect to the safety factor γ and setting the derivative equal to zero gives:

$$\Sigma(I_{v,i} - P_0 \cdot \exp(-\gamma \cdot b_i) \cdot D_i / (b_i \cdot \delta)) = 0 \quad (A7)$$

$$\Sigma(I_{v,i} - P(F_i) \cdot D_i / (b_i \cdot \delta)) = 0 \quad (A8)$$

When the values of $I_{v,i}$, b_i and D_i vary little from section to section, equation (A8) may be approximated by:

$$I_{v,gem} - P(F_{gem}) \cdot D_{gem} / (b_{gem} \cdot \delta)) = 0 \quad (A9)$$

or

$$P(F_{gem}) = I_{v,gem} \cdot b_{gem} \cdot \delta / D_{gem} \quad (A10)$$

To illustrate that an optimization on the basis of averages (equation A10) gives a reasonable approximate of an optimization on the basis of a weighted sum (equation A6), consider the following fictitious numerical example:

Table 19. Statistical properties of 2500 independent sections.

Variable	Average	Coefficient of variation	Distribution type
$I_{v,i}$	1 Meuro	0.3	Lognormal
b_i	1	0.3	Lognormal
D_i	50 Meuro	0.2	Normal
P_0	0,1 per year	-	Deterministic
δ	1 per year	-	Deterministic

According to the approximating procedure based on averages, the optimal average failure probability equals 0.02, so that γ=1.59. The results of more accurate calculations are shown in Table 20.

Table 20, Statistical properties of the parameter values in the optimization of a series system composed of 2500 independent sections.

Safety factor (γ)	Present value of total cost (euro)
1.2	7076
1.4	6903
1.6	6850
1.8	6953
2.0	7070

The outcomes shown in Table 20 are in good agreement with the results of the approximation based on average values.